รายงานวิจัยฉบับสมบูรณ์

เรื่อง

สารออกฤทธิ์ต้านเซลล์มะเร็งเต้านมในกลุ่มเคจแซนโทน จากรากต้นติ้วขน

Anti-breast cancer activity of natural caged-scaffolds from *Cratoxylum formosum* ssp. *pruniflorum* roots

โดย

ดร. ณวงศ์ บุนนาค

คณะการแพทย์แผนไทย

โครงการวิจัยนี้ได้รับทุนสนับสนุนการวิจัยจาก เงินรายได้มหาวิทยาลัย
มหาวิทยาลัยสงขลานครินทร์
ประจำปีงบประมาณ 2556 รหัสโครงการ TTM560546S

Contents

Acknowledgement

The research was supported by a grant from the Prince of Songkla University, Contract No.-TTM560546S. Firstly, I would like to express my sincere thankfulness to my mentor, Assoc. Prof. Dr. Suchada Chantrapromma for her kind help, useful advices and suggestions. I am grateful to Prof. Raymond J. Andersen at Department of Chemistry and Earth, Ocean & Atmospheric Sciences, University of British Columbia, Vancouver, Canada for valuable great helps, guidance, supporting my idea. I would like to thanks Dr. Wisanu Maneerat, Dr. David E. Williams and Dr. Brian O. Patrick for their valuable assistances throughout my year of research. I wish to express my gratitude to Prof. Hoong-Kun Fun and Assoc. Prof. Dr. Chatchanok Karalai for their helpful suggestions, encouragement and assistance during my research activities. NW also thanks Department of Chemistry, Faculty of Science, Prince of Songkla University for the research facilities, and the Faculty of Pharmaceutical Sciences, Prince of Songkla University for providing laboratory facilities.

Nawong Boonnak

บทคัดย่อ

สารผลิตภัณฑ์ธรรมชาติชนิดใหม่ที่หายาก สารประกอบกลุ่มนีโอ-เคจแซนโทน ชื่อพรูนิโฟลโรนที (**1**), และ สารประกอบกลุ่มรีเอเรจ-เคจแซนโทน ชื่อพรูนิโฟลโรนยู (**3**), และสารประกอบกลุ่มเคจ-แซนโทนที่เคยมีการรายงานมาก่อนแล้ว, โคชินไชโนนซี (**2**) ซึ่งถูกแยกได้จากรากของต้นติ้วขน โดยที่โครงสร้างของสารประกอบ (**1**)-(**3**) ที่แยกได้ถูกวิเคราะห์ได้จาก NMR spectroscopic data และ X-ray diffraction จากข้อมูลทาง X-ray ของสารประกอบ (**1**)-(**3**) แสดงให้เห็นว่ามีสารประกอบคู่ enantiomer ตกผลึกออกมาด้วยกันอยู่ใน crystal packing ของสารแต่ละชนิด หลังจากนั้นทำการแยกสารคู่ผสมของสารประกอบ (**1**)-(**3**) ด้วย chiral HPLC ได้เป็นสาร enantiomer pure ของ (–)-**1**/(+)-**1**, (–)-**2**/(+)-**2** และ (–)-**3**/(+)-**3** และทำการหาโครงสร้างสัมบูรณ์ (absolute configurations) ของสารที่แยกได้ต่อด้วยเทคนิค X-ray diffraction และ ECD spectroscopy นอกจากนั้นสารประกอบ (**1**) และ (**3**) ในรูปของผสมในอัตราส่วน 1:1 แสดงฤทธิ์ยับยั้งมะเร็งเต้านมชนิด MCF-7 ด้วยค่า IC_{50} เท่ากับ 0.11 μg/mL

ABSTRACT

Two rare new natural products, the neocaged-xanthone pruniflorone T (**1**), the rearranged caged-xanthone pruniflorone U (**3**), and the known caged-xanthone cochinchinone C (**2**) were isolated from the roots of *Cratoxylum formosum* ssp. *pruniflorum*. The unique structures of **1**-**3** were determined by analysis of NMR and X-ray diffraction data. The X-ray data of **1**-**3** revealed that they all exist with both enantiomers in their crystal packing. Separation of **1**-**3** by chiral HPLC led to the isolation of three pairs of enantiomers, (−)-**1**/ (+)-**1,** (−)-**2**/ (+)-**2** and (−)-**3**/ (+)-**3**, and their absolute configurations were determined by analysis of single-crystal X-ray diffraction and ECD spectroscopic data. A 1:1 mixture of **1** and **3** showed potent in vitro cytotoxicity against a MCF-7 human breast cancer cell line with an IC_{50} value of 0.11 μg/mL.

Executive Summary

Introduction

The natural caged scaffold has been widely isolated from the tropical plants in the genus *Garcinia* (Asano *et al*., 1996; Thoison *et at*., 2000; Rukachaisirikul *et al*., 2003; Reutrakul *et al*., 2007; Shadid *et al*., 2007). Many of the isolated caged-xanthones showed good bioactivity such as anti-HIV-1 (Reutrakul *et al*., 2007), antibacterial (Sukpondma *et al*., 2005) and cytotoxic activities (Shadid *et al*., 2007; Han *et al*., 2006; Cao *et al*., 1998; Wu *et al*., 2004; Yu *et al*., 2006). Gambogic acid, a well known caged-xanthone, exhibited strong cytotoxicity against various human cancer cell lines including BCG-823 gastric carcinoma (Liu *et al*., 2005), SMMC-7721 hepatoma (Yang *et al*., 2007), and SPC-A1 lung cancer (Wu *et al*., 2004) cells. Moreover, gambogic acid has been used as an anti-cancer drug in the People's Republic of China for the treatment of patients with breast carcinoma by intravenous injection (Han *et al*., 2006; Wu *et al*., 2004). The previous results suggested that the unusual caged motif was important for the bioactivity (Zhang *et al*., 2004; Kuemmerle *et al*., 2008; Li *et al*., 2007; Wang *et al*., 2009). Only a few neocaged-, structural isomers of caged-xanthones, and rearranged caged-xanthones, degraded products of caged-xanthones, have been identified.

Moreover, awareness of the stereoselectivity of drug action has intensified since the thalidomide tragedies of the 1960s as differences in the pharmacodynamics and pharmacokinetics of enantiomers have become understood. The separation of enantiomers constitutes a major challenge from the standpoint of efficacy and safety of drug. Although the R and S isomers have the same substituent atoms or groups, they occupy different positions in space, therefore forming different spatial relationships in the asymmetric environment of receptors of enzymes. The X-ray structure determination, using a space group theory is the most powerful technique to distinguish between enantiomerically pure compound and racemic mixture and also provide more detail about 3-D structures of the molecules. From these importances, it led us to search for anti-breast cancer active natural caged-scaffolds from the roots of *Cratoxylum formosum* ssp. *pruniflorum*, which is a rich source of xanthones.

Objectives

- To extract and isolate caged-scaffolds from the roots of *Cratoxylum formosum* ssp. *pruniflorum*
- To identify the absolute configuration of isolated caged-scaffolds
- To search for anti-breast cancer caged-scaffolds

Results and Discussions

Herein, we report the isolation of three different types of caged-scaffolds represented by pruniflorone T (**1**), a new neocaged-xanthone, pruniflorone U (**3**), a rearranged caged-xanthone, and cochinchinone C (**2**), a known caged-xanthone (Mahabusarakam *et al*., 2006), from the roots of *Cratoxylum formosum* ssp. *pruniflorum*. The structures of **1-3** were elucidated by analysis of NMR spectroscopic and single crystal X-ray diffraction data. Compounds **1-3** were evaluated for in vitro cytotoxicity against the MCF-7 human breast cancer cell line.

Neocaged-xanthone pruniflorone T (**1**) was assigned a molecular formula of $C_{23}H_{26}O_5$ on the basis of ^{13}C NMR spectroscopic data and an HREIMS ion at *m*/*z* 382.1774 $[M - CO]^+$ (Mahabusarakam *et al*., 2006).

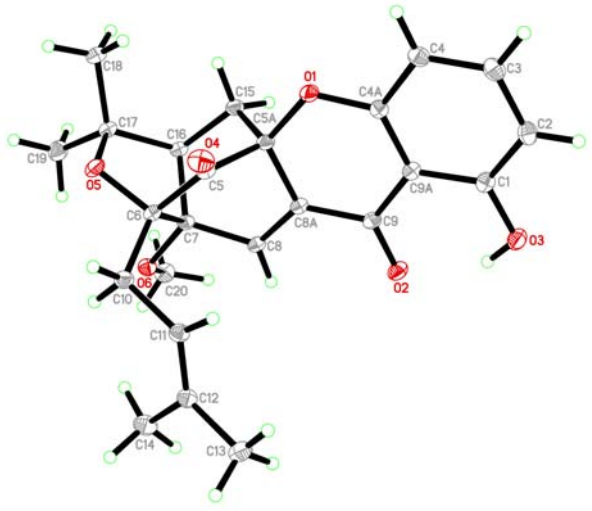

Figure 1. ORTEP diagram of pruniflorone T (**1**)

A single crystal X-ray diffraction analysis of **1** (**Figure 1**) showed that the main skeleton of **1** was a neocaged-xanthone type. The UV spectrum of **1** showed absorption bands at 242, 293, 329, and 396 nm, which were similar to those of the known caged-xanthone

cochinchinone C (**2**) (Mahabusarakam *et al*., 2006). Its IR spectrum indicated the presence of a hydroxy (3445 cm^{-1}) functionality along with unconjugated (1747 cm^{-1}) and conjugated (1645 cm^{-1}) ketone carbonyls.

The ^{1}H and ^{13}C NMR spectroscopic data of **1** (**Table 1**) were similar to those of the known caged-xanthone **2** (Mahabusarakam *et al*., 2006) (**Table 1**) including the presence of ^{13}C NMR resonances typical of unconjugated and conjugated ketone carbonyls at δ_C 198.4 (C-5) and δ_C 179.2 (C-9). The ^{1}H NMR spectrum of **1** (**Table 1**) revealed the hydrogen-bonded phenolic proton at δ_H 11.88 (s, 1-OH) and an ABM spin system for three aromatic protons at δ_H 7.36 (t, J = 8.4 Hz, H-3), 6.57 (dd, J = 0.6, 8.4 Hz, H-4), and 6.47 (dd, J = 0.6, 8.4 Hz, H-2), respectively. Resonances assigned to an olefinic proton at δ_H 7.16 (s, H-8), a methoxy group at δ_H 3.44 (s, 7-OCH_3), and an isoprenyl group at δ_H 4.42 (br t, J = 7.8 Hz, H-11), 2.54 (d, J = 7.8 Hz, H_2-10), and 1.50 (s, H_3-13/H_3-14) were also identified in the ^{1}H NMR spectrum. A methine proton resonance at δ_H 2.44 (H-16) showed vicinal coupling (J = 9.6 Hz) with the proton resonance at δ_H 1.80 (H-15), and the latter also showed geminal coupling (J = 12.9 Hz) with the proton resonance at δ_H 2.48 (H-15), indicating the presence of a -CH_2-CH- subunit. In the HMBC spectrum of **1** (**Figure 2**), the diastereotopic methylene protons H_2-15 were correlated to C-5, C-9, C-5a, and C-8a, whereas the C-16 methine proton was correlated to C-6, C-7, and C-17, indicating that the -CH_2-15 and -CH-16 carbons were linked to C-5a and C-7, respectively. Furthermore, strong HMBC correlations (**Figure 2**) from H-10 to C-5, C-6, and C-7 confirmed the attachment of an isoprenyl side chain to C-6. Therefore, the structure of compound **1** was assigned as a neocaged-xanthone, namely pruniflorone T.

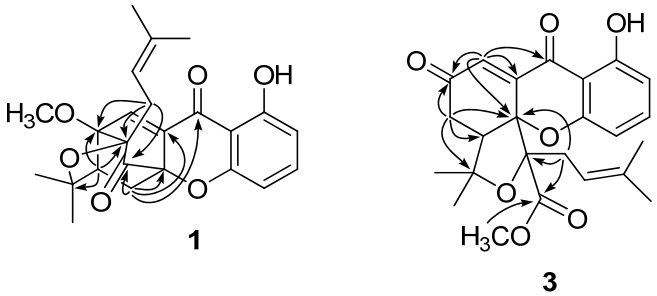

Figure 2. Selected HMBC ($^{1}H \rightarrow ^{13}C$) correlations of **1** and **3**

Table 1. ^{1}H and ^{13}C NMR Spectroscopic Data of 1-3 in $CDCl_3$

position	Neocaged-xanthone (**1**)		Caged-xanthone (**2**)		Rearranged caged-xanthone (**3**)	
	δ_C,[a] type	δ_H[b] (*J* in Hz)	δ_C,[a] type	δ_H[b] (*J* in Hz)	δ_C,[a] type	δ_H[b] (*J* in Hz)
1-OH	162.9 C	11.88 s	162.9 C	12.10 s	162.6 C	11.65 s
2	109.8 CH	6.47 dd (0.6, 8.4)	109.5 CH	6.55 dd (0.9, 8.4)	110.2 CH	6.61 br d (8.4)
3	139.3 CH	7.36 t (8.4)	138.9 CH	7.41 t (8.4)	140.8 CH	7.48 t (8.4)
4	107.8 CH	6.57 dd (0.6, 8.4)	107.4 CH	6.52 dd (0.9, 8.4)	106.9 CH	6.51 br d (8.4)
4a	160.0 C		159.4 C		159.5 C	
5a	83.5 C		88.8 C		90.9 C	
5	198.4 C		84.1 C		95.1 C	
6	84.0 C		201.1 C		171.7 C	
7	88.6 C		84.8 C		197.0 C	
8	138.3 CH	7.16 s	135.3 CH	7.51 d (1.2)	128.9 CH	6.65 s
9	179.2 C		180.7 C		185.3 C	
8a	130.7 C		132.1 C		145.8 C	
9a	106.5 C		106.1 C		107.8 C	
10	28.1 CH_2	2.54 d (7.8)	29.7 CH_2	2.39 br d (13.2)	37.9 CH_2	2.86 dd (12.6, 16.5)
				1.58 dd (9.6, 13.2)		2.64 dd (6.6, 16.5)
11	117.9 CH	4.42 br t (7.8)	49.4 CH	2.53 d (9.6)	55.9 CH	3.13 dd (6.6, 12.6)
12	136.7 C		83.9 C		84.7 C	
13	25.8 CH_3	1.50 s	30.4 CH_3	1.68 s	30.0 CH_3	1.73 s
14	17.8 CH_3	1.50 s	29.0 CH_3	1.32 s	25.4 CH_3	1.41 s
15	34.2 CH_2	2.48 br d (12.9)	29.2 CH_2	2.64 d (7.8)	36.6 CH_2	2.46 m
		1.80 dd (9.6, 12.9)				
16	41.6 CH	2.44 d (9.6)	118.4 CH	4.41 br t (7.8)	116.9 CH	4.99 br t (6.9)
17	83.6 C		135.7 C		136.3 C	
18	29.8 CH_3	1.43 s	25.5 CH_3	1.37 s	17.9 CH_3	1.40 s
19	28.6 CH_3	1.25 s	16.7 CH_3	1.01 s	25.9 CH_3	1.62 s
6-OCH_3	–	–	–	–	51.8 CH_3	3.58 s
7-OCH_3	51.9 CH_3	3.44 s	54.1 CH_3	3.64 s	–	–

[a] Measured at 75 MHz. [b] Measured at 300 MHz.

The rearranged caged-xanthone pruniflorone U (**3**) was assigned a molecular formula of $C_{24}H_{26}O_7$ on the basis of ^{13}C NMR spectroscopic data (**Table 1**) and an HREIMS ion at *m/z* 426.1684 $[M]^+$. The single crystal X-ray diffraction analysis of **3** (**Figure 3**) showed that the main skeleton of **3** was a rearranged caged-xanthone. The UV spectrum of **3** showed absorption bands at 243, 252, 312, and 385 nm. IR absorptions at 3615, 1748, 1710, and 1633 cm^{-1} implied the existence of a hydroxy and three carbonyl groups. The presence of the carbonyl functionalities was confirmed by the observation of resonances at δ_C 197.0 (C-7), δ_C 185.3 (C-9) and δ_C 171.7 (C-6) in the ^{13}C NMR data (**Table 1**).

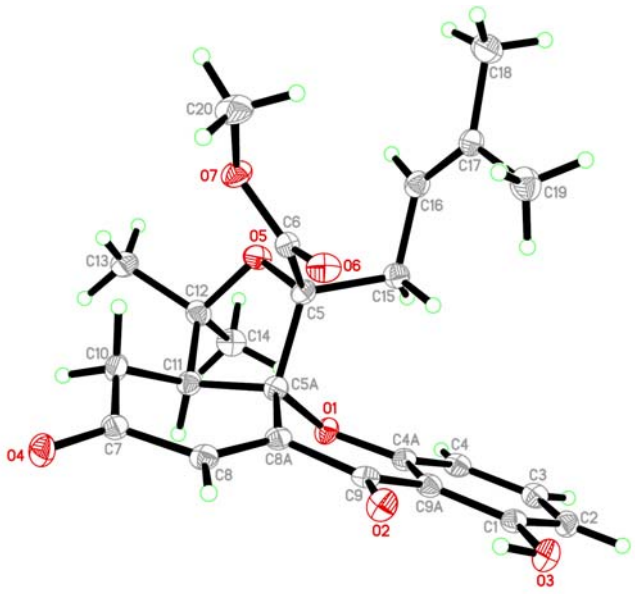

Figure 3. ORTEP diagram of pruniflorone U (**3**)

The ^1H NMR spectrum of **3** (**Table 1**) revealed resonances assigned to a hydrogen-bonded phenolic proton at δ_H 11.65 (s, 1-OH) and three aromatic protons which coupled as and an ABM system at δ_H 7.48 (t, J = 8.4 Hz, H-3), 6.61 (br d, J = 8.4 Hz, H-2), and 6.51 (br d, J = 8.4 Hz, H-4) for the three aromatic protons. A proton resonance at δ_H 6.65 (s) was assigned to the C-8 olefinic proton. The resonance at δ_H 3.13 (dd), assigned to the methine proton H-11, showed small (J = 6.6 Hz) and large (J = 12.6 Hz) coupling constants with the non-equivalent C-10 methylene proton resonances at δ_H 2.64 and δ_H 2.86, respectively. In the NOESY spectrum, a diastereotopic C-10 methylene proton at δ_H 2.64 showed a correlation with H-11 (δ_H 3.13), which indicated that the orientation of a diastereotopic C-10 methylene proton at δ_H 2.64 should be β-oriented. The attachment of an α,β-unsaturated cyclohexenone

moiety at C-8a and C-5a was assigned by the HMBC correlations from the H-8 (δ_H 6.65) resonance to the C-9, C-5a, C-8a, and C-10 resonances and from H-10 (δ_H 2.86) to C-5a.

The ^{1}H NMR spectrum of **3** also showed resonances at δ_H 1.73 (s, H_3-13) and δ_H 1.41 (s, H_3-14) assigned to a 2,2-dimethyltetrahydrofuran ring. The attachment of the tetrahydrofuran ring at C-11 and C-5a was confirmed by the HMBC correlations between H-10 (δ_H 2.86) and C-7, C-11, C12, and C-5a. Resonances typical of an isoprenyl group were present at δ_H 4.99 (br t, J = 6.9 Hz, H-16), 2.46 (m, H_2-15), 1.62 (s, H_3-19), and 1.40 (s, H_3-18). The attachment of isoprenyl and methyl ester groups at C-5 was confirmed by the HMBC correlations between H_2-15 (δ_H 2.46) and C-5, C-5a, and C-6 and between 6-OCH_3 (δ_H 3.58) and C-6 shown in **Figure 2**. Therefore, the structure of compound **3** was assigned as a rearranged caged-xanthone, namely pruniflorone U.

The X-ray analyses of **1**-**3** revealed that both **1** (CCDC727003) and **3** (CCDC774999) crystallized in a centrosymmetric triclinic *P*-1 space group (containing an inversion center), whereas **2** (Chantrapromma *et al*., 2005) crystallized in a centrosymmetric monoclinic $P2_1/c$ space group (containing a *c*-glide plane). Owing to the fact that crystals of an enantiomeric pure compound cannot crystallize in a space group that contains an inversion center, mirror plane, or glide plane (Glusker *et al*., 1994), and the crystals of **1**-**3** crystallalized in space groups containing an inversion center (for **1** and **3**) and a glide plane (for **2**), it was apparent that the crystals of **1**-**3** are racemates.

The crystal packings of **1**-**3** as shown **Figures 4-6** revealed that molecules (**1**), (**2**) and (**3**) cannot be superimposed on molecules ***ent*-(1)**, ***ent*-(2)** and ***ent*-(3)**, respectively. In these diagrams, molecules (**1**) and (**3**) are related to molecules ***ent*-(1)** and ***ent*-(3)** by inversion (Glusker *et al*., 1994), whereas molecule (**2**) is related to molecule ***ent*-(2)** by a *c*-glide plane (Glusker *et al*., 1994). Therefore, the X-ray data obtained for **1**-**3** showed that single crystals of **1**-**3** exist as racemates. Moreover, the X-ray data in **Figures 4b-6b** and **Figures 4c-6c**, showed that the crystals of **1**-**3** were stabilized by intermolecular interactions between two enantiomers (using blue and red ovals in **Figures 4c-6c**) in their crystal lattices.

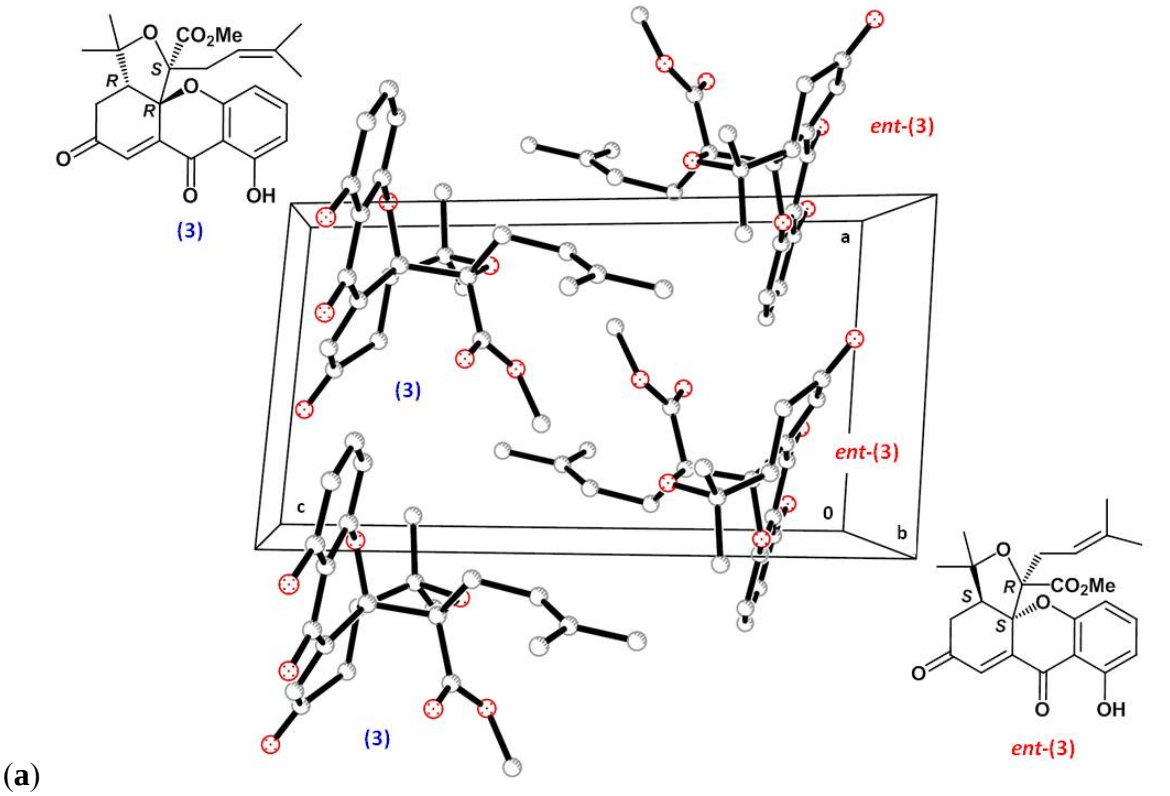

(**a**)

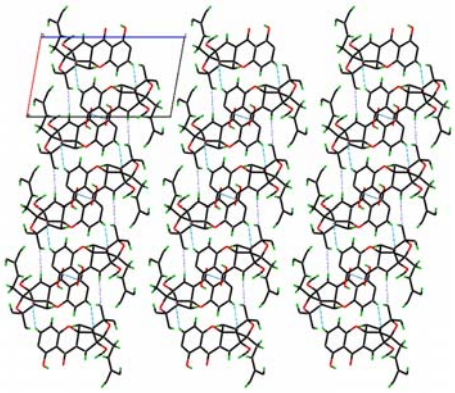

(**b**)

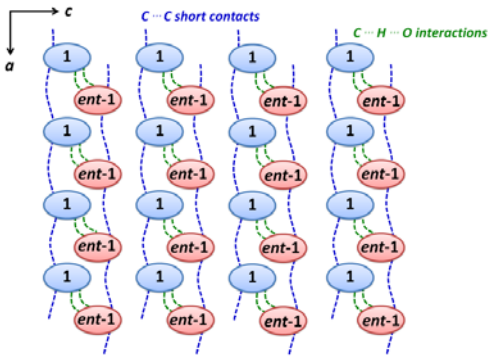

(**c**)

Figure 4. Crystal structure of neocaged-xanthone (**1**); (**a**) crystal packing of **1** showing the non-superimposition of molecule (**1**) (5a*R*,6*R*,7*R*,16*S*–(**1**)) and molecule *ent*-(**1**) (5a*S*,6*S*,7*S*,16*R*–(**1**)) (**b**) Intermolecular interactions and molecular arrangement of **1** (**c**) Schematic representation of interactions between molecule (**1**) (blue oval) and molecule *ent*-(**1**) (red oval) in the crystal packing

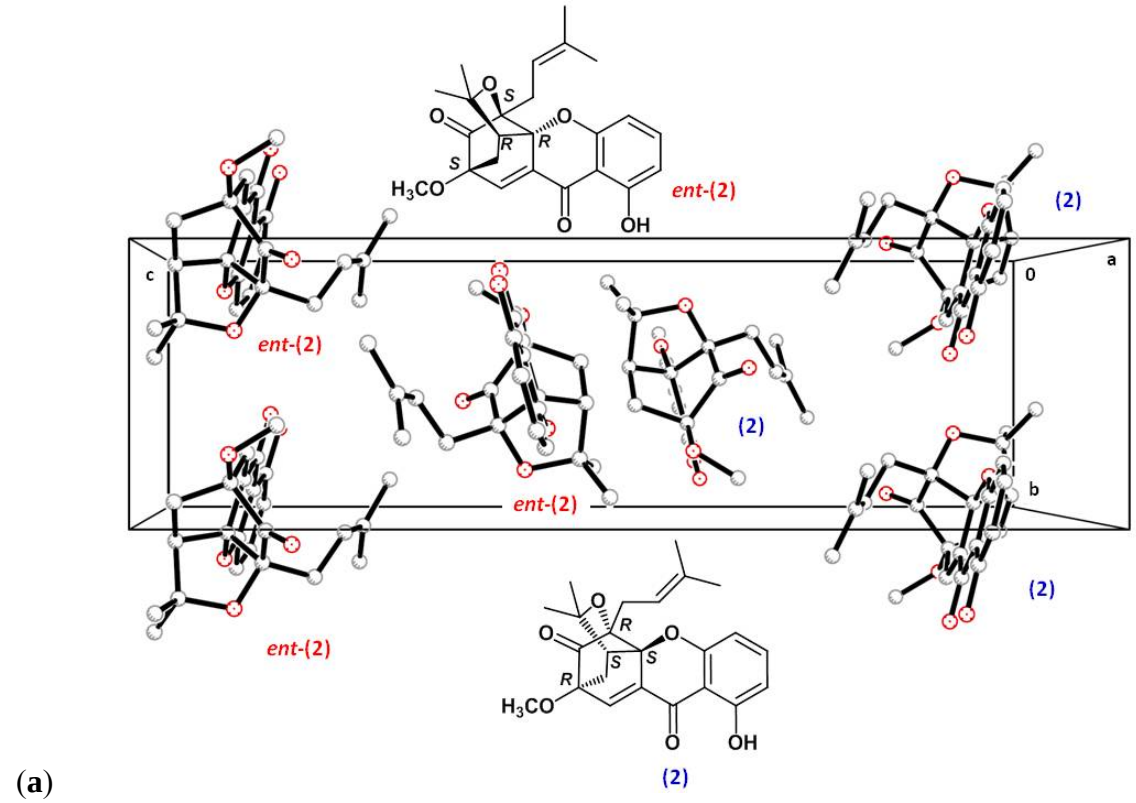

(**a**)

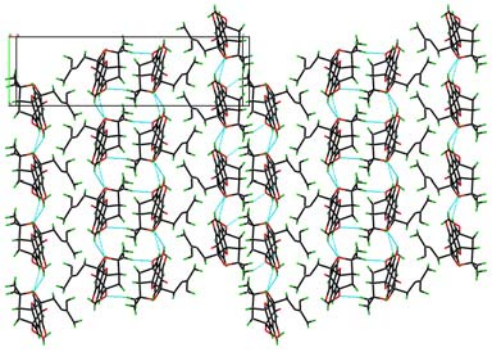

(**b**)

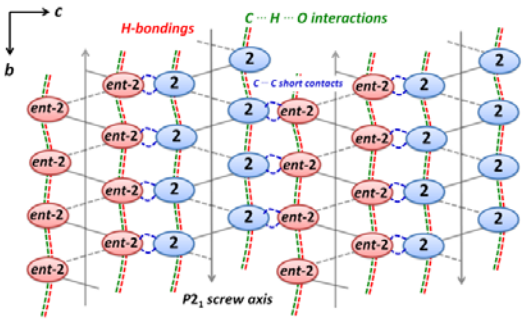

(**c**)

Figure 5. Crystal structure of caged-xanthone (**2**) (Chantrapromma *et al.*, 2005); (**a**) crystal packing of **2** showing the non-superimposition of molecule (**2**) (5*R*,5a*S*,7*R*,11*S*–(**2**)) and molecule *ent*-(**2**) (5*S*,5a*R*,7*S*,11*R*–(**2**)) (**b**) Intermolecular interactions and molecular arrangement of **2** (**c**) Schematic representation of interactions between molecule (**2**) (blue oval) and molecule *ent*-(**2**) (red oval) in the crystal packing

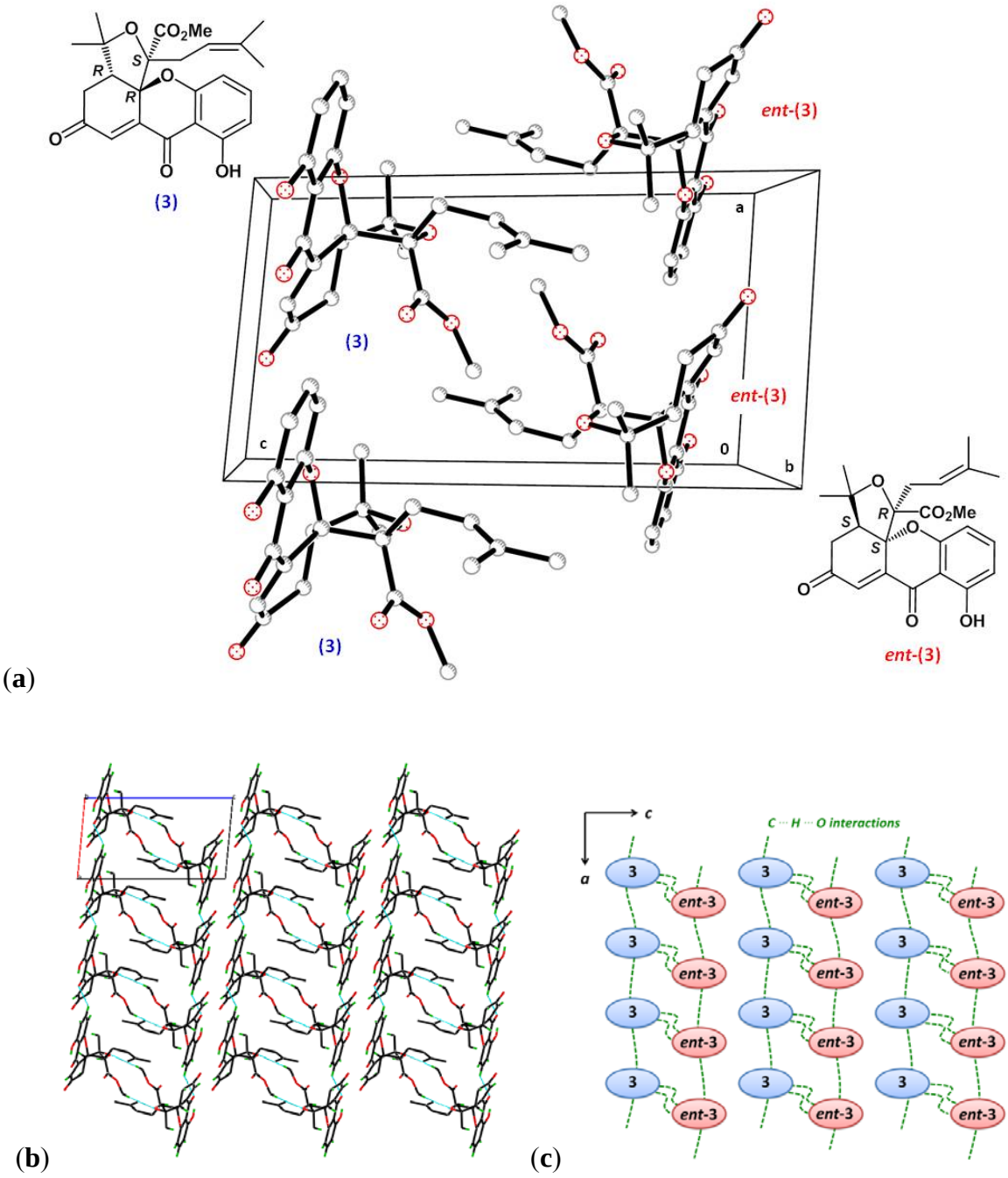

Figure 6. Crystal structure of rearranged caged-xanthone (**3**); (**a**) crystal packing of **3** showing the non-superimposition of molecule (**3**) (5*S*,5a*R*,11*R*–(**3**)) and molecule *ent*-(**3**) (5*R*,5a*S*,11*S*–(**3**)) (**b**) Intermolecular interactions and molecular arrangement of **3** (**c**) Schematic representation of interactions between molecule (**3**) (blue oval) and molecule *ent*-(**3**) (red oval) in the crystal packing

Surprisingly, the specific rotations of the isolated samples of **1**-**3** are +13.5 (*c* 0.14, $CHCl_3$), +125.1 (*c* 0.14, $CHCl_3$) and −24.0 (*c* 0.10, $CHCl_3$), respectively, demonstrating that the bulk samples of **1**-**3** are optically active, whereas the X-ray data of **1**-**3** showing that **1**-**3** contained both enantiomers in their crystal packing suggests that **1**-**3** are racemates. The combination of both observations suggests that the isolated samples of **1**-**3** are partial racemates. A previous report by Odile and coworkers (Thoison *et al*., 2000), showed that bractatin, a caged-xanthone isolated from *Garcinia bracteata* leaves, was a parital racemate that could be separated using a chiral column to give two peaks in an HPLC chromatogram. The partial racemization of **1** and **2** can be explained by the proposed biosynthesis shown in Scheme 1 in which the Claisen rearrangement step generates intermediates **1** and **2** as partial racemates (Hayden *et al*., 2006). This infers that Claisen rearrangement to give **1** and **2** might proceed via a mixture of non-enzymatic and enzymatic processes. **Scheme 1** proposes that the caged motif construction occurs via a Diels Alder reaction affording the partial *rac*-**1** and partial *rac*-**2**, respectively, whereas partial *rac*-**3** would be formed via a ring expansion and degradation of partial *rac*-**2**.

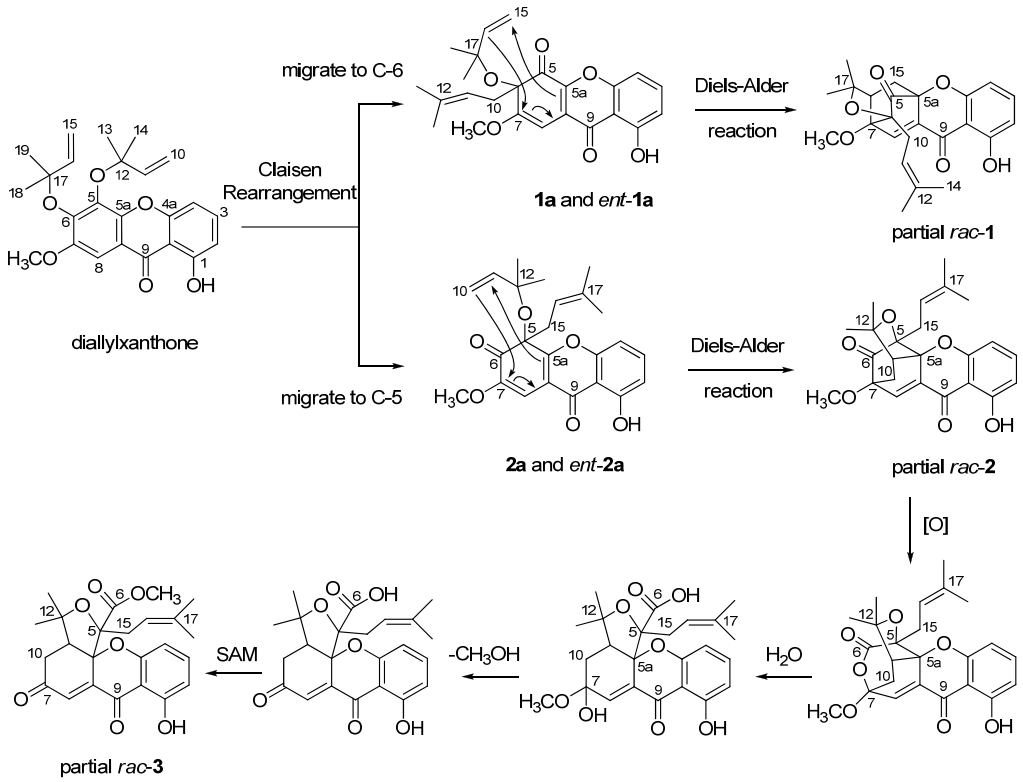

Scheme 1. Plausible biosynthesis of **1**-**3**

The above results implied that compounds **1**-**3** were partial racemates. To clarify this assumption, we have further subjected all compounds to HPLC separation on a chiral column to determine the ratio of the two enantiomers in each mixture. The chiral HPLC analysis of each of the isolated samples **1**-**3** showed well resolved peaks of two enantiomers in unequal ratios (**Figure 7**).

a)

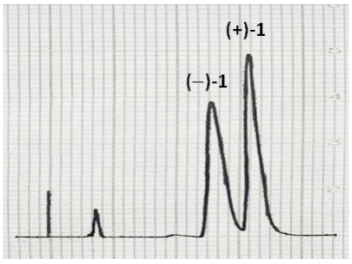

b)

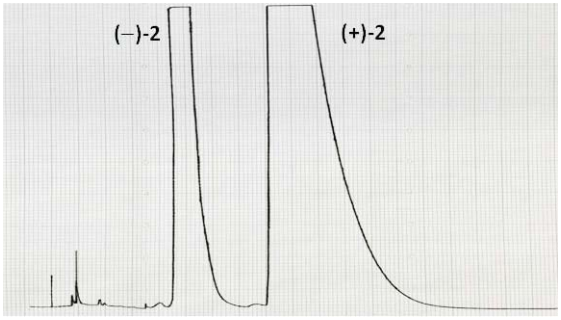

c)

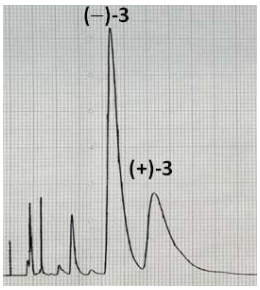

Figure 7. Chiral HPLC using a Chiral Pack AD-H, 5μ 4.6 x 250 mm column, with detection at 225 nm and a flow rate of 1 mL/min for: **(a)** Chiral HPLC chromatogram of (−)-neocaged xanthone and (+)-neocaged xanthone (**1**) by using 1:99 *i*PrOH/*n*-hexane as eluent; **(b)** Chiral HPLC chromatogram of (−)-caged-xanthone (**2**) and (+)-caged-xanthone (**2**) by using 0.5:99.5 *i*PrOH/*n*-hexane as eluent; **(c)** Chiral HPLC chromatogram of (−)-rearranged caged-xanthone (**3**) and (+)-rearranged caged-xanthone (**3**) by using 1:99 *i*PrOH/*n*-hexane as eluent.

The ratio of two enantiomers of compound **1-3** were as follows: 1.0:1.1 for the mixture of (–)-**1** [(1.1 mg), $[\alpha]^{25}_{D}$ = –61] and (+)-**1** [(1.2 mg), $[\alpha]^{25}_{D}$ = +79] in compound **1** (**Figure 7a**); 1.0:1.9 for the mixture of (–)-**2** [(1.8 mg), $[\alpha]^{25}_{D}$ = –459] and (+)-**2** [(3.4 mg), $[\alpha]^{25}_{D}$ = +509] in compound **2** (**Figure 7b**); and 1.1:1.0 for the mixture of (–)-**3** [(0.8 mg), $[\alpha]^{25}_{D}$ = –161] and (+)-**3** [(0.7 mg), $[\alpha]^{25}_{D}$ = +172] in compound **3** (**Figure 7c**), respectively. Comparison of the spectroscopic data of (–)-**1**/ (+)-**1** with **1**, (–)-**2**/ (+)-**2** with **2**, and (–)-**3**/ (+)-**3** with **3**, revealed that the ^{1}H and ^{13}C NMR spectra of each of the isolated enantiomers and their precursor mixtures in an achiral environmental were identical. These results confirmed our hypothesis that compounds **1**-**3** were partial racemates.

To establish the absolute configuration of the three different caged-scaffolds **1**-**3**, pure enantiomers of each scaffold [(–)-neocaged-xanthone pruniflorone T (**1**), (–)-caged-xanthone cochinchinone C (**2**) and (–)-rearranged caged-xanthone pruniflorone U (**3**)] were further recrystallized in CH_2Cl_2 to obtain single crystals for X-ray structure determination using CuK_{α} radiation. Yellow plate-like single crystals of the (–)-neocaged-xanthone **1** were monoclinic, with a = 8.4151(3) Å, b = 8.0906(3) Å, c = 15.1668(5) Å and chiral space group $P2_1$. From the X-ray data analysis, the absolute configuration of (–)-neocaged-xanthone pruniflorone T (**1**) (**Figures 8** and **10**) was established as 5a*R*, 6*R*, 7*R*, and 16*S* through the refinement of Flack's parameter [x = 0.01(2)].

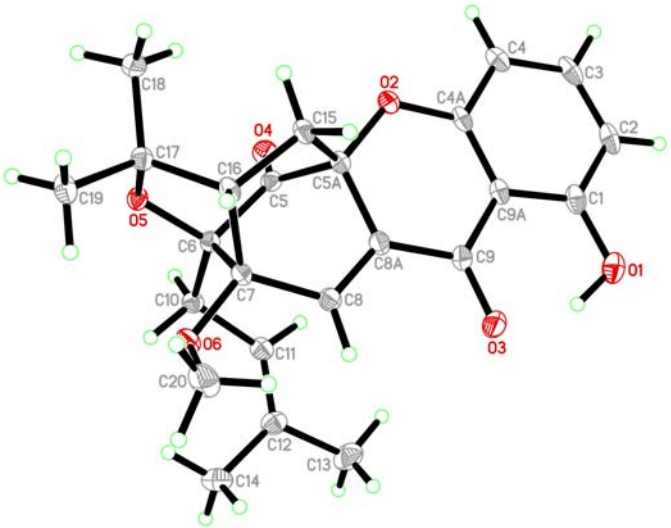

Figure 8. ORTEP diagram of (–)-pruniflorone T (**1**).

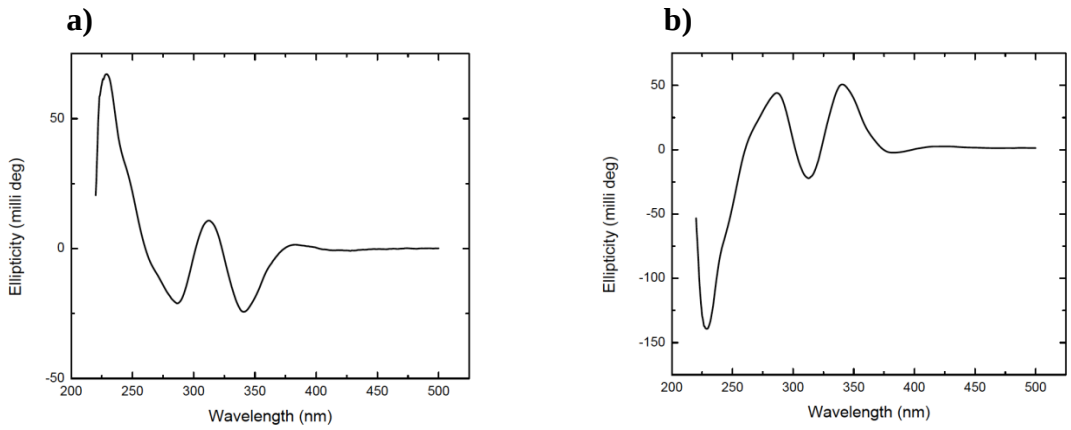

Figure 9. ECD spectra recorded in CH_2Cl_2: **a)** (–)-Neocaged-xanthone pruniflorone T (**1**) (0.20 mg/mL); **b)** (+)-Neocaged-xanthone pruniflorone T (**1**) (0.12 mg/mL) (pathlength of 0.2 cm, bandwidth 2 nm, data pitch 0.5 nm, scan rate 200 nm/min and response 4 s).

Moreover, (+)-neocaged-xanthone **1** showed the opposite sign in terms of the Cotton effects in the electronic circular dichroism (ECD) curve (**Figure 9**) and specific rotation as compared with the (–)-neocaged-xanthone **1**, but their NMR data were identical in an achiral environmental. Thus, the absolute configuration of (+)-neocaged-xanthone **1** (**Figure 10**) is (5a*S*, 6*S*, 7*S*, 16*R*).

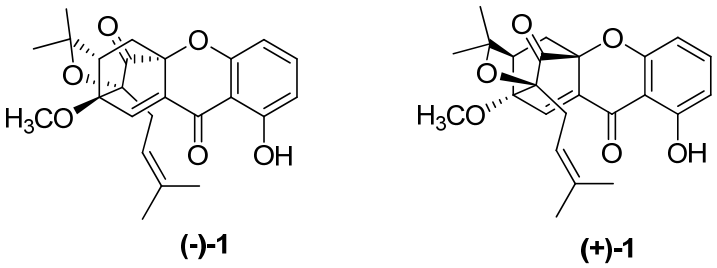

Figure 10. The absolute configurations of (–)-5a*R*, 6*R*, 7*R*, 16*S*-**1** and (+)-5a*S*, 6*S*, 7*S*, 16*R*-**1**.

The absolute configuration of (–)-caged-xanthone cochinchinone C (**2**) was confirmed to be the same as (–)-**1** based on single-crystal X-ray diffraction analysis. The yellow needle single crystals of the (–)-caged-xanthone **2** were, orthorhombic, with a = 7.2698(8) Å, b = 11.4350(1) Å, c = 24.6320(3) Å and chiral space group $P2_12_12_1$. The X-ray diffraction analysis using anomalous scattering of CuK_α radiation and resulted in a Flack parameter of

0.02 (3), which showed that the absolute configuration of (−)-caged-xanthone cochinchinone C (**2**) (**Figures 11** and **13**) as (5*R*, 5a*S*, 7*R*, 11*S*).

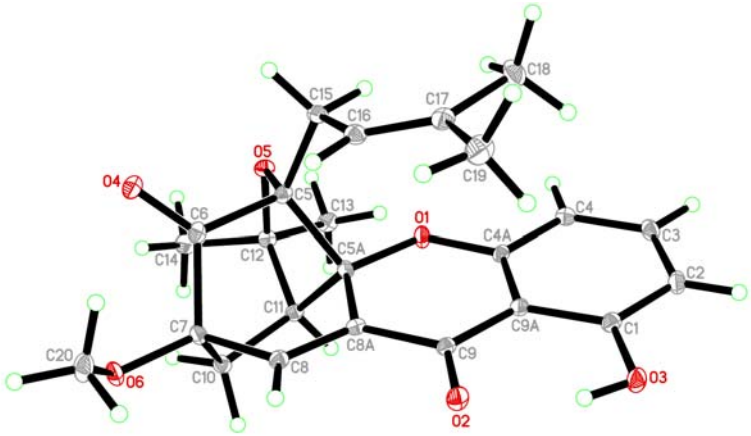

Figure 11. ORTEP diagram of (−)-cochinchinone C (**2**).

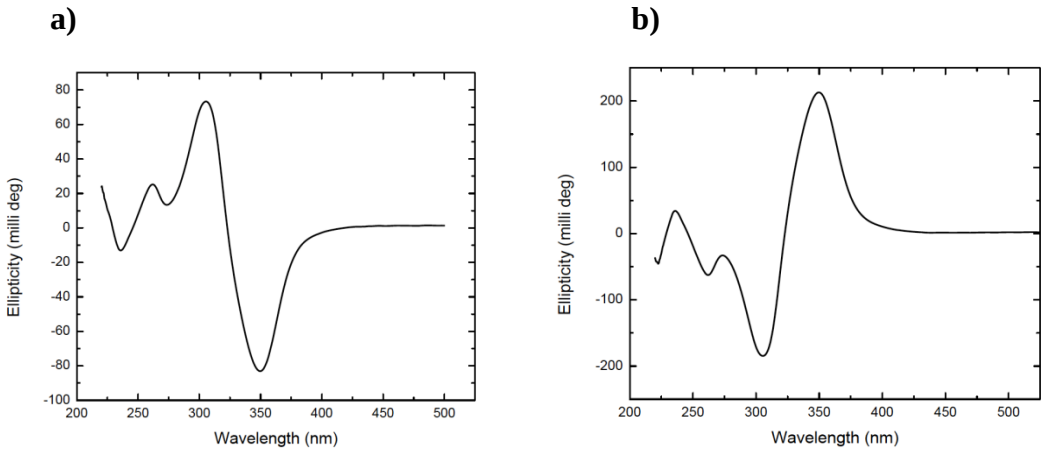

Figure 12. ECD spectra recorded in CH_2Cl_2: **a)** (−)-Caged-xanthone **2** (0.02 mg/mL); **b)** (+)-Caged-xanthone **2** (0.13 mg/mL) (pathlength of 0.2 cm, bandwidth 2 nm, data pitch 0.5 nm, scan rate 200 nm/min and response 4 s).

The signs of the ECD cotton effects and specific rotations of (+)-cochinchinone C (**2**) and (−)-cochinchinone C (**2**) were opposite (**Figure 12**). Therefore, the absolute configuration of (+)-cochinchinone C (**2**) (**Figure 13**) was (5*S*, 5a*R*, 7*S*, 11*R*).

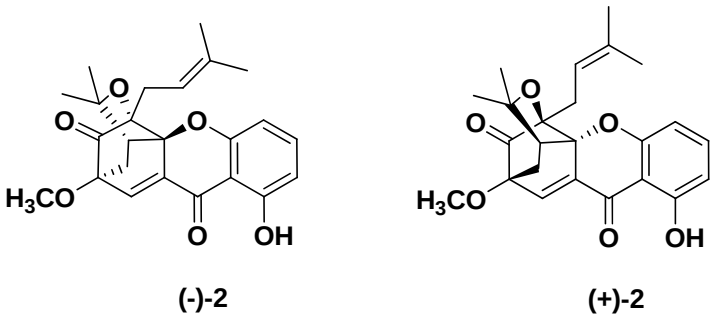

Figure 13. The absolute configurations of (−)-5*R*, 5a*S*, 7*R*, 11*S*-**2** and (+)-5*S*, 5a*R*, 7*S*, 11*R*-**2**

Finally, yellow needle single crystals of the (−)-rearranged caged-xanthone pruniflorone U (**3**) were, monoclinic, with a = 13.4658(12) Å, b = 7.9997(7) Å, c = 20.8660(2) Å and with a chiral space group ($P2_1$). The absolute configuration of (−)-rearranged caged-xanthone pruniflorone U (**3**) was assigned as (5*S*, 5a*R*, 11*R*) by the single crystal X-ray diffraction analysis (**Figures 14** and **16**) with a Flack parameter of 0.02 (3).

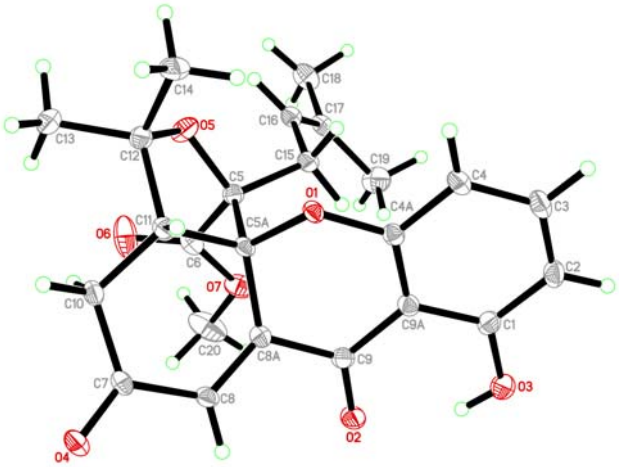

Figure 14. ORTEP diagram of (−)-rearranged caged-xanthone pruniflorone U (**3**).

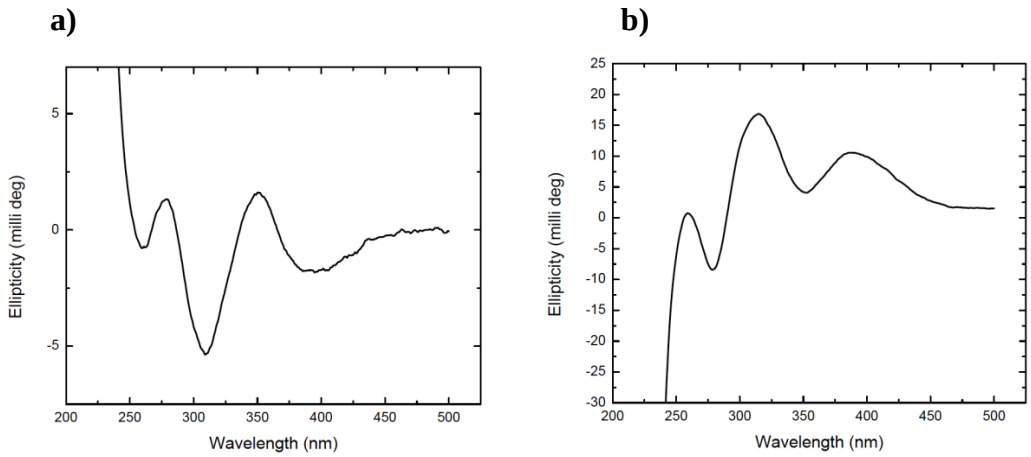

Figure 15. ECD spectra recorded in CH_2Cl_2: **a)** (−)-Rearranged caged-xanthone pruniflorone U (**3**) (0.02 mg/mL); **b)** (+)-Rearranged caged-xanthone pruniflorone U (**3**) (0.14 mg/mL) (pathlength of 0.2 cm, bandwidth 2 nm, data pitch 0.5 nm, scan rate 200 nm/min and response 4 s).

In a similar way, the absolute configuration of (+)-pruniflorone U (**3**) (**Figure 16**) was assigned as (5*R*, 5a*S*, 11*S*) by comparison of the ECD curve (**Figure 15**) and specific rotation with those of (−)-pruniflorone U (**3**).

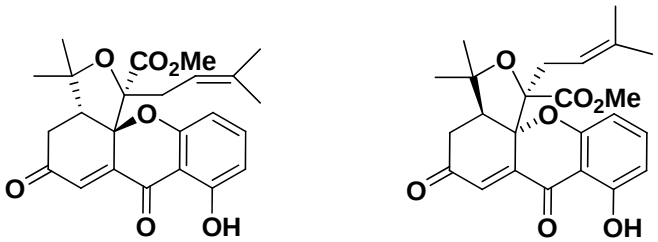

Figure 16. The absolute configurations of (−)-5*S*, 5a*R*, 11*R*-**3** and (+)-5*R*, 5a*S*, 11*S*-**3**.

Only stable compounds of sufficient quantity were evaluated for in vitro cytotoxicity against the MCF-7 human breast cancer cell line (**Table 2**). Cochinchinone C (**2**) exhibited better activity than pruniflorone T (**1**) and pruniflorone U (**3**) with an IC_{50} value of 0.36 μg/mL. Interestingly, a 1:1 mixture of **1** and **3** significantly increased the cytotoxicity against MCF-7 compared with the pure forms (**1** and **3**) with an IC_{50} value of 0.11 μg/mL.

Table 2. Cytotoxicity of **1**-**3** Against the MCF-7 Human Breast Cancer Cell Line

Compounds	**1**	**2**	**3**	**1+3**[a]	**camptothecin**
IC_{50} (μg/mL)	>5	0.36	>5	0.11	<0.024

[a] a 1:1 mixture of **1** and **3**

Conclusions

In summary, this paper describes the isolation of three different types of caged-scaffolds **1-3** from the roots of *C. formosum* ssp. *pruniflorum*. Two of the scaffolds are found in the new natural products pruniflorone T **(1)** and pruniflorone U **(3)**. Single crystal X-ray diffraction analysis data obtained for the isolated samples of **1-3**, revealed that natural **1-3** exist in both enantiomeric forms in their crystal packings, but are also optical active, suggesting that natural **1** and **3** are slightly partial racemates and natural **2** are partial racemate. To confirm this possibility, the enantiomeric mixtures of natural **1-3** were further purified by chiral HPLC yielding each enantiomer as a pure compound [(−)-**1** (1.1 mg), (+)-**1** (1.2 mg), (−)-**2** (1.8 mg), (+)-**2** (3.4 mg), (−)-**3** (0.8 mg), and (+)-**3** (0.7 mg), respectively]. The HPLC analysis confirmed that the three caged-scaffolds; neocaged-xanthone (**1**), caged-xanthone (**2**) and rearranged caged-xanthone (**3**), were partial racemates. We have proposed that the scaffolds are produced in the plant via a mixture of non-enzymatic and enzymatic processes. The absolute configuration of the caged-scaffolds **1-3** were established by single crystal X-ray diffraction analysis using CuKα radiation. Interestingly, a 1:1 mixture of the new natural products pruniflorone T (**1**) and pruniflorone U (**3**) exhibited potent cytotoxicity against the MCF-7 human breast cancer cell line with an IC_{50} value of 0.11 μg/mL.

Material and Methods

General Experimental Procedures

Optical rotations were measured on a JASCO P-1020 polarimeter. Ultraviolet (UV) absorption spectra were measured on a SPECORD S 100 (Analytikjena) spectrophotometer. Infrared spectra (IR) were recorded on a Perkin-Elmer 783 FTS FT-IR spectrometer. The ^{1}H and ^{13}C NMR spectra were recorded on 300 MHz Bruker FTNMR Ultra Shield and 600 MHz

Bruker AV-600 spectrometers in $CDCl_3$ with TMS as the internal standard. Chemical shifts are reported in δ (ppm) and coupling constants (J) are expressed in Hertz. Electronic circular dichroism (ECD) spectra were recorded on a JASCO J-810 CD spectropolarimeter. Mass spectra were measured on a MAT 95 XL mass spectrometer (Thermo Finnigan). Chiral HPLC was performed on a Chiralpak AD-H column of 4.6 x 250 nm and attached to the Photodiode Array Detector. Quick Column chromatography (QCC) and column chromatography (CC) were carried out on silica gel (Merck) type 100 (0.063-0.20 mm) and silica gel 60 F_{254} (Merck) with a gradient system of acetone-*n*-hexane or as otherwise stated, or silica gel 60 RP-18 (40-63 μm) (Merck) with pure MeOH.

Plant Material

Roots of *C. formosum* ssp. *pruniflorum* were collected in May 2004 from Nong Khai Province, in the northeastern part of Thailand. Identification was made by Prof. Puangpen Sirirugsa, Department of Biology, Faculty of Science, Prince of Songkla University and a specimen (No. 0012677) was deposited at Prince of Songkla University Herbarium.

Extraction and Isolation

Air-dried roots of *C. formosum* ssp. *pruniflorum* (5.30 kg) were extracted with CH_2Cl_2 (2 × 20 L, for 5 days) at room temperature. The crude CH_2Cl_2 extract was evaporated under reduced pressure to afford a brownish crude (60.0 g) extract, which was subjected to QCC on silica gel using *n*-hexane as the first eluent and then increasing polarity with acetone to give six fractions (F1-F6). Fraction F4 was separated by QCC eluting with a gradient of CH_2Cl_2–*n*-hexane (0 – 70% over 120 min) to afford 11 subfractions (F4A-F4K). Subfraction F4B was further purified by QCC with a gradient of EtOAc–*n*-hexane (0 – 40% over 90 min) to give six subfractions (F2B1-F2B6). Subfraction F2B4 was further purified by CC eluting with 30% acetone–*n*-hexane to give nine subfractions (F2B4A-F2B4I). Subfraction F2B4F was further purified by CC eluting with 30% CH_2Cl_2-*n*-hexane to give **1** (4.3 mg), **2** (80.3 mg) and mixture of β-sitosterol and stigmasterol (7.5 mg). Compound **1** was recrystallized in $CHCl_3$–MeOH (9:1, *v/v*) to yield yellow needle single crystals. Subfraction F2B4E was further separated by CC on reversed-phase silica gel C18 eluting with MeOH to give **2** (15.5 mg) and **3** (3.5 mg). Compound **3** was recrystallized in $CHCl_3$–MeOH (9:1, *v/v*) to yield yellow needle single crystals.

*Pruniflorone T (**1**)*. Yellow powder, m.p. 167-169 °C; $[\alpha]^{25}_{D}$ = +14 (*c* 0.1, $CHCl_3$), UV ($CHCl_3$) λ_{max} (log ε) 242 (3.36), 293 (3.34), 329 (3.54), 396 (2.78) nm; IR (neat) ν_{max} 3445, 1747, 1645 cm^{-1}; HREIMS $[M - CO]^+$ *m/z* 382.1774 for $C_{23}H_{26}O_5$ $[M - CO]^+$ (calcd. 382.1780). EIMS *m/z* (rel. int.): (A parent ion at *m/z* 410 was not observed.), 382 (3) $[M - CO]^+$, 313 (10), 279 (20), 256 (23), 178 (18), 167 (33), 149 (75), 127 (28), 113 (40), 111 (26), 99 (40), 97 (34), 85 (77), 83 (84), 71 (100), 69 (57).

Chiral HPLC Separation and ECD Spectroscopic Data of (–)-**1** and (+)-**1**

Separation of the two enantiomers of partial *rac*-**1** (2.3 mg) was performed by semipreparative HPLC on an enantioselective column (Chiral Pack AD-H 5 μm, 4.6 mm × 25 mm, eluent *n*-hexane/*i*PrOH 99:1 v/v, 1 mL/min). Compound (–)-**1** (1st eluted) {(1.1 mg), $[\alpha]^{25}_{D}$ = –61 (*c* 0.4, CH_2Cl_2), m.p. 215-217 °C} and (+)-**1** (2nd eluted) {(1.2 mg), $[\alpha]^{25}_{D}$ = +79 (*c* 0.8, CH_2Cl_2), m.p. 212-214 °C} were obtained. ECD spectra of compounds (–)-**1** (0.20 mg/mL) and (+)-**1** (0.12 mg/mL) were recorded at 25 °C in CH_2Cl_2, with path length of 0.2 cm, bandwidth 2 nm, data pitch 0.5 nm, scan rate 200 nm/min, and response 4 s. UV absorption spectra were recorded at 25 °C in CH_2Cl_2 in the 200-500 nm region.

*Cochinchinone C (**2**)*. Yellow powder, m.p. 158-159 °C; $[\alpha]^{25}_{D}$ = +125 (*c* 0.1, $CHCl_3$), UV ($CHCl_3$) λ_{max} (log ε) 262 (3.28), 310 (4.06), 350 (3.82), 400 (3.35) nm; IR (neat) ν_{max} 3428, 1746, 1644, 1604 cm^{-1}; HREIMS $[M - CO]^+$ *m/z* 382.1785 for $C_{23}H_{26}O_5$ $[M - CO]^+$ (calcd. 382.1780). EIMS *m/z* (rel. int.): (A parent ion at *m/z* 410 was not observed.), 382 $[M - CO]^+$ (48), 313 (100), 285 (32), 271 (9), 243 (16), 227 (5), 203 (5), 137 (8), 69 (7).

Chiral HPLC Separation and ECD Spectroscopic Data of (–)-**2** and (+)-**2**

Separation of the two enantiomers of partial *rac*-**2** (5.2 mg) was performed by semipreparative HPLC on an enantioselective column (Chiral Pack AD-H 5 μm, 4.6 mm × 25 mm, eluent *n*-hexane/*i*PrOH 99.5:0.5 v/v, 1 mL/min). Compound (–)-**2** (1st eluted) {(1.8 mg), $[\alpha]^{25}_{D}$ = –459 (*c* 0.7, CH_2Cl_2), m.p. 163-164 °C } and (+)-**2** (2nd eluted) {(3.4 mg), $[\alpha]^{25}_{D}$ = +509 (*c* 0.7, CH_2Cl_2), m.p. 166-167 °C } were obtained. ECD spectra of compounds (–)-**2** (0.02 mg/mL) and (+)-**2** (0.13 mg/mL) were recorded at 25 °C in CH_2Cl_2, with path length of 0.2 cm, bandwidth 2 nm, data pitch 0.5 nm, scan rate 200 nm/min, and response 4 s. UV absorption spectra were recorded at 25 °C in CH_2Cl_2 in the 200-500 nm region.

*Pruniflorone U (**3**)*. Yellow powder, m.p. 97-99 °C; $[\alpha]^{25}_{D}$ = –24 (*c* 0.1, $CHCl_3$), UV ($CHCl_3$) λ_{max} (log ε) 243 (3.93), 252 (3.91), 312 (4.01), 385 (3.37) nm; IR (neat) ν_{max} 3615, 1748, 1710, 1633 cm^{-1}; HREIMS *m/z* 426.1684 for $C_{24}H_{26}O_7$ (calcd. 426.1679). EIMS *m/z* (rel. int.): 426 $[M]^+$ (2), 382 (7), 313 (13), 270 (100), 242 (19), 227 (42), 213 (9), 200 (8), 137 (8), 69 (7).

Chiral HPLC Separation and ECD Spectroscopic Data of (–)-**3** and (+)-**3**

Separation of the two enantiomers of partial *rac*-**3** (1.5 mg) was performed by semipreparative HPLC on an enantioselective column (Chiral Pack AD-H 5 μm, 4.6 mm × 25 mm, eluent *n*-hexane/*i*PrOH 99:1 v/v, 1 mL/min). Compound (–)-**3** (1st eluted) {(0.8 mg), $[\alpha]^{25}_{D}$ = –161 (*c* 0.2, CH_2Cl_2), m.p. 150-152 °C } and (+)-**3** (2nd eluted) {(0.7 mg), $[\alpha]^{25}_{D}$ = +172 (*c* 0.5, CH_2Cl_2), m.p. 147-148 °C } were obtained. ECD spectra of compounds (–)-**3** (0.02 mg/mL) and (+)-**3** (0.14 mg/mL) were recorded at 25 °C in CH_2Cl_2, with path length of 0.2 cm, bandwidth 2 nm, data pitch 0.5 nm, scan rate 200 nm/min, and response 4 s. UV absorption spectra were recorded at 25 °C in CH_2Cl_2 in the 200-500 nm region.

*X-ray crystallographic studies of **1** and **3***

Crystallographic data were collected at 100.0 (1) K with the Oxford Cryosystem Cobra low-temperature attachment. The data were collected using a CCD diffractometer with a graphite monochromated Mo Ka radiation at a detector distance of 5 cm using *APEX2* (Bruker, 2005). The collected data were reduced using *SAINT* program (Sheldrick, 1998), and the empirical absorption corrections were performed using *SADABS* program (Bruker, 2005). The structures were solved by direct methods and refined by least-squares using the *SHELXTL* software package (Sheldrick, 1998). All non-hydrogen atoms were refined anisotropically, whereas all H atoms were placed in calculated positions with an O–H distance of 0.82 Å and C–H distances in the range 0.93–0.98 Å after checking their positions in the difference map. The U_{iso} values were constrained to be $1.5U_{eq}$ of the carrier atoms for methyl H atoms and $1.2U_{eq}$ for hydroxyl and the other H atoms. The final refinement converged well. Materials for publication were prepared using *SHELXTL*[2] and *PLATON* (Spek, 2003).

Crystal data for **1**: $C_{24}H_{26}O_6$, *M*=410.45, 0.55×0.30×0.16 mm^3, triclinic, *P*-1, *a*=8.2330(3) Å, *b*=8.4002(3) Å, *c*=14.8363(5) Å, α=100.909(2)°, β=99.445(2)° γ=92.198(2)°,

V=991.31(6) Å^3, Z=2, D_x =1.375 Mg.m^{-3}, μ(MoKα)=0.098 mm^{-1}, 28505 reflection measured, 7135 unique reflections, R=0.0461, R_w=0.1228.

Crystal data for **3**: $C_{24}H_{26}O_7$, M=426.45, 0.60×0.35×0.12 mm^3, triclnic, P-1, a=7.7224(6) Å, b=9.9926(8) Å, c=14.1397(12) Å, α=103.086(4)°, β=92.580(4)° γ=100.991(4)°, V=1038.84(15) Å^3, Z=2, D_x =1.363 Mg m^{-3}, μ(MoKα)=0.100 mm^{-1}, 11097 reflection measured, 3600 unique reflections, R=0.0485, R_w=0.1155.

*Determination of Absolute Configurations of compounds (–)-**1**, (–)-**2** and (–)-**3** by X-ray Structure analysis*

The data were collected using a CCD diffractometer with cross-coupled multilayer optics CuKα radiation at a detector distance of 49.80 mm. Data were collected and integrated using the Bruker SAINT (Bruker, 2010) software package. Data were corrected for absorption effects using the multi-scan technique (SADABS) (Sheldrick, 2008). The data were corrected for Lorentz and polarization effects. The structure was solved by direct methods (Altomare *et al*., 1999). The material crystallizes with two crystallographically independent molecules in the asymmetric unit. All non-hydrogen atoms were refined anisotropically. All OH hydrogen atoms were located in difference maps and refined isotropically. All other hydrogen atoms were placed in calculated positions. The absolute configuration was established on the basis of the refined Flack x-parameter (Parsons & Flack 2004).

$$R1 = \Sigma \, ||Fo| - |Fc|| \, / \, \Sigma \, |Fo| = 0.031$$

$$wR2 = [\Sigma \, (\, w(Fo^2 - Fc^2)^2 \,) / \, \Sigma \, w(Fo^2)^2]^{1/2} = 0.077$$

Neutral atom scattering factors were taken from Cromer and Waber (Cromer & Waber 1974). Anomalous dispersion effects were included in Fcalc (Ibers & Hamilton 1964), the values for Δf' and Δf'' were those of Creagh and McAuley (Creagh & McAuley 1992). The values for the mass attenuation coefficients are those of Creagh and Hubbell (Creagh & Hubbell 1992). All refinements were performed using the SHELXL-97 (Bruker, 2008) via the WinGX (Farrugia, 1999) interface.

Crystal data for (–)-**1**: $C_{24}H_{26}O_6$, M = 410.45; monoclinic system, space group $P2_1$, a =8.4151(3) Å, b = 8.0906(3) Å, c = 15.1668(5) Å, $\alpha = \gamma = 90°$, β = 98.855(2)°, V = 1020.30(6)

Å^3, Z = 2, d = 1.336 g/cm^3. A crystal of dimensions was 0.03 × 0.13 × 0.14 mm^3. μ(Cu-Kα) = 0.0784 mm^{-1}. The data were collected at a temperature of -100.0 ± 0.1°C to a maximum 2θ value of 131.72°. Data were collected in a series of ϕ and ω scans in 1° oscillations using both 10.0 and 30.0-second exposures. Of the 26945 reflections that were collected, 7264 were unique (R_{int} = 0.028); equivalent reflections (excluding Friedel pairs) were merged. The absolute configuration was established on the basis of the refined Flack x-parameter (Parsons & Flack 2004),-0.09(8). The final assignments for the chiral centers are as follows: C5A=R, C6=R and C7=R, C16A=R. The structure was solved by direct methods and refined by a full-matrix least squares on F^2. Final R indices [$I>2\sigma(I)$]: R_1= 0.031, wR_2 = 0.081. The standard deviation of an observation of unit weight was 1.04. The weighting scheme was based on counting statistics. The maximum and minimum peaks on the final difference Fourier map corresponded to 0.14 and –0.15 e$^-$/Å^3, respectively.

Crystal data for (–)-**2**: $C_{24}H_{26}O_6$, M = 410.45; orthorhombic system, space group $P2_12_12_1$, a = 7.2698(8) Å, b = 11.4350(1) Å, c = 24.6320(3) Å, $\alpha = \beta = \gamma$ = 90°, V = 2047.7(4) Å^3, Z = 4, d = 1.331 g/cm^3. A crystal of dimensions was 0.13 × 0.23 × 0.31 mm^3. μ(Cu-Kα) = 7.81 cm^{-1}. The data were collected at a temperature of -183.0 ± 0.1°C to a maximum 2θ value of 131.14°. Data were collected in a series of ϕ and ω scans in 1° oscillations using both 2.0 and 5.0-second exposures. Of the 21717 reflections that were collected, 3494 were unique (R_{int} = 0.033); equivalent reflections (excluding Friedel pairs) were merged. The absolute configuration was established on the basis of the refined Flack x-parameter (Parsons & Flack 2004),-0.04(4). The final assignments for the chiral centers are as follows: C5=R, C5A=S, C7=R and C11=R. The structure was solved by direct methods and refined by a full-matrix least squares on F^2. Final R indices [$I>2\sigma(I)$]: R_1= 0.026, wR_2 = 0.064. The standard deviation of an observation of unit weight was 1.07. The weighting scheme was based on counting statistics. The maximum and minimum peaks on the final difference Fourier map corresponded to 0.19 and –0.28 e$^-$/Å^3, respectively.

Crystal data for (–)-**3**: $C_{24}H_{26}O_7$, M = 426.45; monoclinic system, space group $P2_1$, a =13.4658(12) Å, b = 7.9997(7) Å, c = 20.8660(2) Å, $\alpha = \gamma$ = 90°, β = 106.550(5)°, V = 2154.6(3) Å^3, Z = 4, d = 1.315 g/cm^3. A crystal of dimensions was 0.10 × 0.29 × 0.34 mm^3. μ(Cu-Kα) = 7.99 cm^{-1}. The data were collected at a temperature of -100.0 ± 0.1°C to a

maximum 2θ value of 131.72°. Data were collected in a series of ϕ and ω scans in 1° oscillations using both 3.0 and 10.0-second exposures. Of the 26945 reflections that were collected, 7264 were unique (R_{int} = 0.028); equivalent reflections (excluding Friedel pairs) were merged. The absolute configuration was established on the basis of the refined Flack x-parameter (Parsons & Flack 2004),-0.02(5). The final assignments for the chiral centers are as follows: C5=S, C5A=R C11=S. The structure was solved by direct methods and refined by a full-matrix least squares on F^2. Final R indices [$I>2\sigma(I)$]: R_1= 0.031, wR_2 = 0.077. The standard deviation of an observation of unit weight was 1.07. The weighting scheme was based on counting statistics. The maximum and minimum peaks on the final difference Fourier map corresponded to 0.14 and –0.15 $e^-/Å^3$, respectively.

The crystallographic-information files for **1** (CCDC727003), **3** (CCDC774999), (–)-**1** (CCDC969759), (–)-**2** (CCDC969760), and (–)-**3** (CCDC969761) have been deposited in the Cambridge Crystallographic Data Centre. These data can be obtained free of charge via http://www.ccdc.cam.ac.uk/data_request/cif, or by e-mailing data_request@ccdc.cam.ac.uk, or by contacting the Cambridge Crystallographic Data Centre, 12, Union Road, Cambridge CB2 1EZ, UK; fax: +44 1223 336033.

Cytotoxicity Assay

The cancer cell line MCF-7 (human breast adenocarcinoma) was grown in Dulbecco's modified eagle medium: nutrient mixture F12 (D-MEM/F12) supplemented with 10% fetal bovine serum (FBS). Cells were seeded in 96 wells (3000 cell/well) and allowed to adhere for 24 h at 37°C with 5% CO_2 in a fully humidified incubator. Then 100 mL of 25 mg/mL crude extract or fivefold diluted pure compound in medium (final concentration 0.008, 0.04, 0.2, 1, and 5 mg/mL) were dispensed into wells of the cell plates and incubated further for 72 h. After removal of the sample medium, the cells were topped up with 200 mL D-MEM/F12 medium and incubated. After 72 h, cells were fixed with cold 40% trichloroacetic acid and kept at 4°C for 1 h and washed with tap water. The viable cells were conducted by using sulphorhodamine B (SRB) following the method of Skehan and coworker (Skehan *et al*., 1990). The absorbance was measured at 492 nm using a microplate reader. The results were based on the ability of the extracts to inhibit cell growth compared to control (cells in media without extract) and calculated for IC_{50} using probit analysis. Camptothecin, which was used as a standard, showed cytotoxic activity at <0.024 mg/mL (Salae *et al*., 2010).

References

Altomare, A.; Burla, M. C.; Camalli, M.; Cascarano, G. L.; Giacovazzo, C.; Guagliardi, A.; Moliterni, A. G. G.; Polidori, G.; Spagna, R. SIR97. *J. Appl. Cryst*. **1999**, *32*, 115–119.

Asano, J.; Chiba, K.; Tada, M.; Yoshii, T. *Phytochemistry* **1996**, *41,* 815–820.

Bruker. APEX2, SAINT and SADABS; Bruker AXS Inc.: Madison, WI, **2005**.

Bruker. SAINT Version 7.68A. Bruker AXS Inc; Madison, Wisconsin, USA, **1997–2010**.

Bruker. SHELXTL Version 2008/4. Bruker AXS Inc.: Madison, Wisconsin, USA, **2008**.

Cao, S.-G.; Sng, V. H. L.; Wu, X.-H.; Sim, K.-Y.; Tan, B. H. K.; Pereira, J. T.; Goh, S. H. *Tetrahedron* **1998**, *54,* 10915–10924.

Chantrapromma, S.; Boonnak, N.; Fun, H.-K. *Acta Cryst.* **2005**, *E61*, o3505–o3507.

Creagh, D. C.; McAuley, W. J. "*International Tables for Crystallography*", *Vol C*, A.J.C. Wilson, ed., Kluwer Academic Publishers, Boston, Table 4.2.6.8, pages 219–222, **1992**.

Creagh, D. C.; Hubbell, J. H. "*International Tables for Crystallography*", *Vol C*, A.J.C. Wilson, ed., Kluwer Academic Publishers, Boston, Table 4.2.4.3, pages 200–206, **1992**.

Cromer, D. T.; Waber, J. T. "*International Tables for X-ray Crystallography*", *Vol. IV*, The Kynoch Press, Birmingham, England, Table 2.2 A, **1974**.

Farrugia, L. J. WinGX–V1.80.05. *J. Appl. Cryst*. **1999**, *32*, 837.

Glusker, J. P.; Lewis, M.; Rossi, M. *Crystal Structure Analysis for Chemistry and Biologists*; John Wiley & Sons: New Jersey, **1994**.

Han, Q.-B.; Wang, Y.-L.; Yang, L.; Tso, T.-F.; Qiao, C.-F.; Song, J.-Z.; Xu, L.-J.; Chen, S.-L.; Yang, D.-J.; Xu, H.-X. *Chem. Pharm. Bull.* **2006**, *54,* 265–267.

Hayden, A. E.; Xu, H.; Nicolaou, K. C.; Houk, K. N. *Org. Lett*., **2006**, *8*, 2989–2992.

Ibers, J. A.; Hamilton, W. C. *Acta Cryst*. **1964**, *17*, 781.

Kuemmerle, J.; Jiang, S.; Tseng, B.; Kasibhatla, S.; Drewe, J.; Cai, S.-X. *Bioorg. Med. Chem.* **2008**, *16,* 4233–4241.

Li, N. G.; You, Q. D.; Huang, X. F.; Wang, J. X.; Guo, Q. L.; Chen, X. G.; Li, Y.; Li, H. Y. *Chin. Chem. Lett.* **2007***, 18,* 659–662.

Liu, W.; Guo, Q.-L.; You. Q.-D.; Zhao, L.; Gu, H.-Y.; Yuan, S.-T. *World J. Gastroenterol*. **2005**, *11*, 3655–3659.

Mahabusarakam, W.; Nuangnaowarat, W.; Taylor, W. C. *Phytochemistry* **2006**, *67,* 470–474.

Parsons, S.; Flack, H. D. *Acta Cryst*. **2004**, *A60*, s61.

Reutrakul, V.; Anantachoke, N.; Pohmakotr, M.; Jaipetch, T.; Sophasan, S.; Yoosook, C.; Kasisit, J.; Napaswat, C.; Santisuk, T.; Tuchinda, P. *Planta Med.* **2007**, *73,* 33–40.

Rukachaisirikul, V.; Painuphong, P.; Sukpondma, Y.; Koysomboon, S.; Sawangchote, P.; Taylor, W. C. *J. Nat. Prod.* **2003**, *66,* 933–938.

Salae, A. W.; Karalai, C.; Ponglimanont, C.; Kanjana-Opas, A.; Yuenyongsawad, S. *Can. J. Chem*. **2010**, *88*, 922–927.

Shadid, K. A.; Shaari, K.; Abas, K. F.; Israf, D. A.; Hamzah, A. S.; Syakroni, N.; Saha, K.; Lajis, N. H. *Phytochemistry* **2007**, *68,* 2537–2544.

Sheldrick, G. M. SADABS, *Acta Cryst*. **2008**, *A64*, 112−122.

Sheldrick, G. M. SHELXTL Version 5.1. Bruker AXS; USA: Madison, WI, **1998**.

Skehan, P.; Storeng, R.; Scudiero, D.; Monks, A.; McMahon, J.;Vistica, D.; Warren, J. T.; Bokesch, H.; Kenney, S.; Boyd, M. R. *J. Natl. Cancer Inst*. **1990**, *82*, 1107–1112.

Spek, A. L. *J. Appl. Crystallogr*. **2003**, *36*, 7–13.

Sukpondma, Y.; Rukachaisirikul, V.; Phongpaichit, S. *Chem. Pharm. Bull.* **2005**, *53,* 850–852.

Thoison, O.; Fahy, J.; Dumontet, V.; Chironi, A.; Riche, C.; Tri, M. V. Sevenet, T. *J. Nat. Prod.* **2000**, *63,* 441–446.

Wang, J.; Zhao, L.; Hu, Y.; Guo, Q.; Zhang, L.; Wang, X.; Li, N.; You, Q. *Eur. J. Med. Chem.* **2009**, *44,* 2611–2620.

Wu, Z.-Q.; Guo, Q.-L.; You, Q.-D.; Zhao, L.; Gu,. H.-Y. *Biol. Pharm. Bull.* **2004**, *27,* 1769–1764.

Yang, Y.; Yang, L.; You, Q.-D.; Nie, F.-F.; Gu, H.-Y.; Zhao, L.; Wang, X.-T.; Guo, Q.-L. *Cancer Lett*. **2007**, *256*, 259–266.

Yu, J.; Guo, Q.-L.; You, Q.-D.; Lin, S.-S.; Li, S.; Gu, H.-Y.; Zhang, H.-W.; Tan, Z.; Wang, X. *Cancer Chemother Pharmacol*. **2006**, *58,* 434–443.

Zhang, H.-Z.; Kasibhatla, S.; Wang, Y.; Herich, J.; Guastella, J.; Tseng, B.; Drewe, J.; Cai, S.-X. *Bioorg. Med. Chem.* **2004**, *12,* 309–317.

Appendix

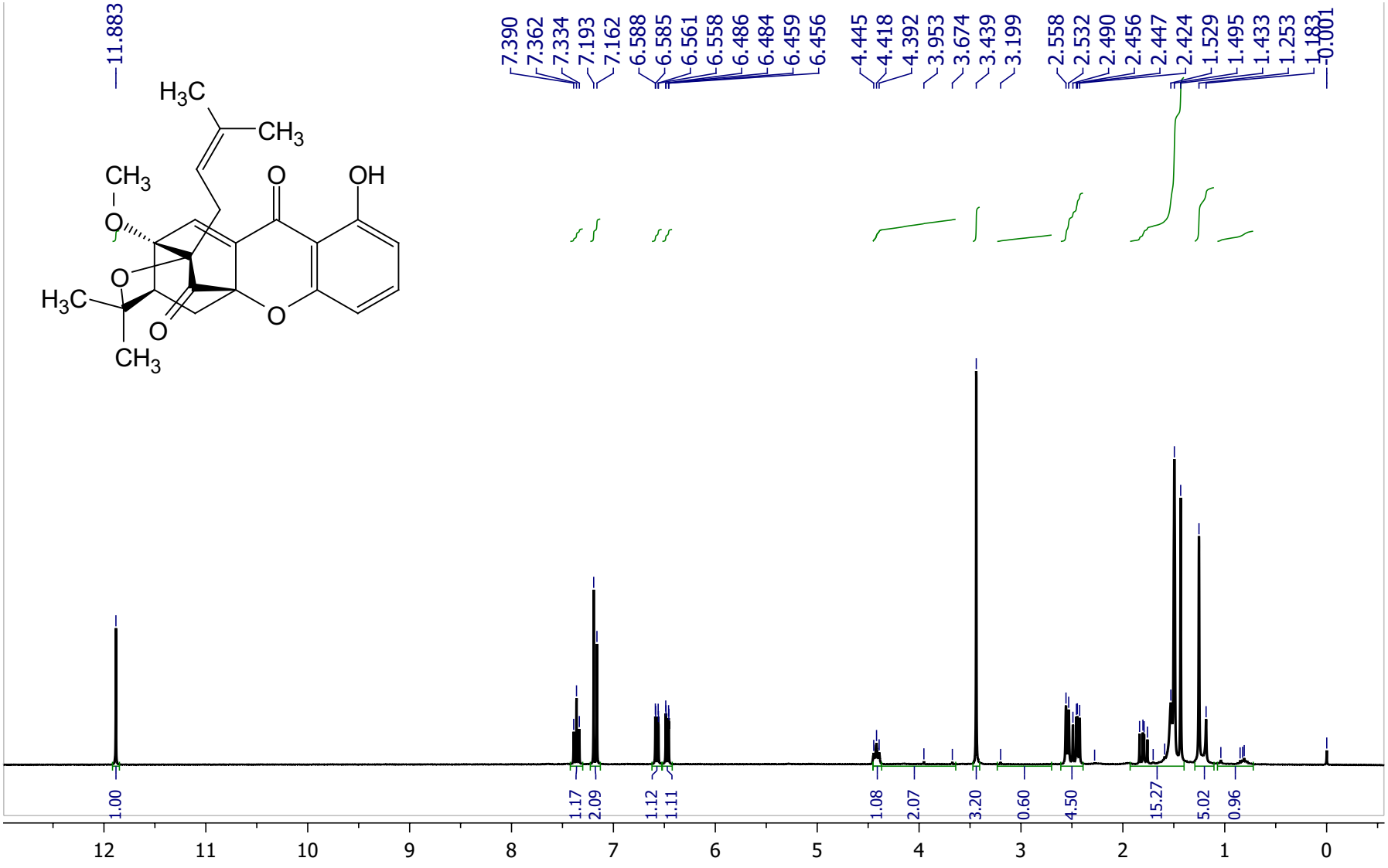

Figure A1. ^{1}H NMR (300 MHz, $CDCl_3$) spectrum of **1**

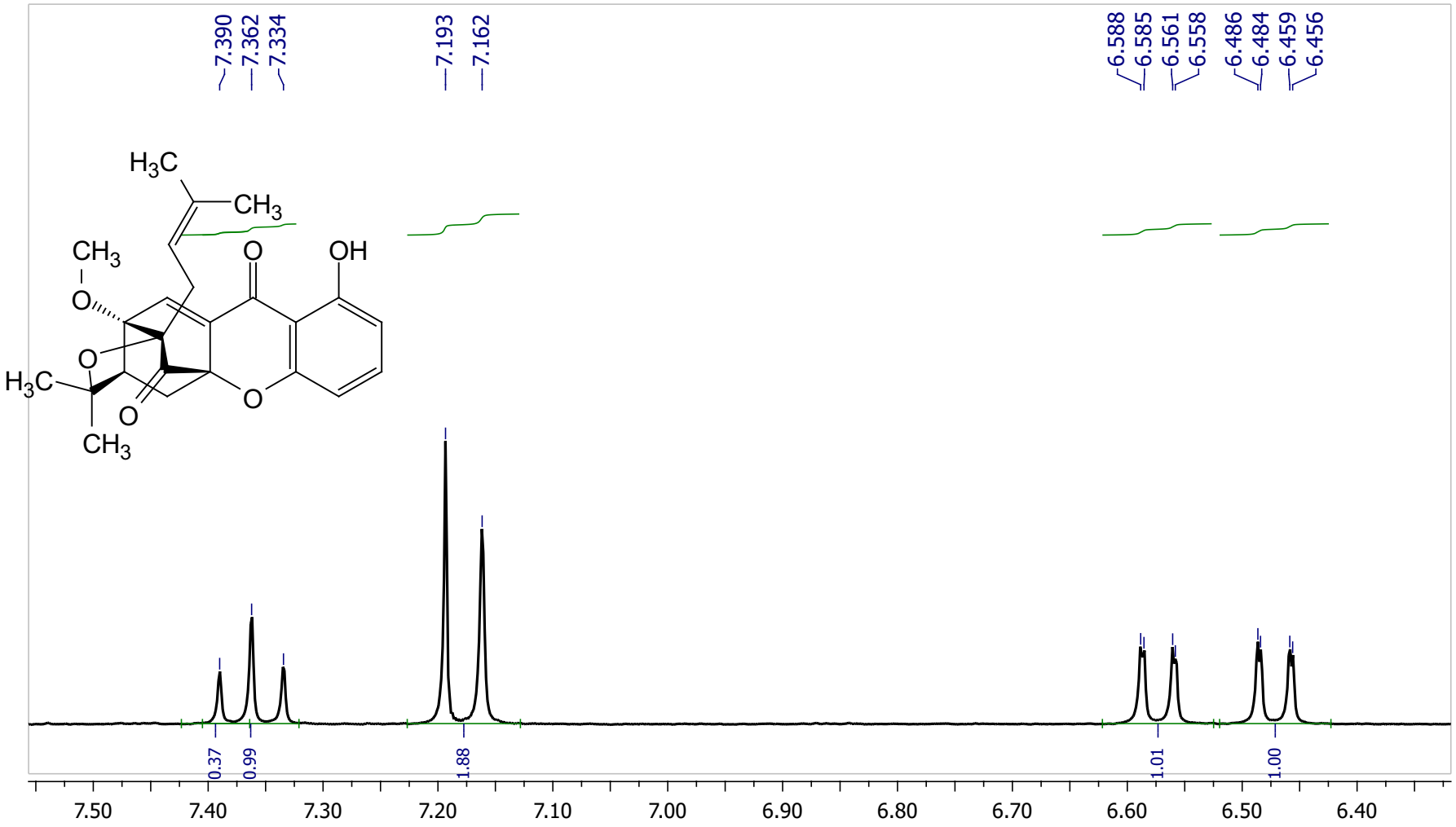

Figure A2. ^{1}H NMR (300 MHz, $CDCl_3$) spectrum of **1** (expansion)

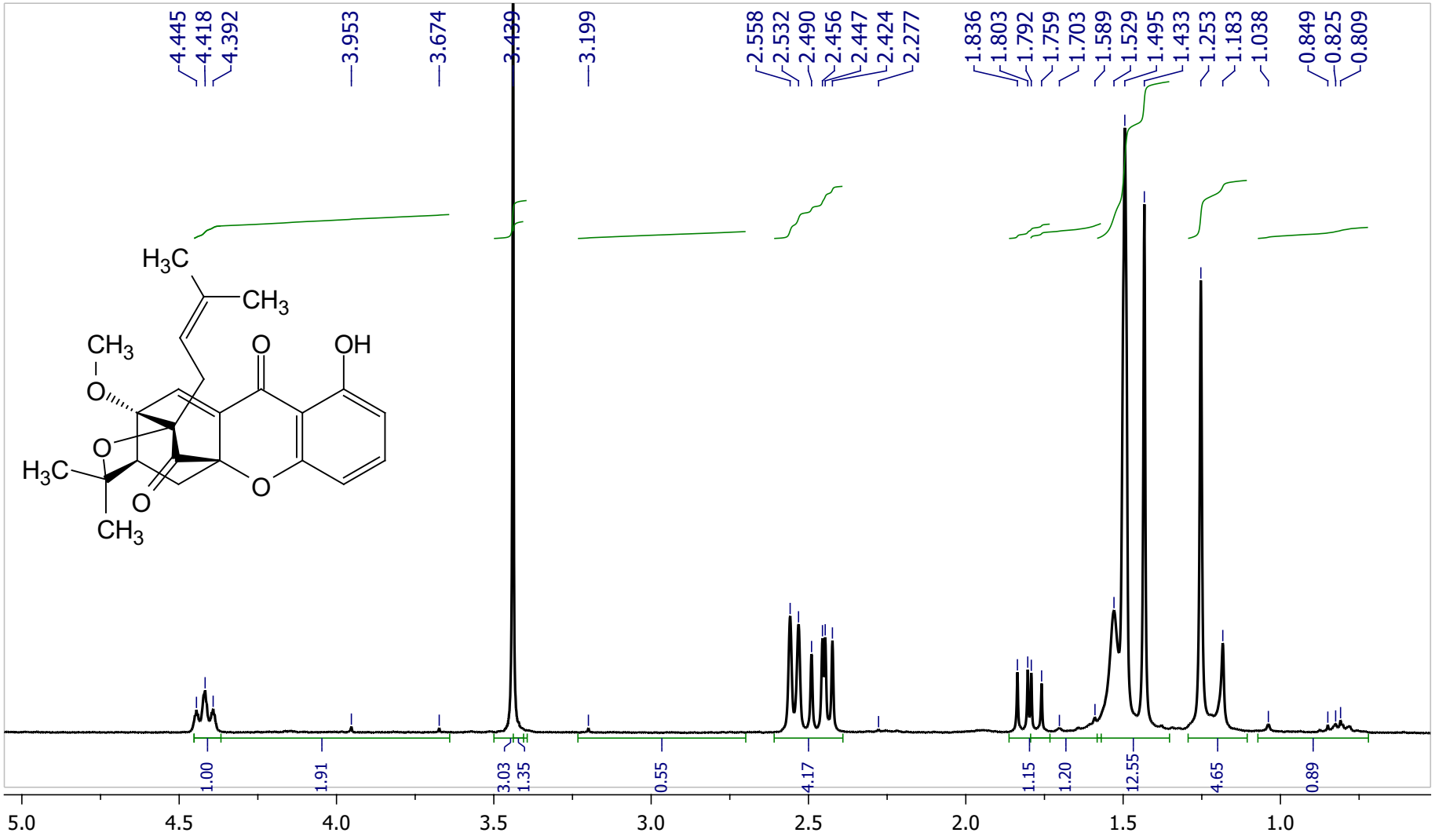

Figure A3. ^{1}H NMR (300 MHz, $CDCl_3$) spectrum of **1** (expansion)

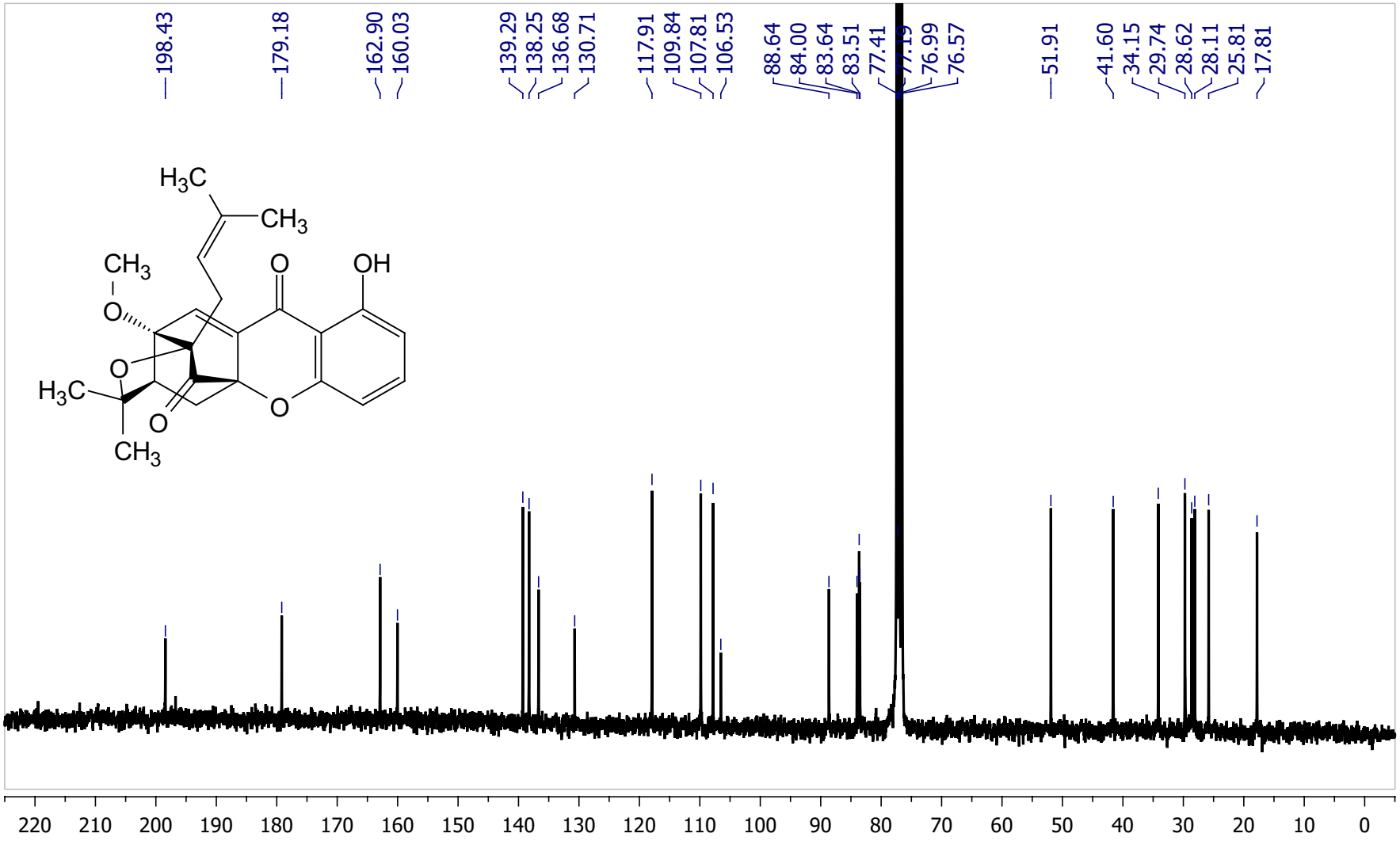

Figure A4. ^{13}C NMR (75 MHz, $CDCl_3$) spectrum of **1**

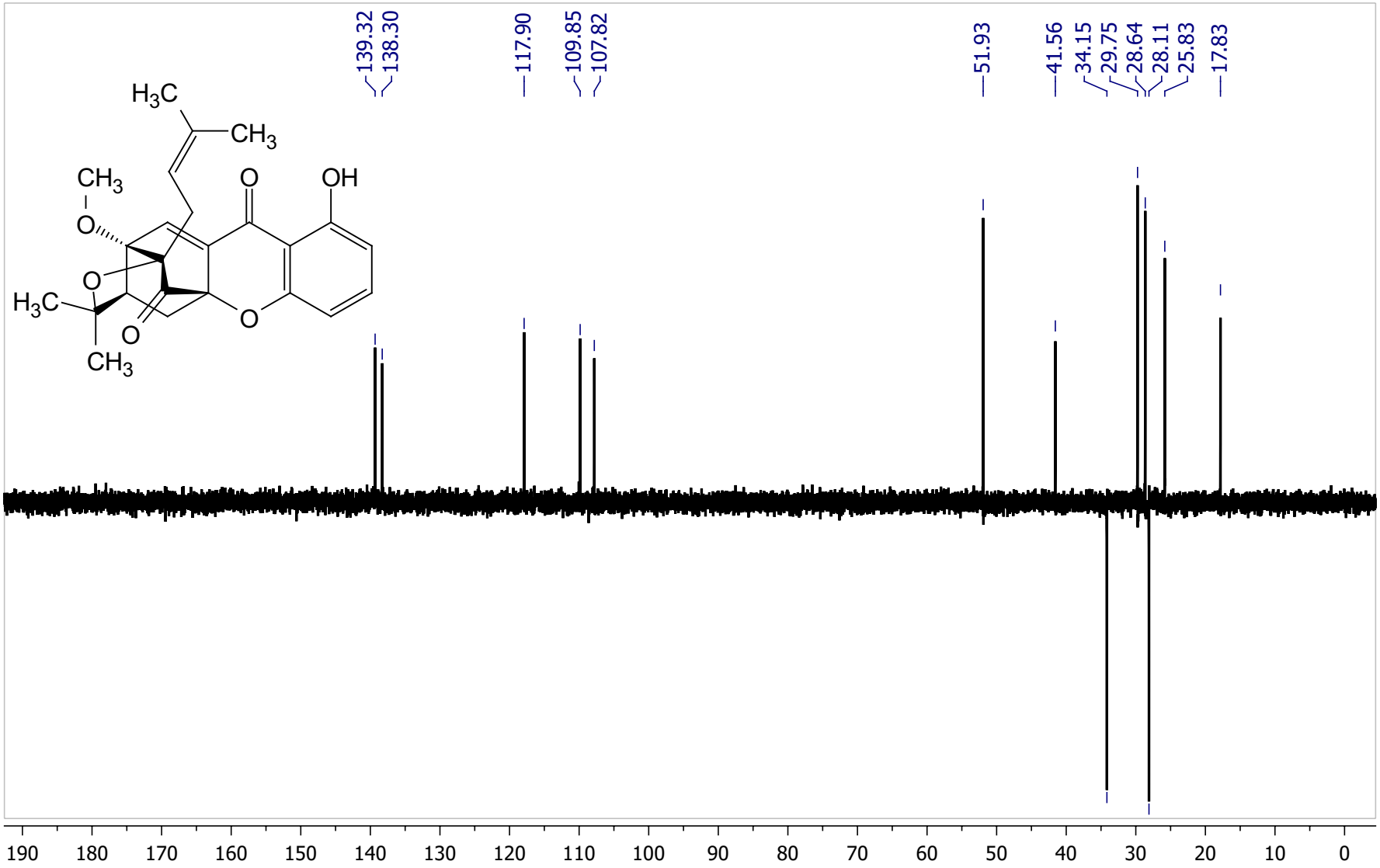

Figure A5. Dept 135 (75 MHz, $CDCl_3$) spectrum of **1**

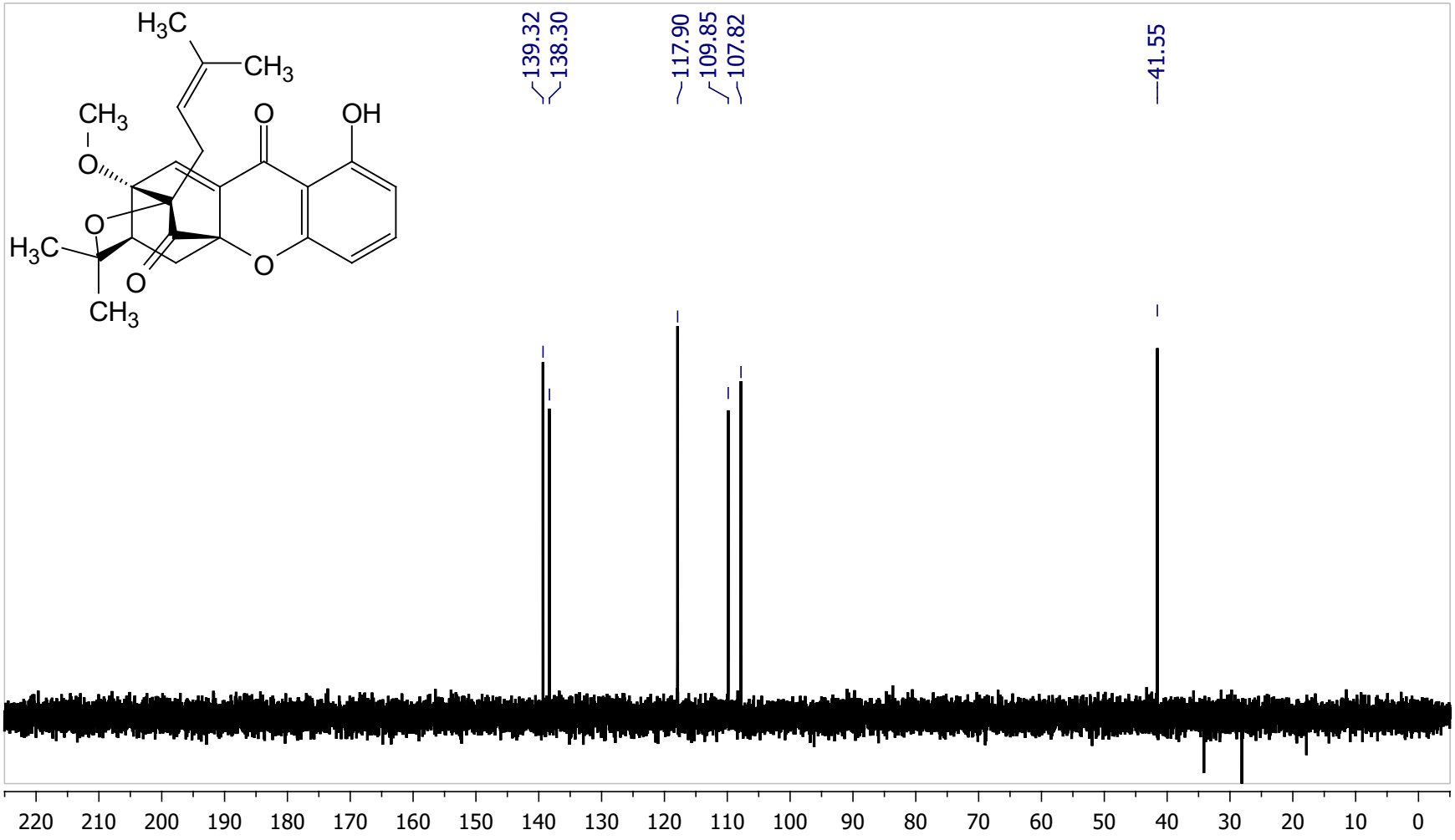

Figure A6. Dept 90 (75 MHz, $CDCl_3$) spectrum of **1**

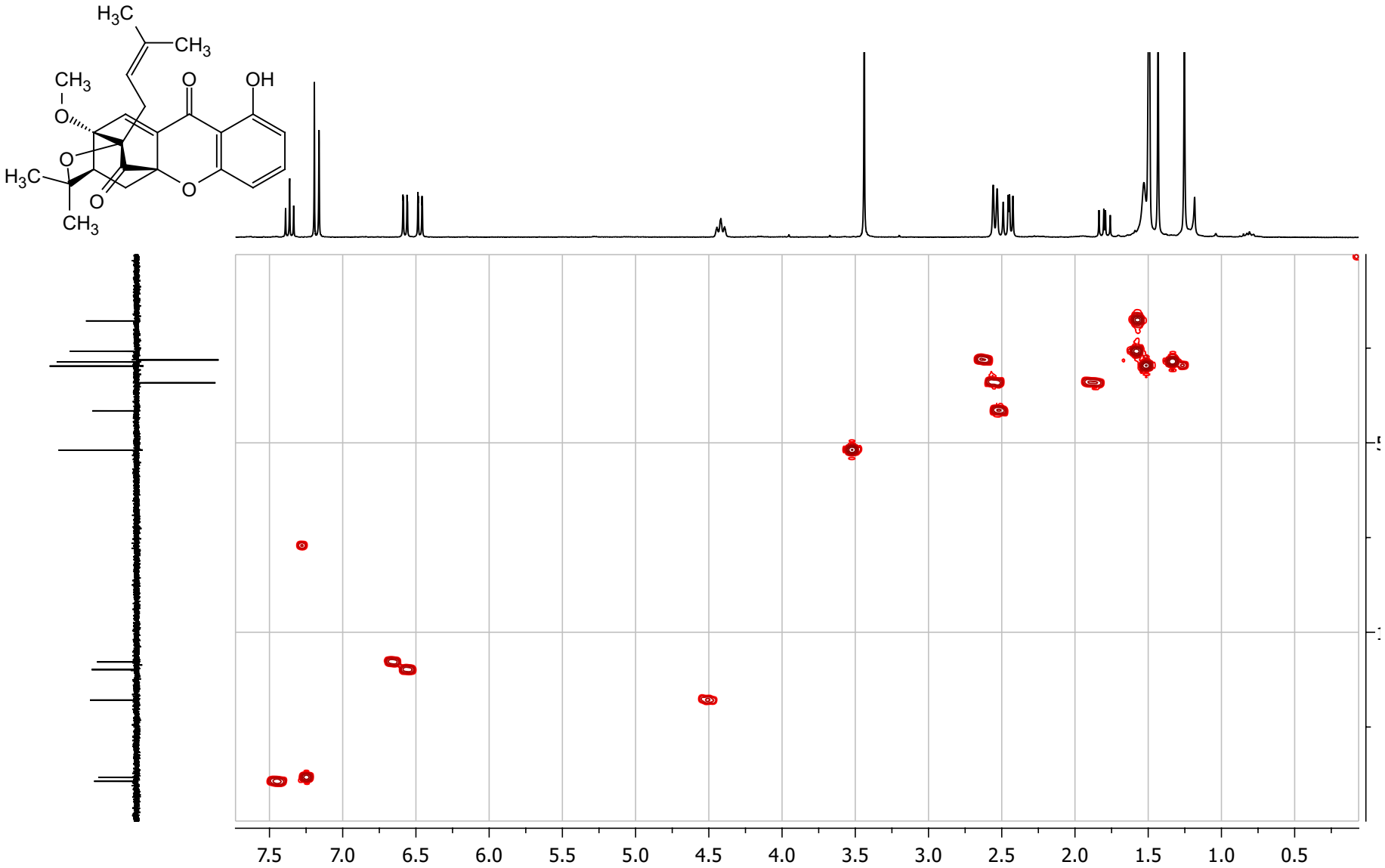

Figure A7. HMQC (300MHz, $CDCl_3$) spectrum of **1**

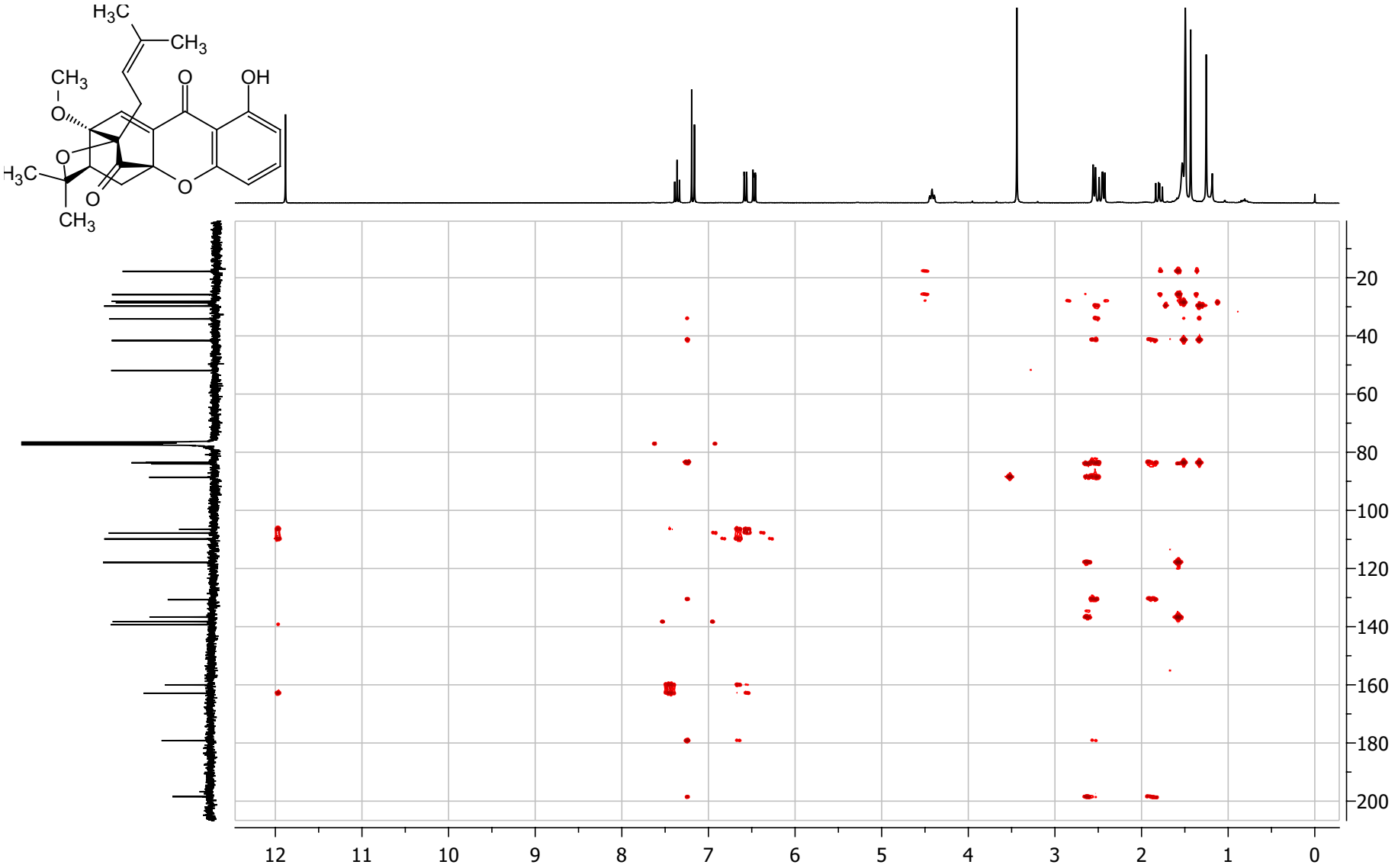

Figure A8. HMBC (300MHz, $CDCl_3$) spectrum of **1**

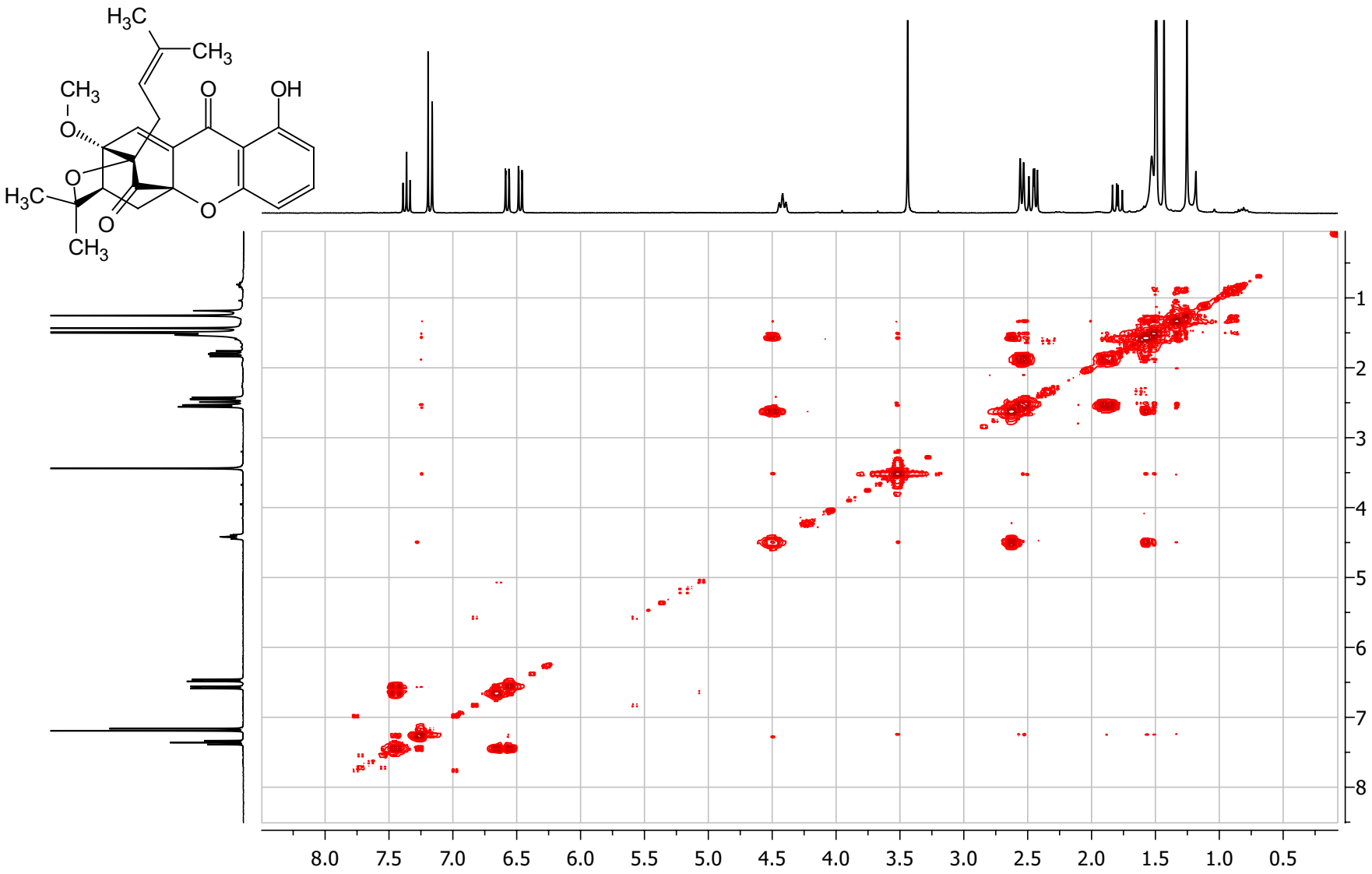

Figure A9. COSY (300MHz, $CDCl_3$) spectrum of **1**

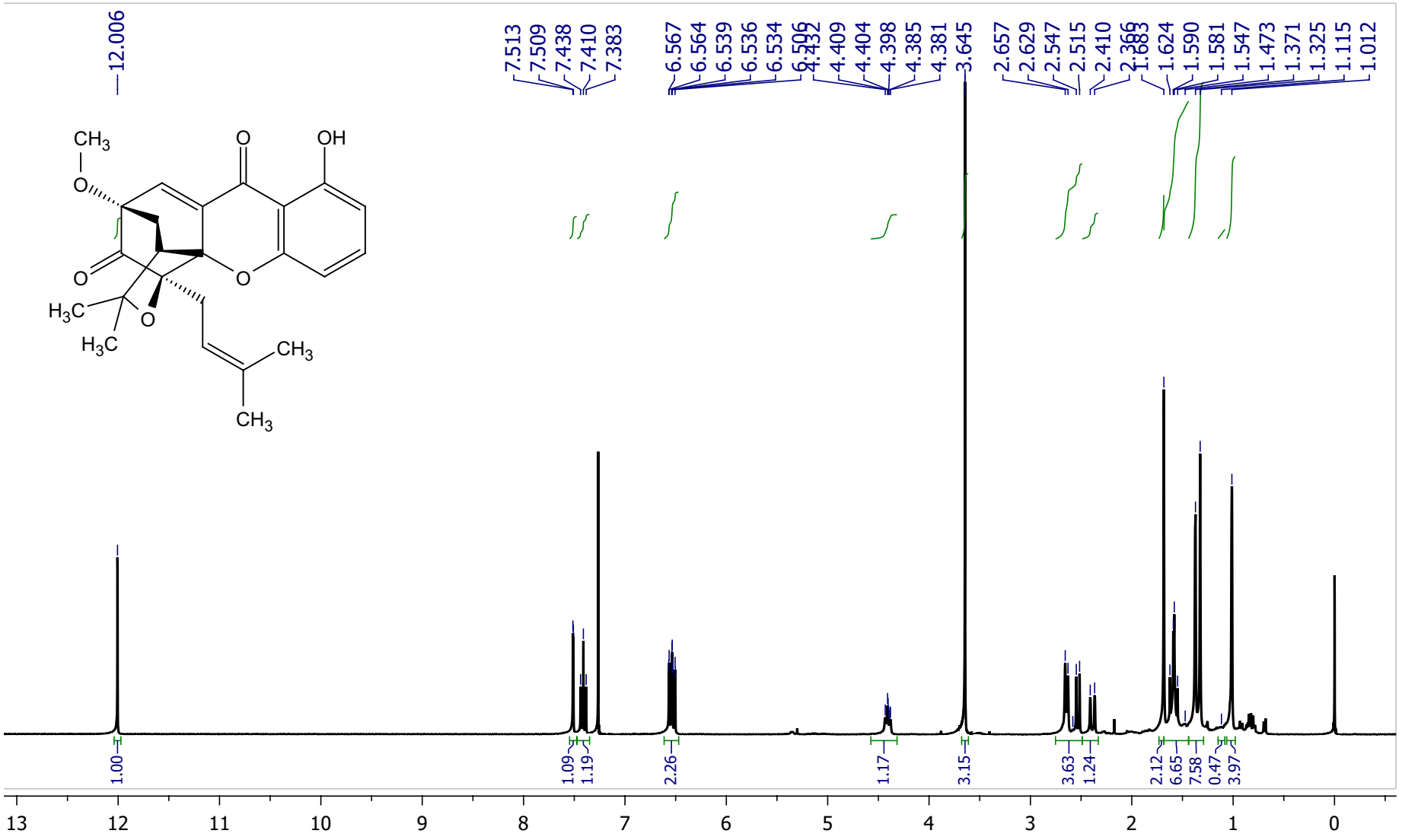

Figure A10. ^{1}H NMR (300 MHz, $CDCl_3$) spectrum of **2**

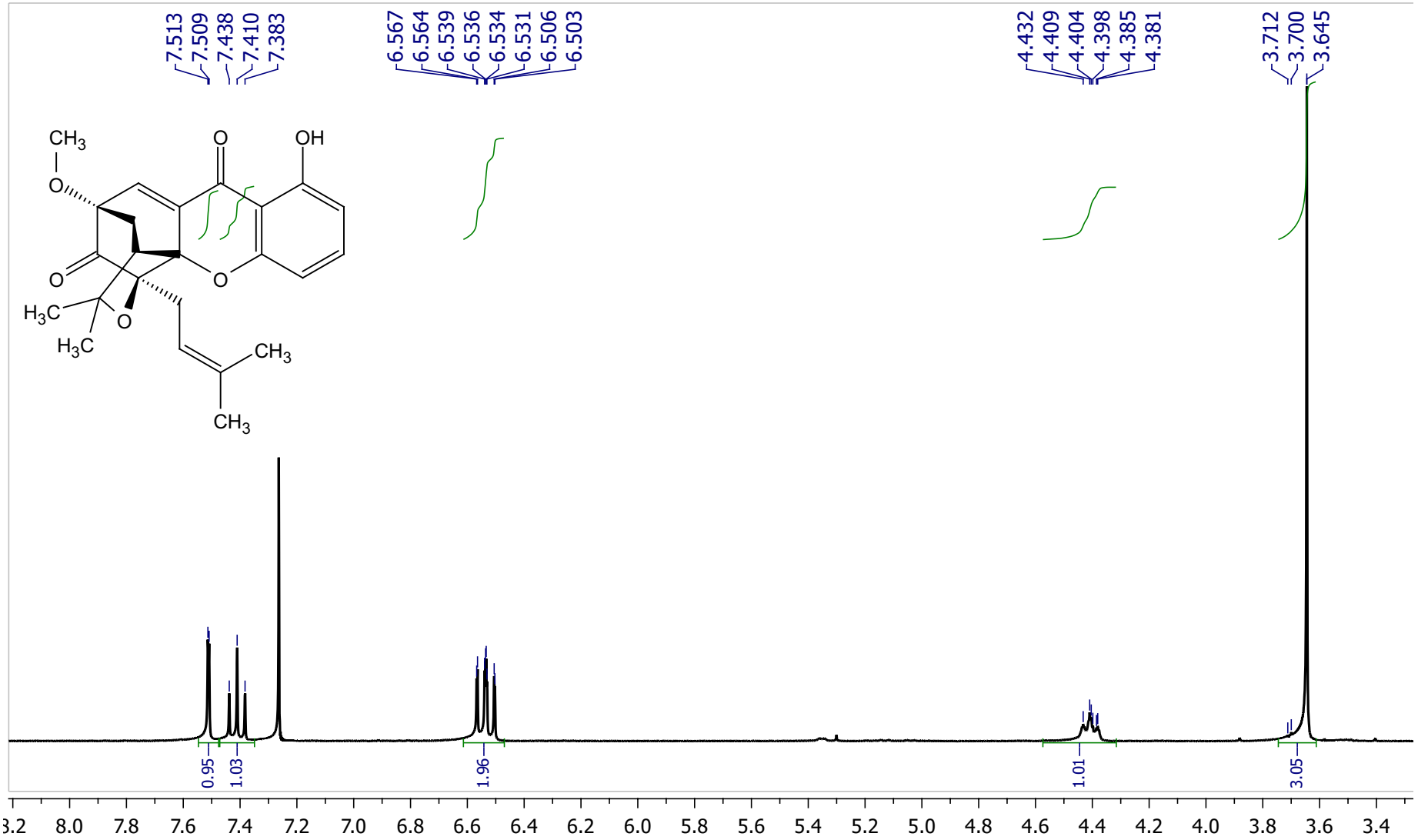

Figure A11. ^{1}H NMR (300 MHz, $CDCl_3$) spectrum of **2** (expansion)

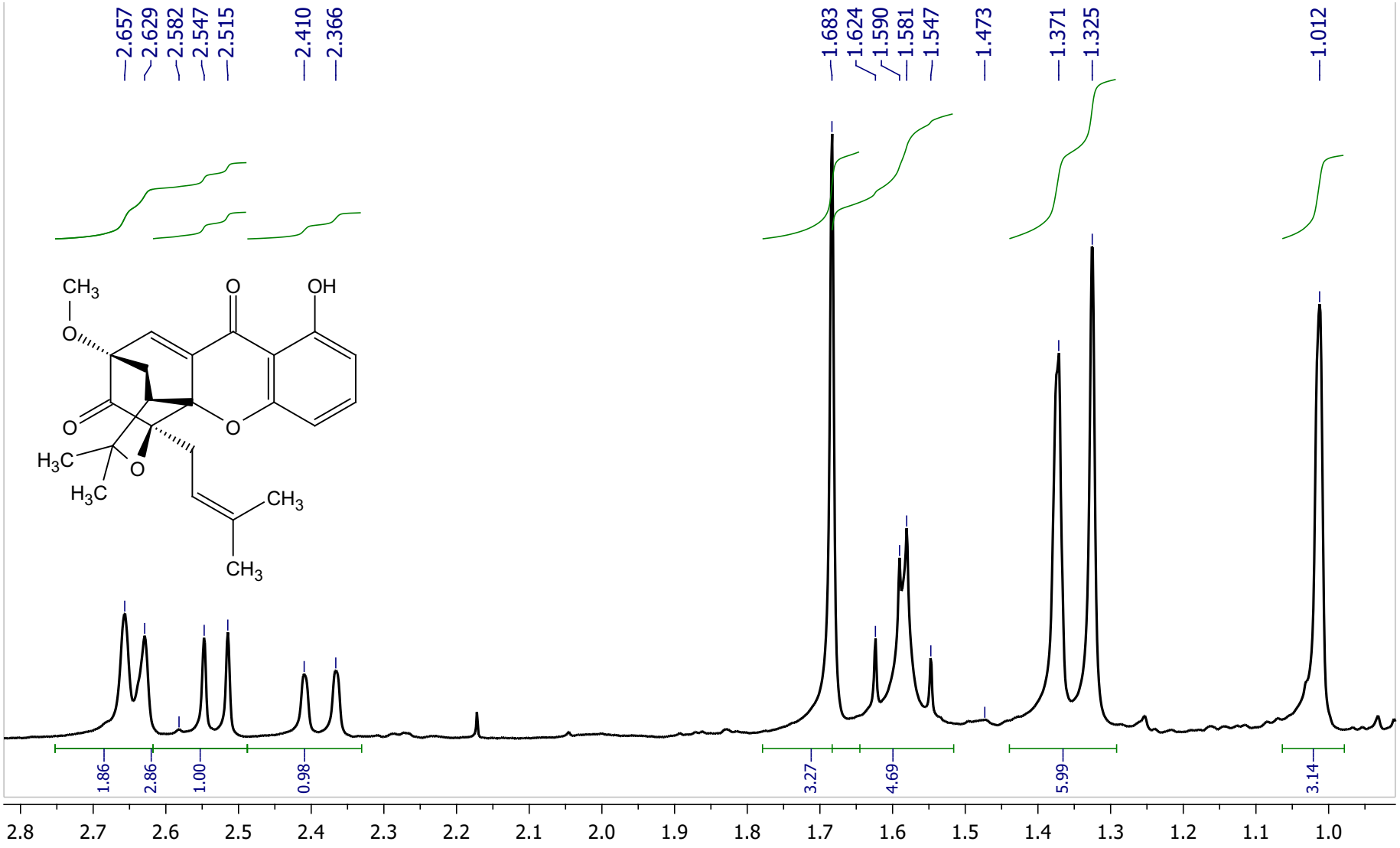

Figure A12. ^{1}H NMR (300 MHz, $CDCl_3$) spectrum of **2** (expansion)

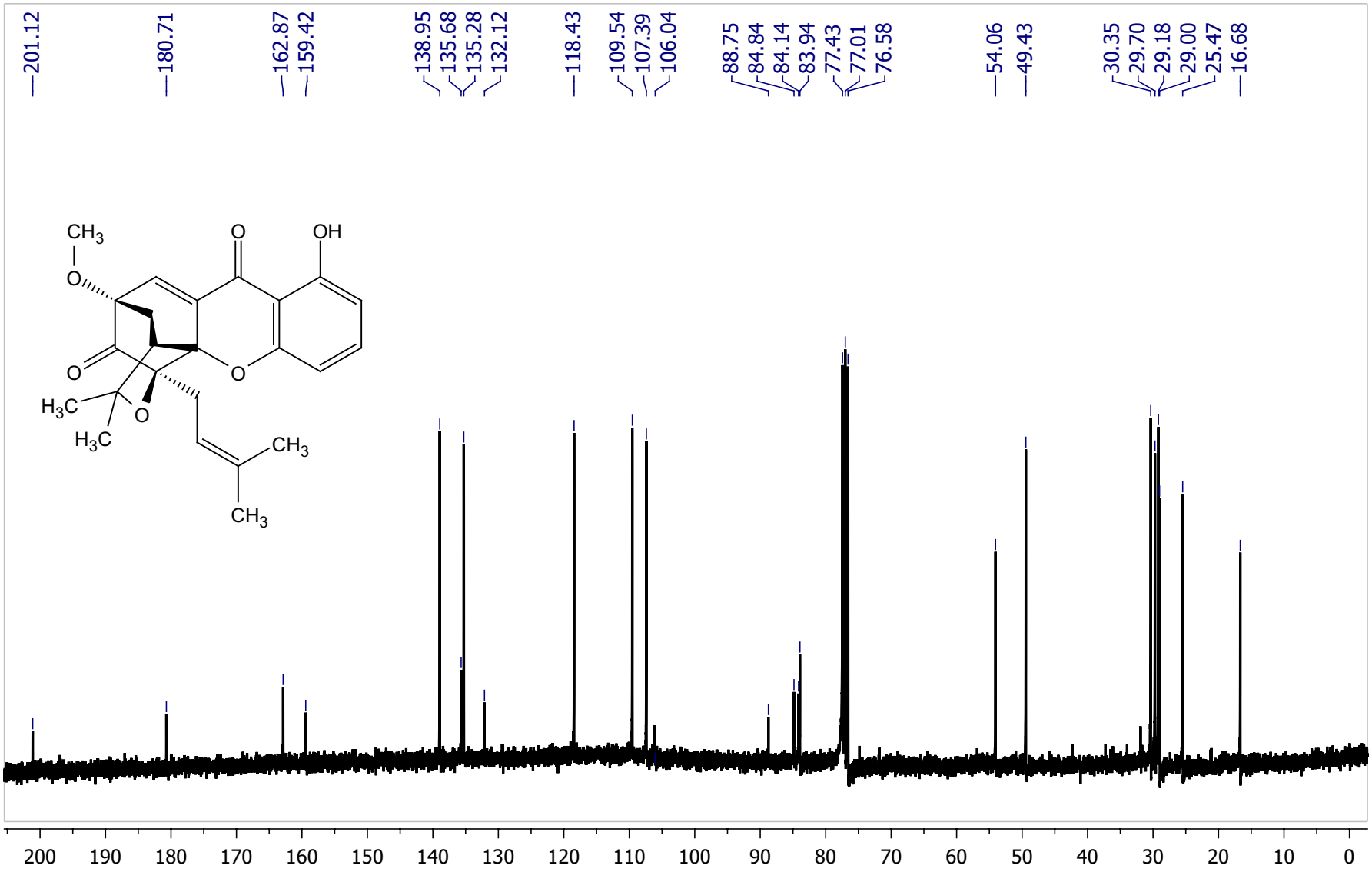

Figure A13. ^{13}C NMR (75 MHz, $CDCl_3$) spectrum of **2**

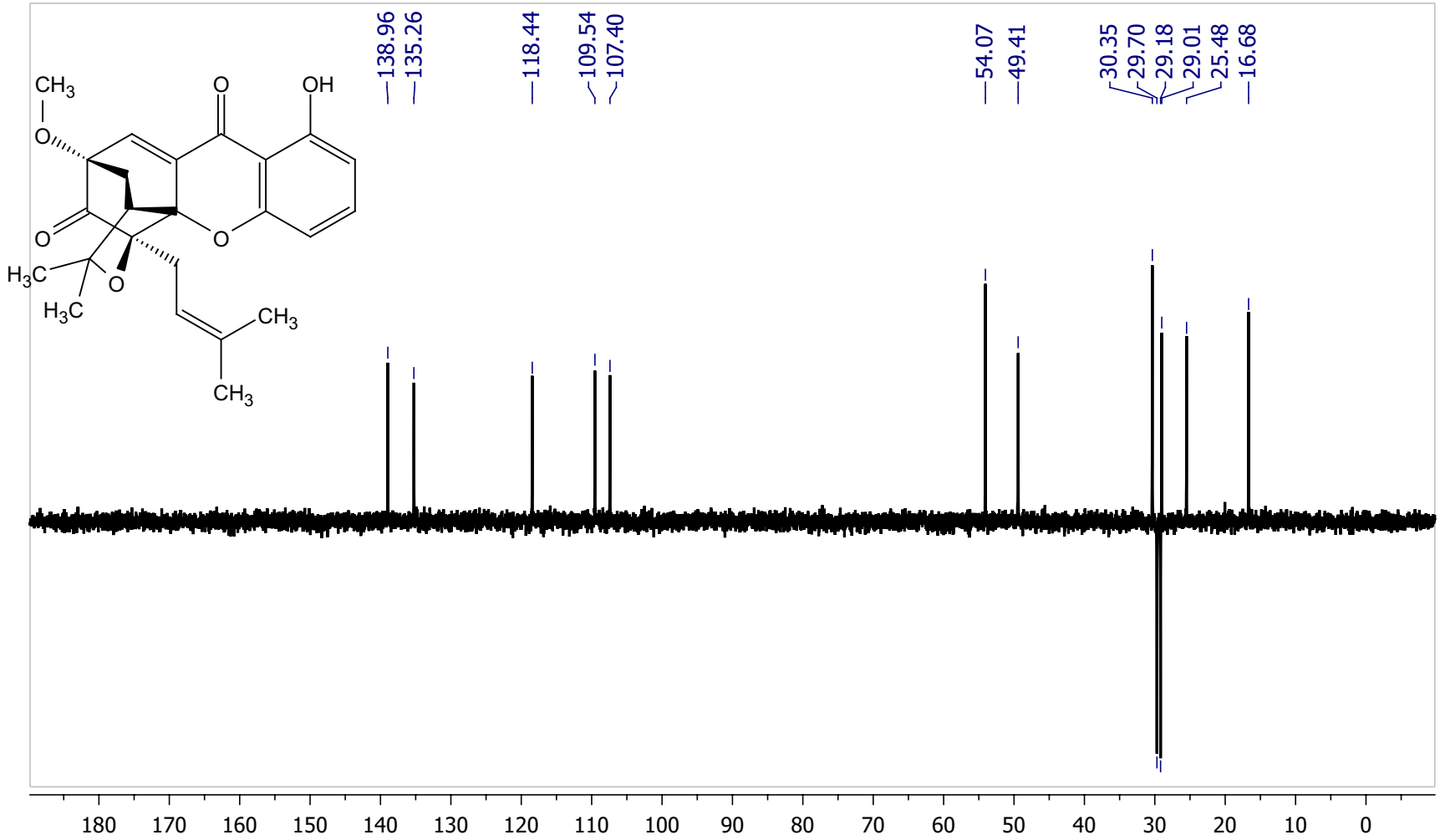

Figure A14. Dept 135 (75 MHz, $CDCl_3$) spectrum of **2**

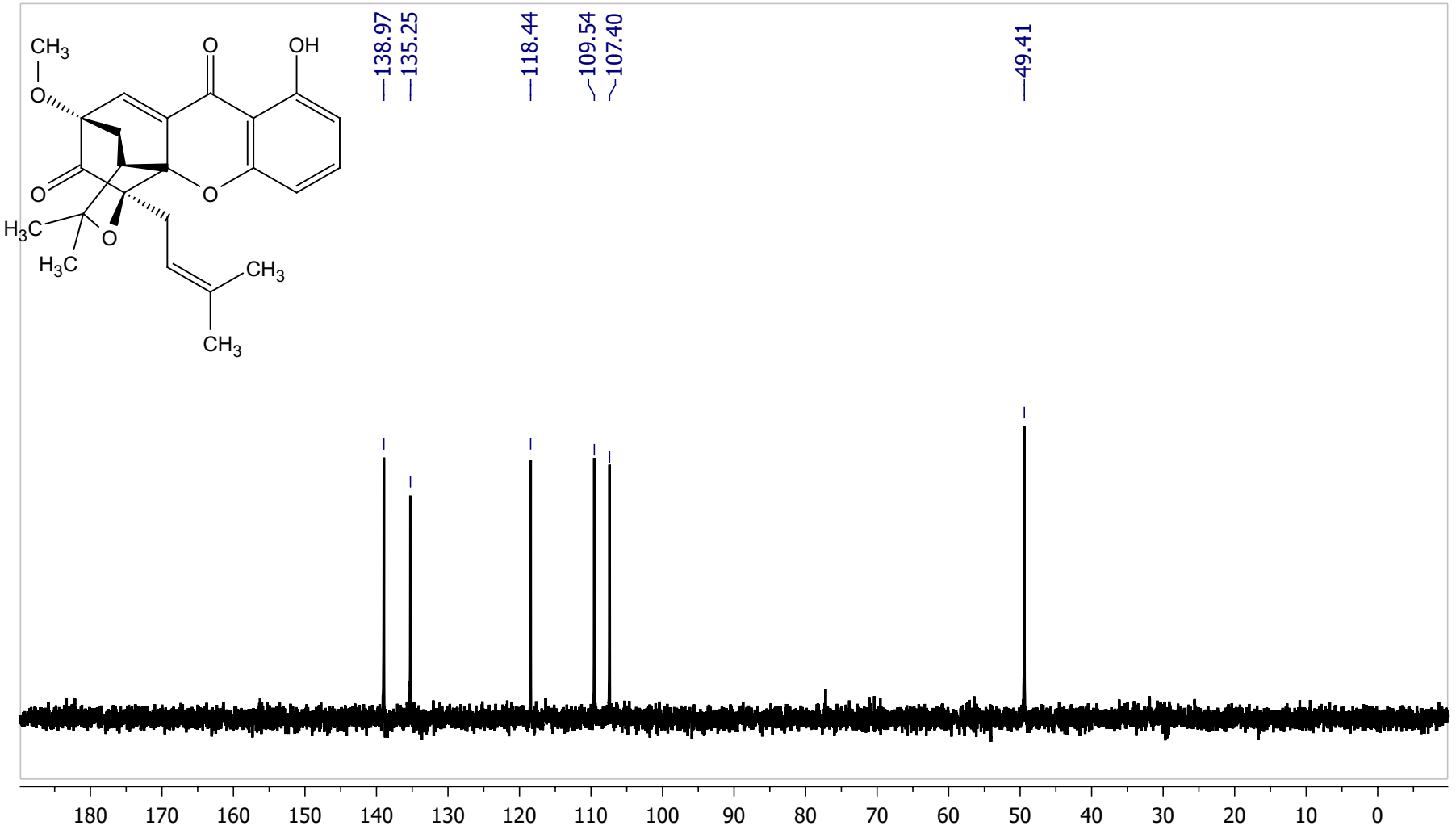

Figure S15. Dept 90 (75 MHz, $CDCl_3$) spectrum of **2**

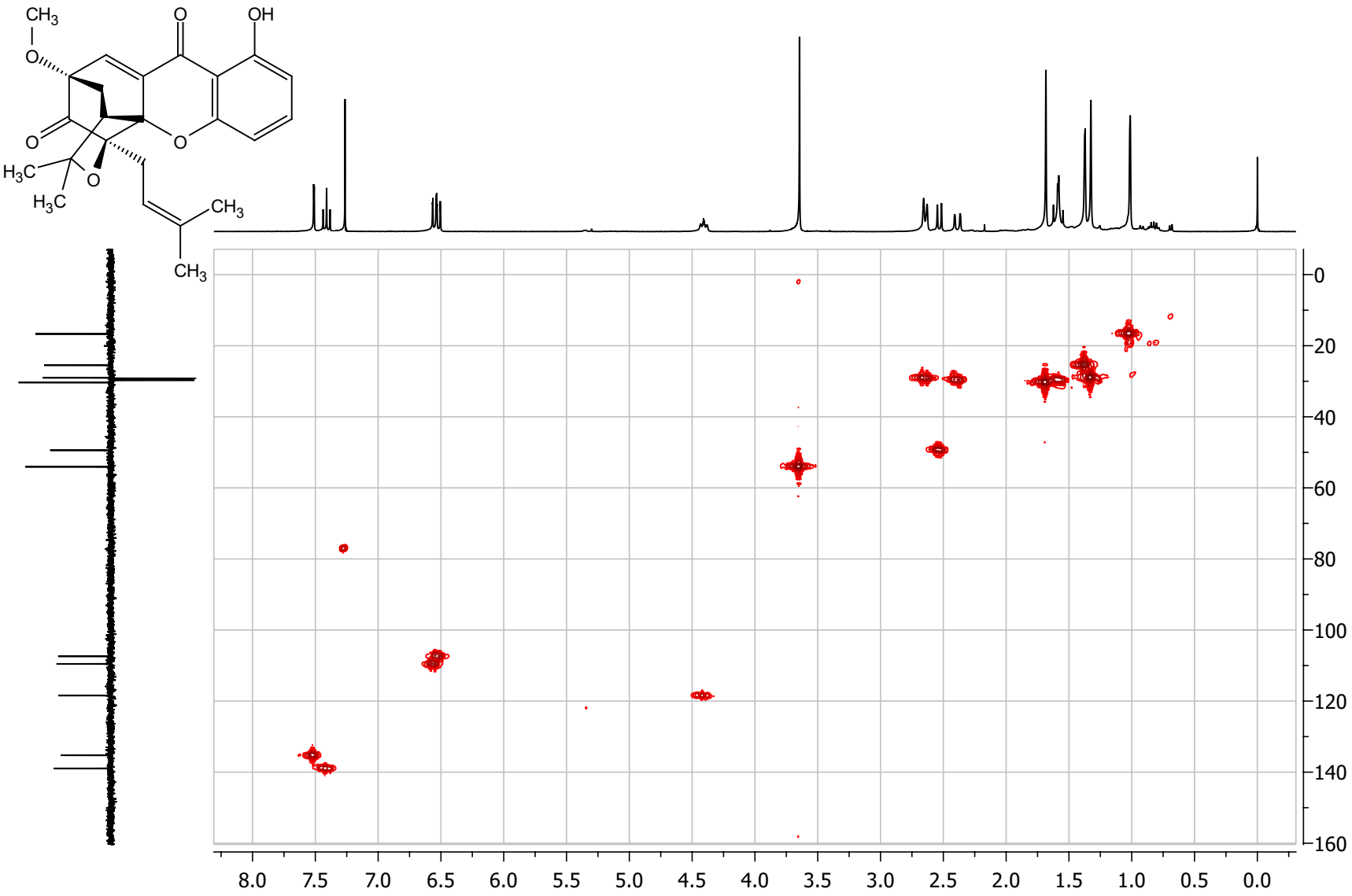

Figure S16. HMQC (300MHz, $CDCl_3$) spectrum of **2**

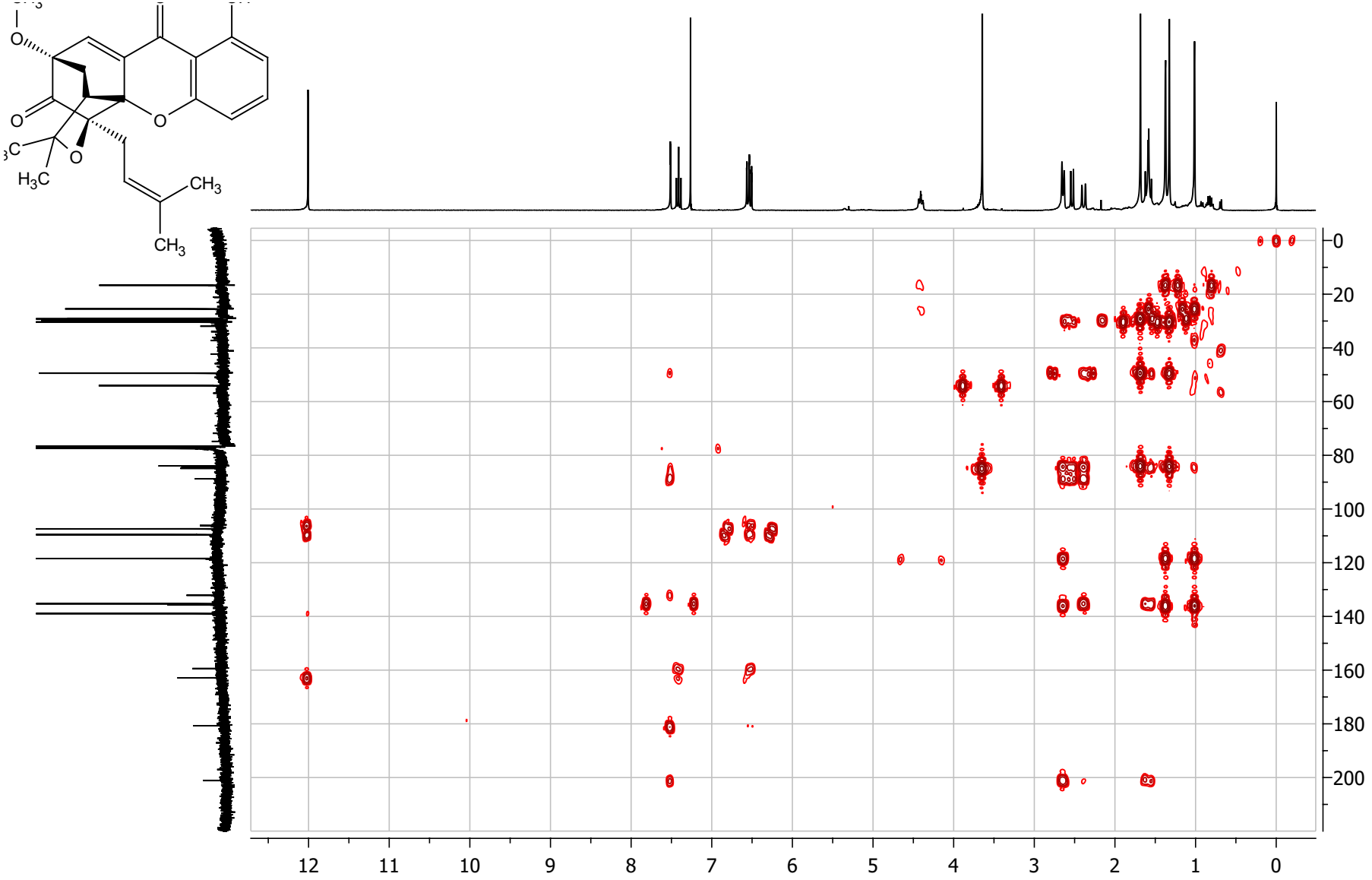

Figure A17. HMBC (300MHz, $CDCl_3$) spectrum of **2**

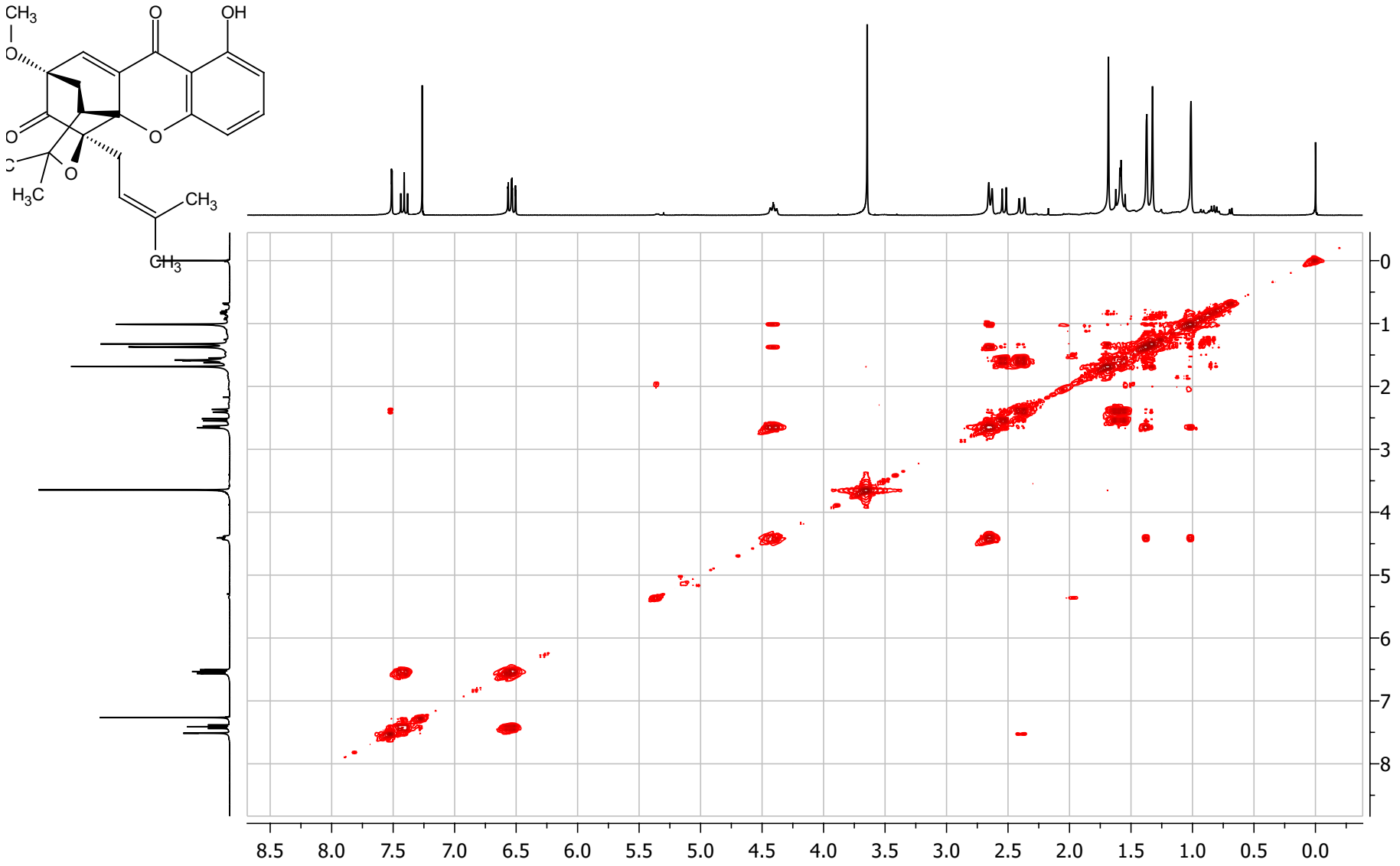

Figure A18. COSY (300MHz, $CDCl_3$) spectrum of **2**

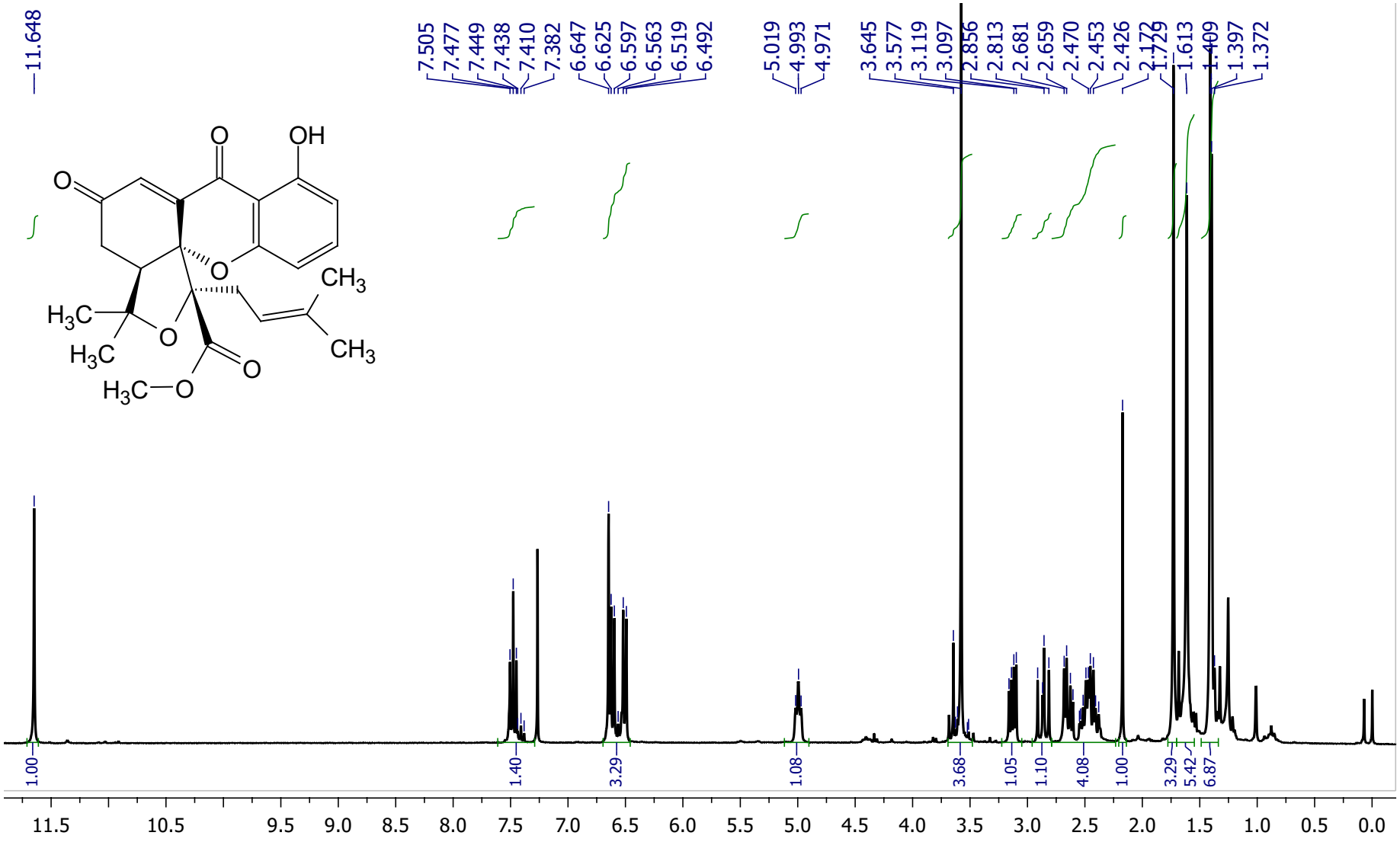

Figure A19. ^{1}H NMR (300 MHz, $CDCl_3$) spectrum of **3**

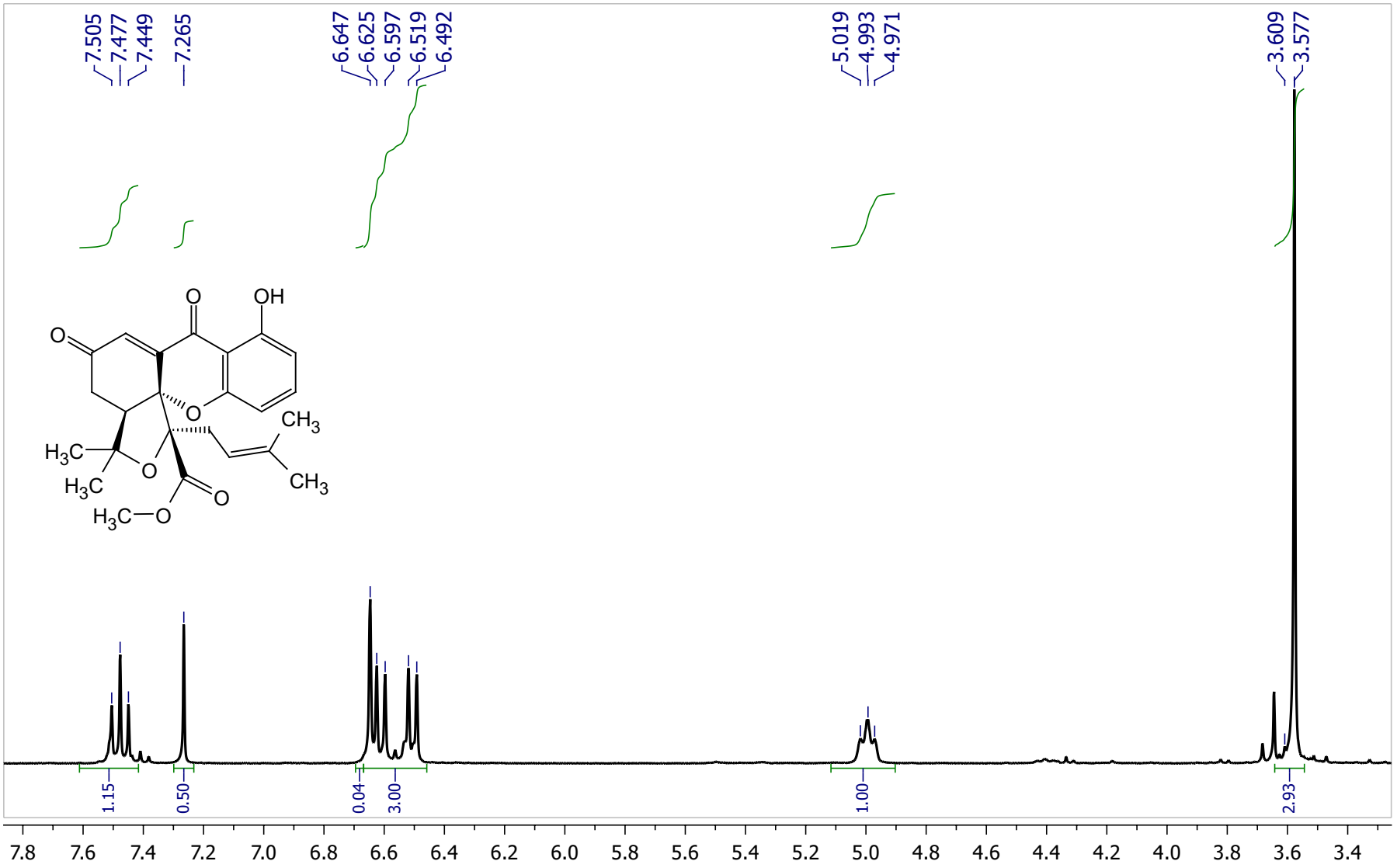

Figure A20. ^{1}H NMR (300 MHz, $CDCl_3$) spectrum of **3** (expansion)

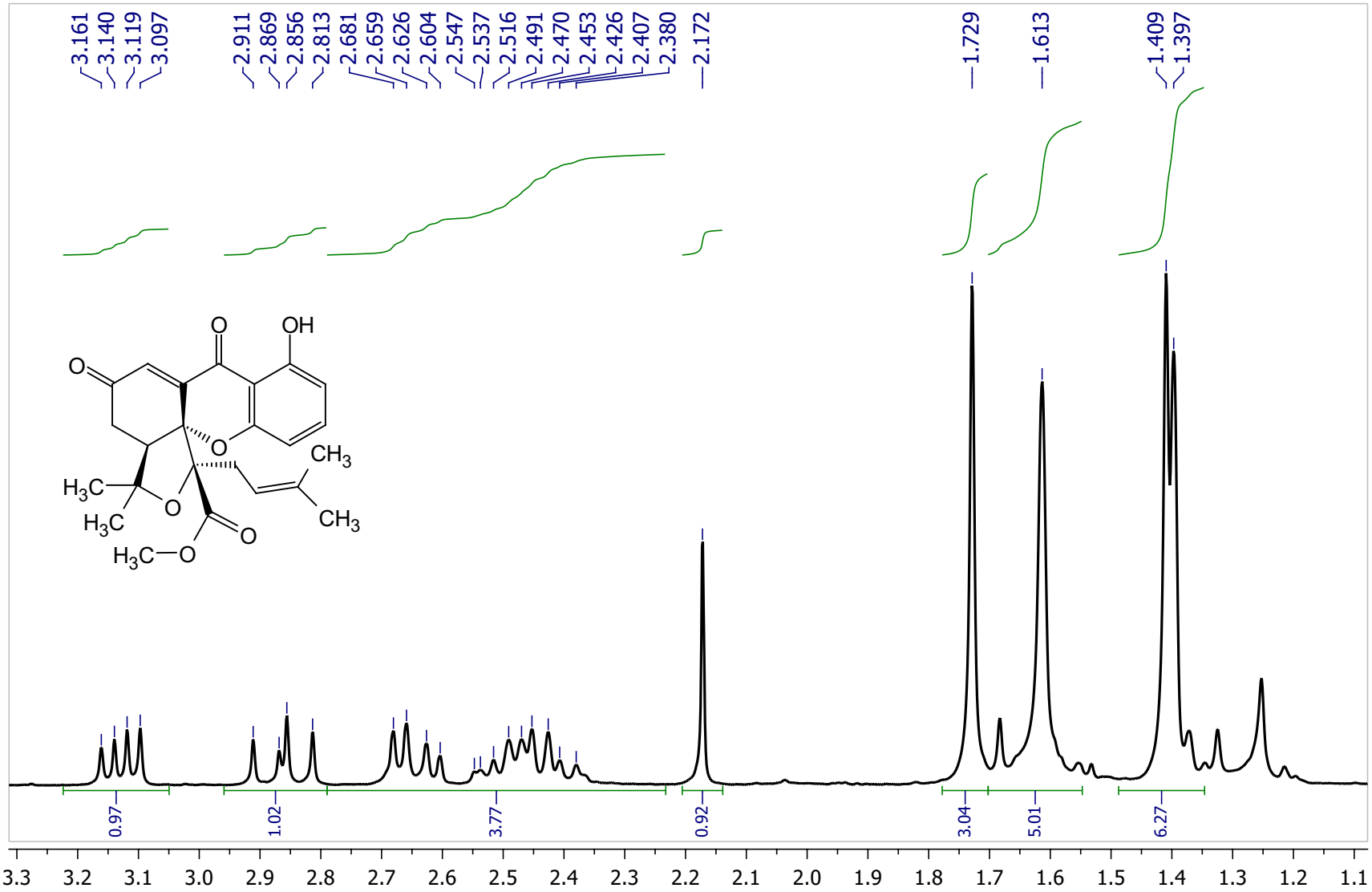

Figure A21. ^{1}H NMR (300 MHz, $CDCl_3$) spectrum of **3** (expansion)

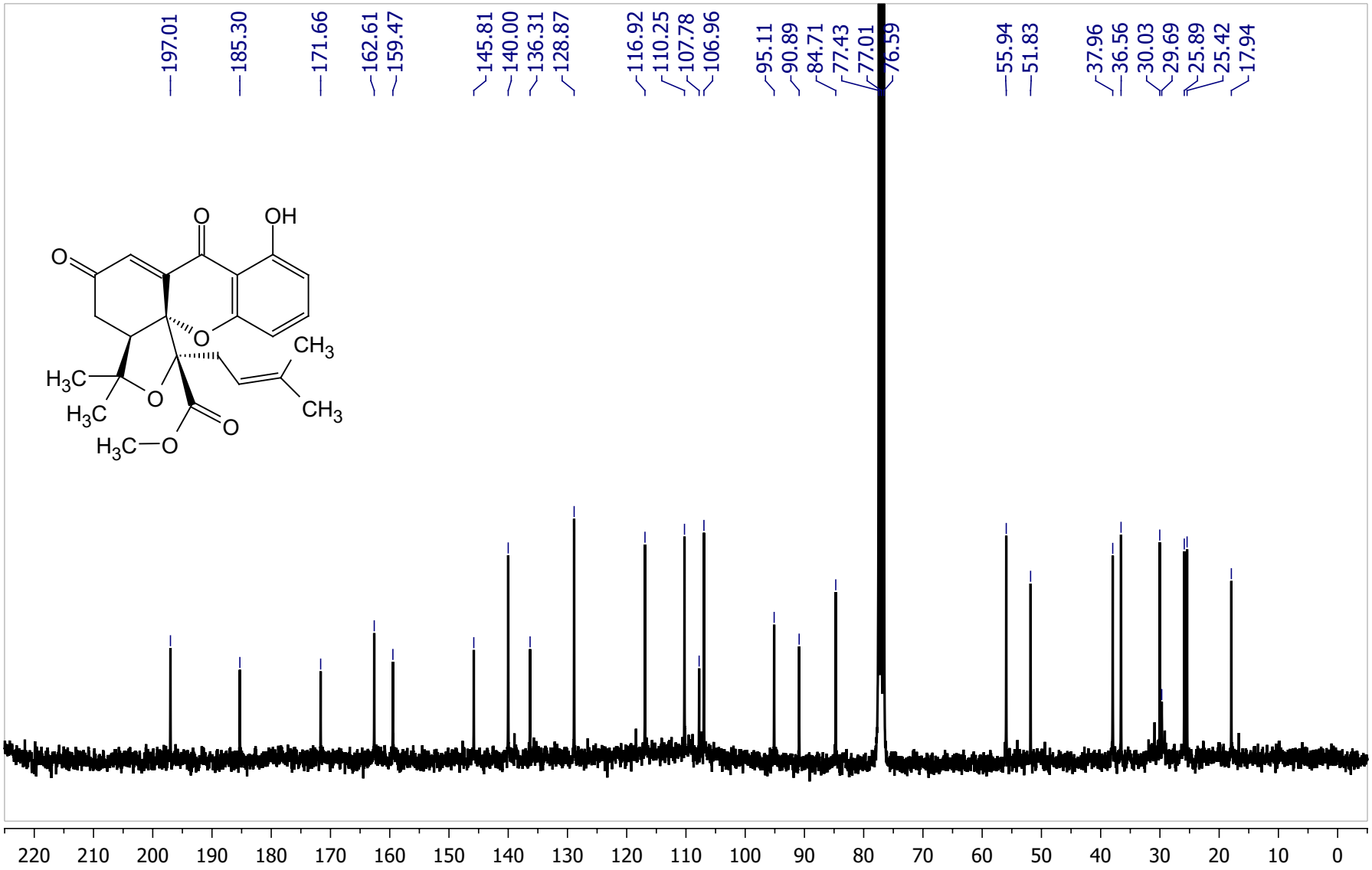

Figure A22. ^{13}C NMR (75 MHz, $CDCl_3$) spectrum of **3**

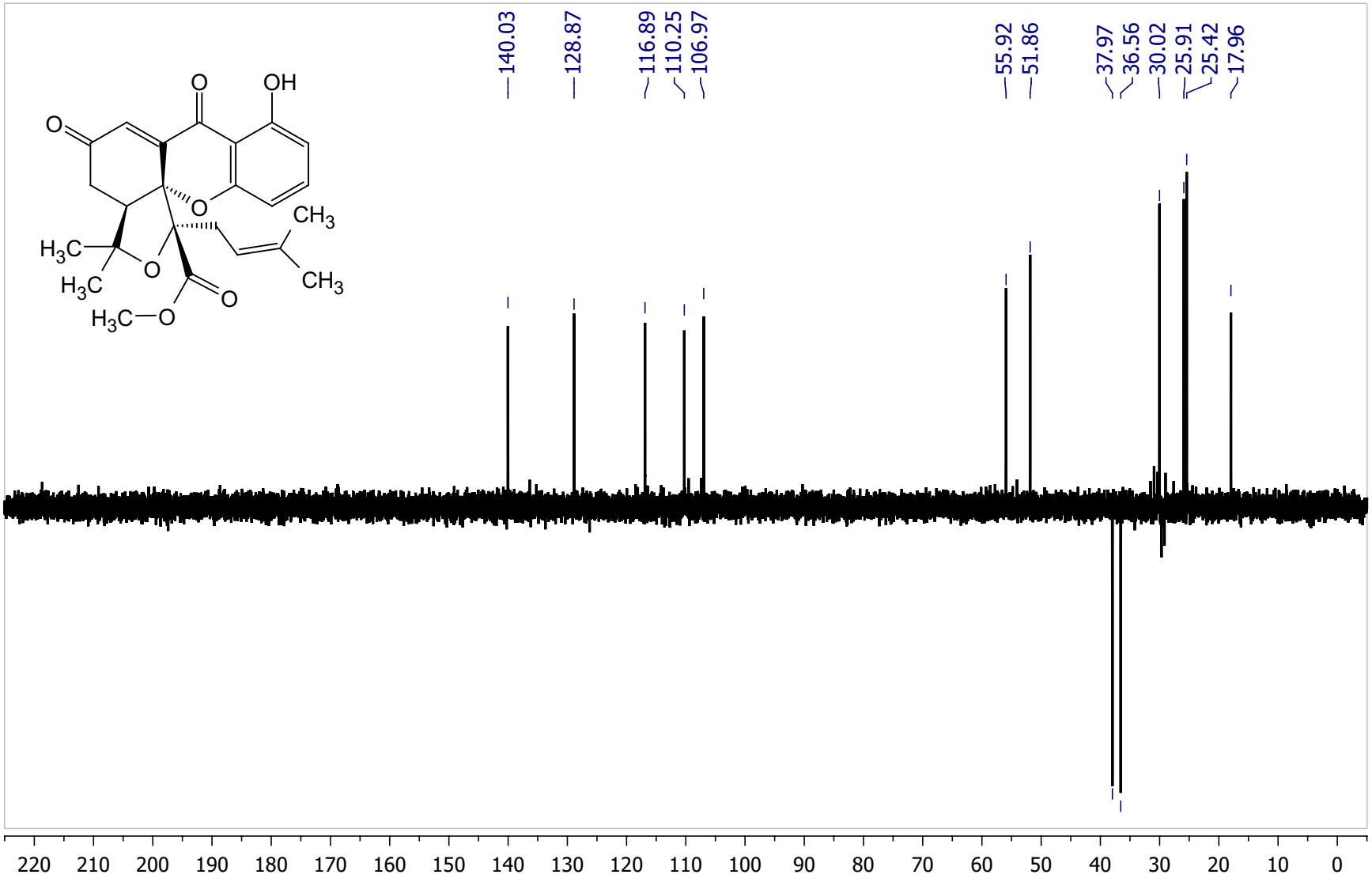

Figure A23. Dept 135 (300 MHz, $CDCl_3$) spectrum of **3**

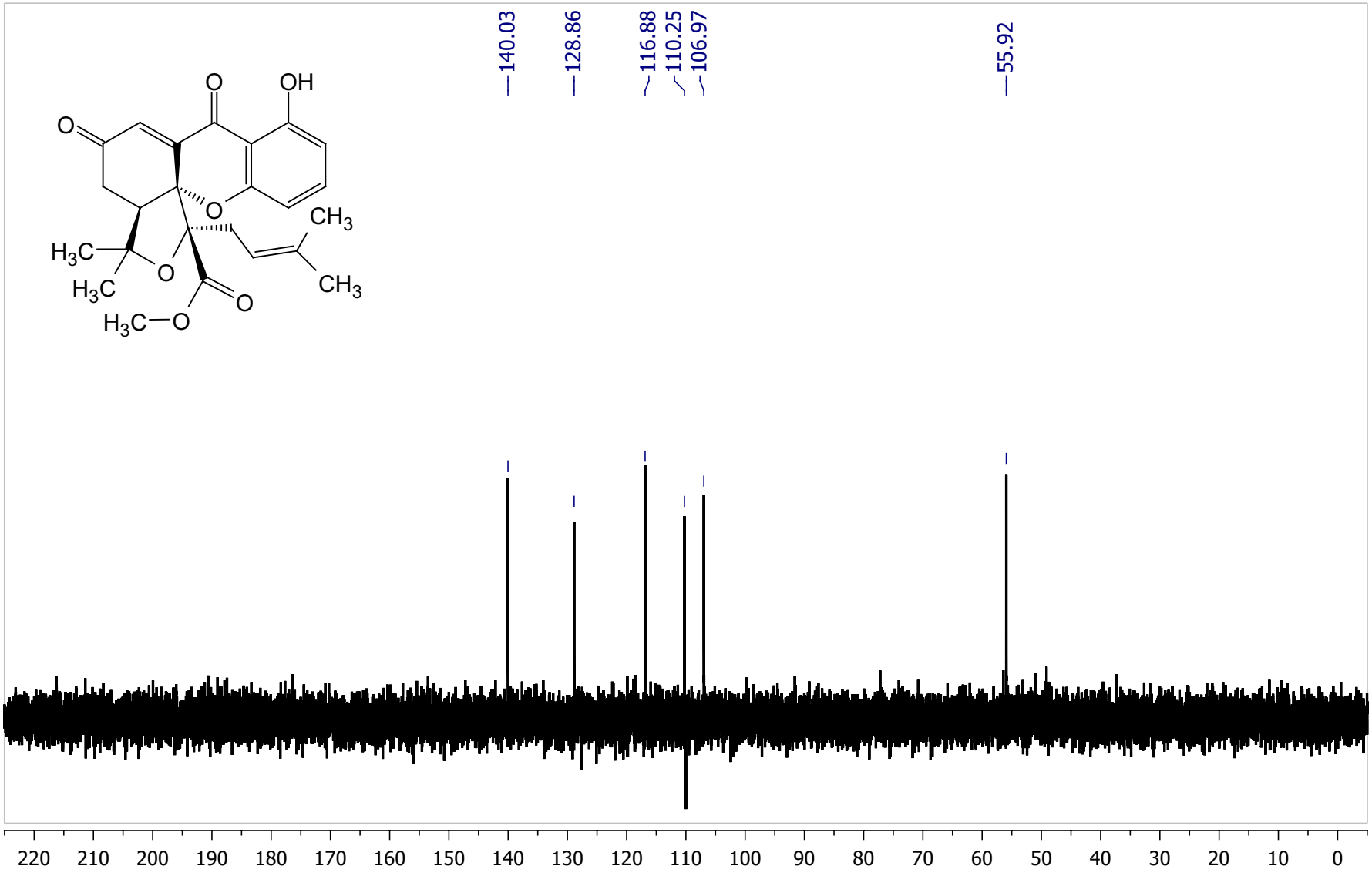

Figure A24. Dept 90 (75 MHz, $CDCl_3$) spectrum of **3**

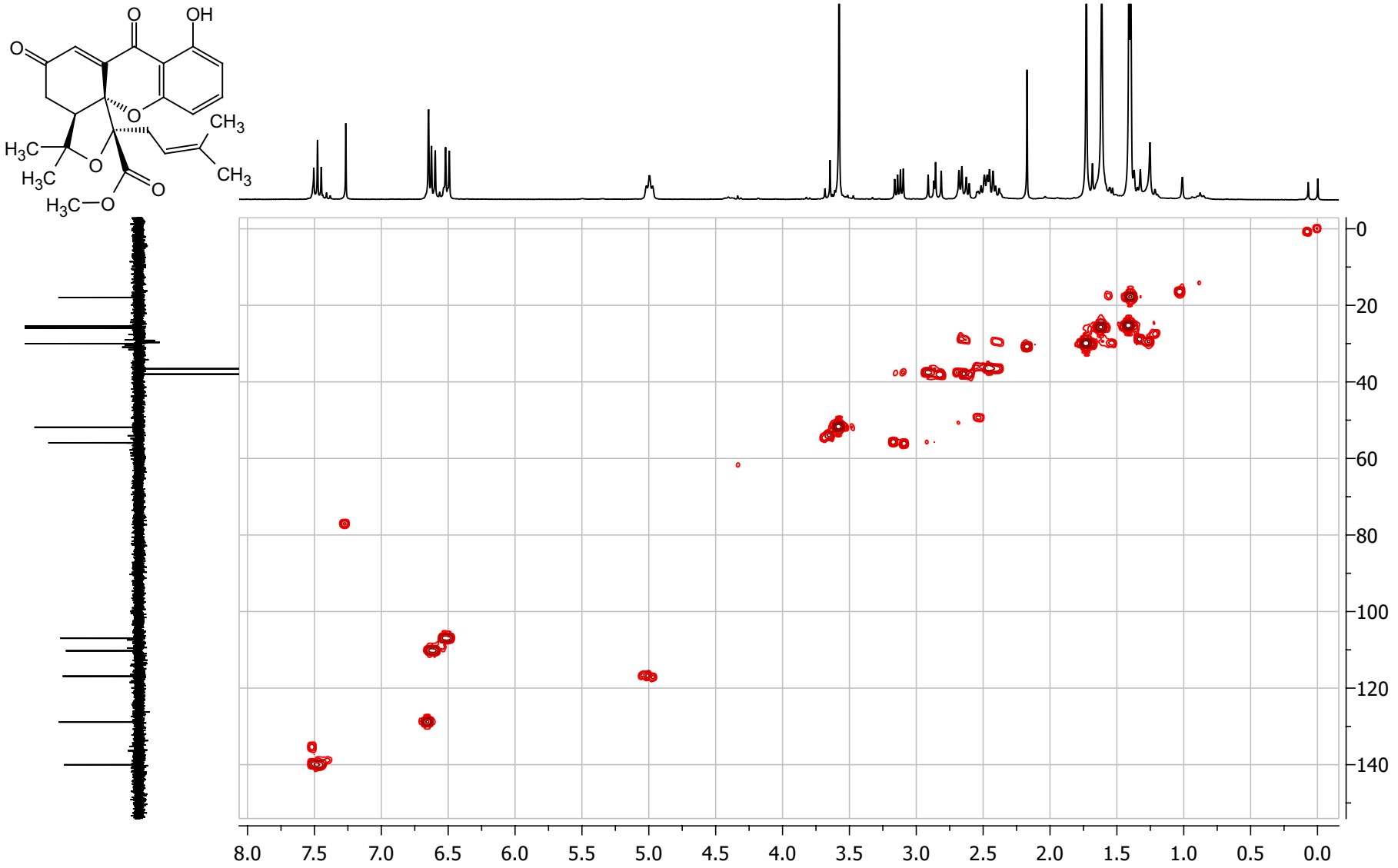

Figure A25. HMQC (300MHz, $CDCl_3$) spectrum of **3**

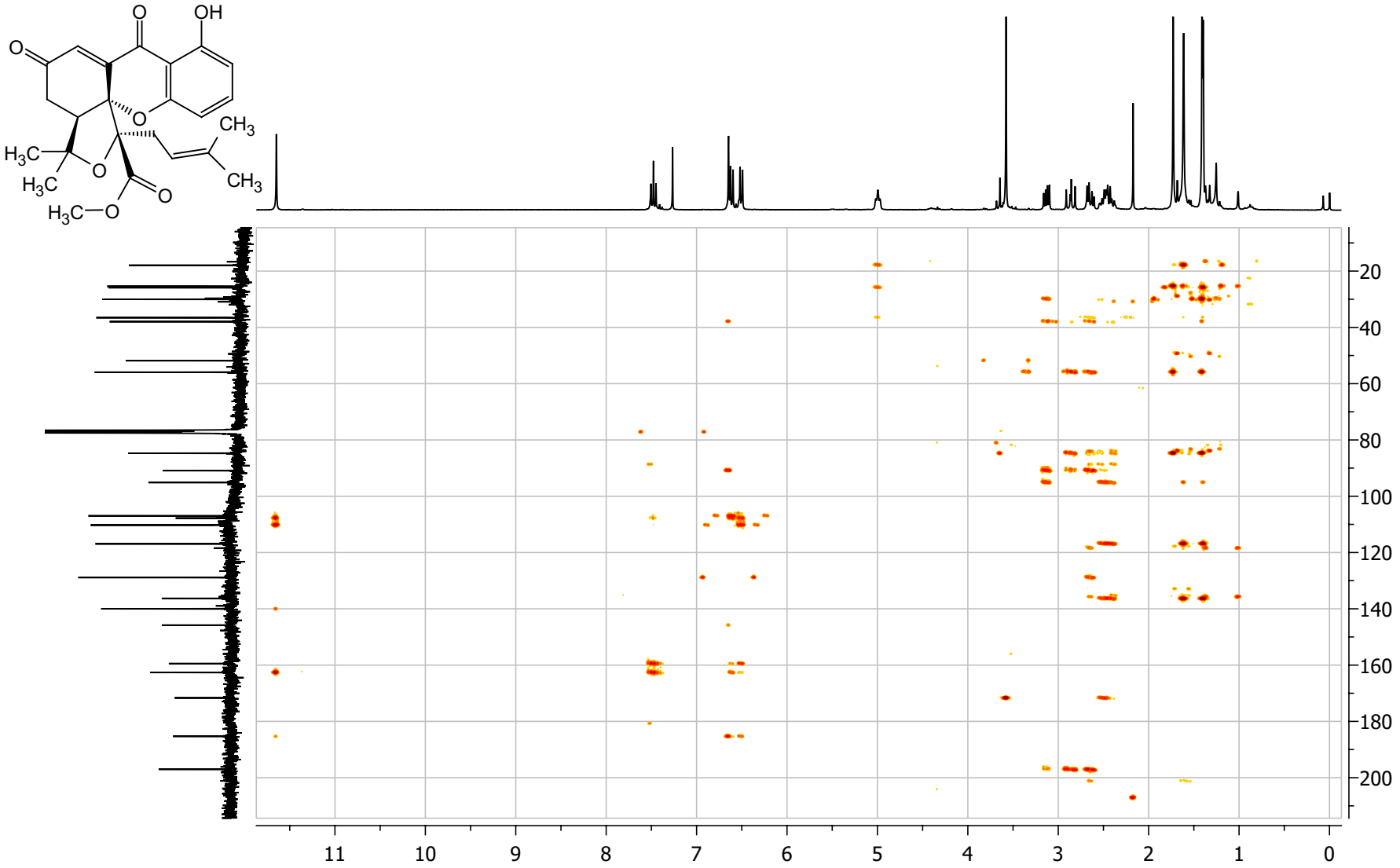

Figure A26. HMBC (300MHz, $CDCl_3$) spectrum of **3**

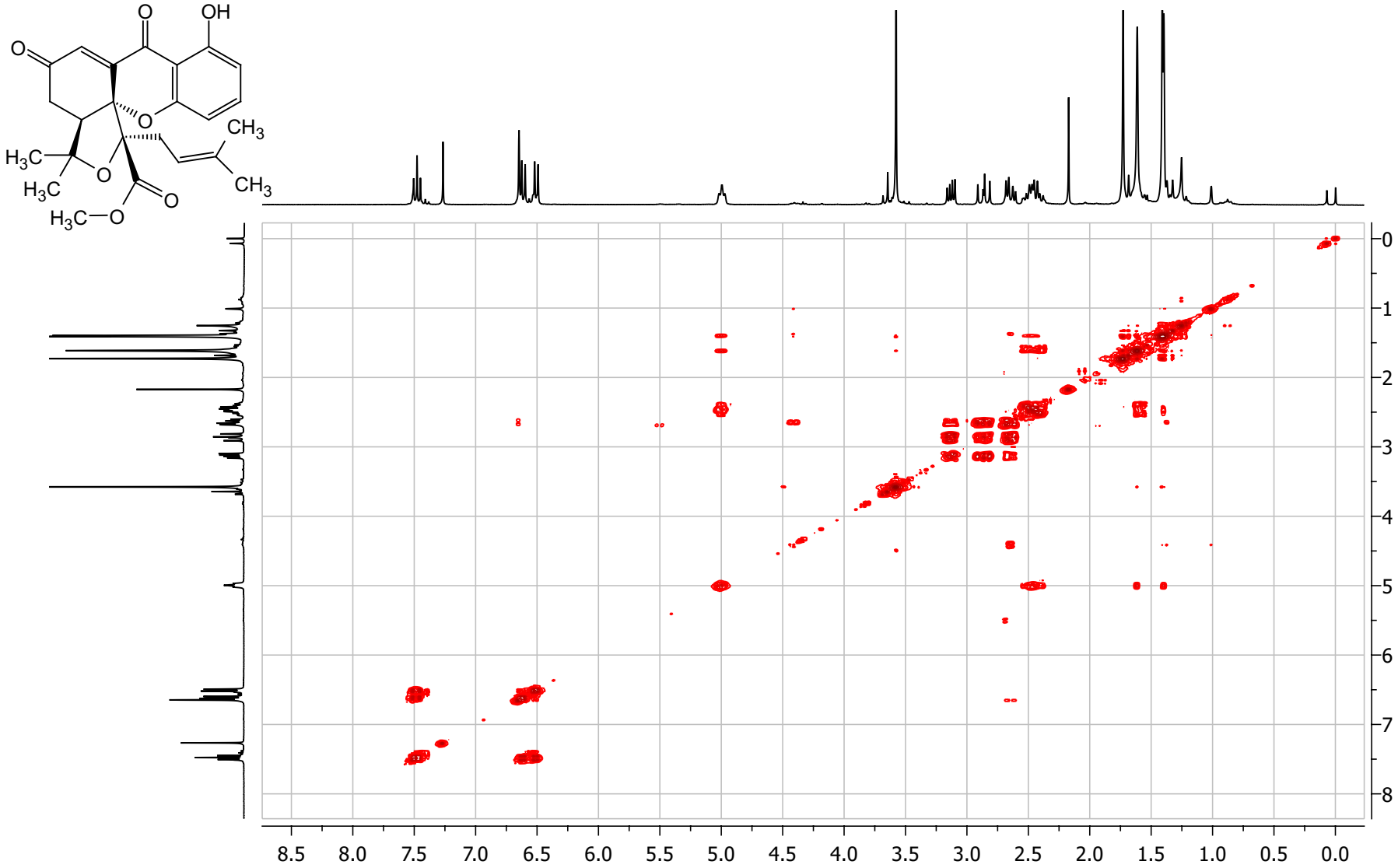

Figure A27. COSY (300MHz, $CDCl_3$) spectrum of **3**

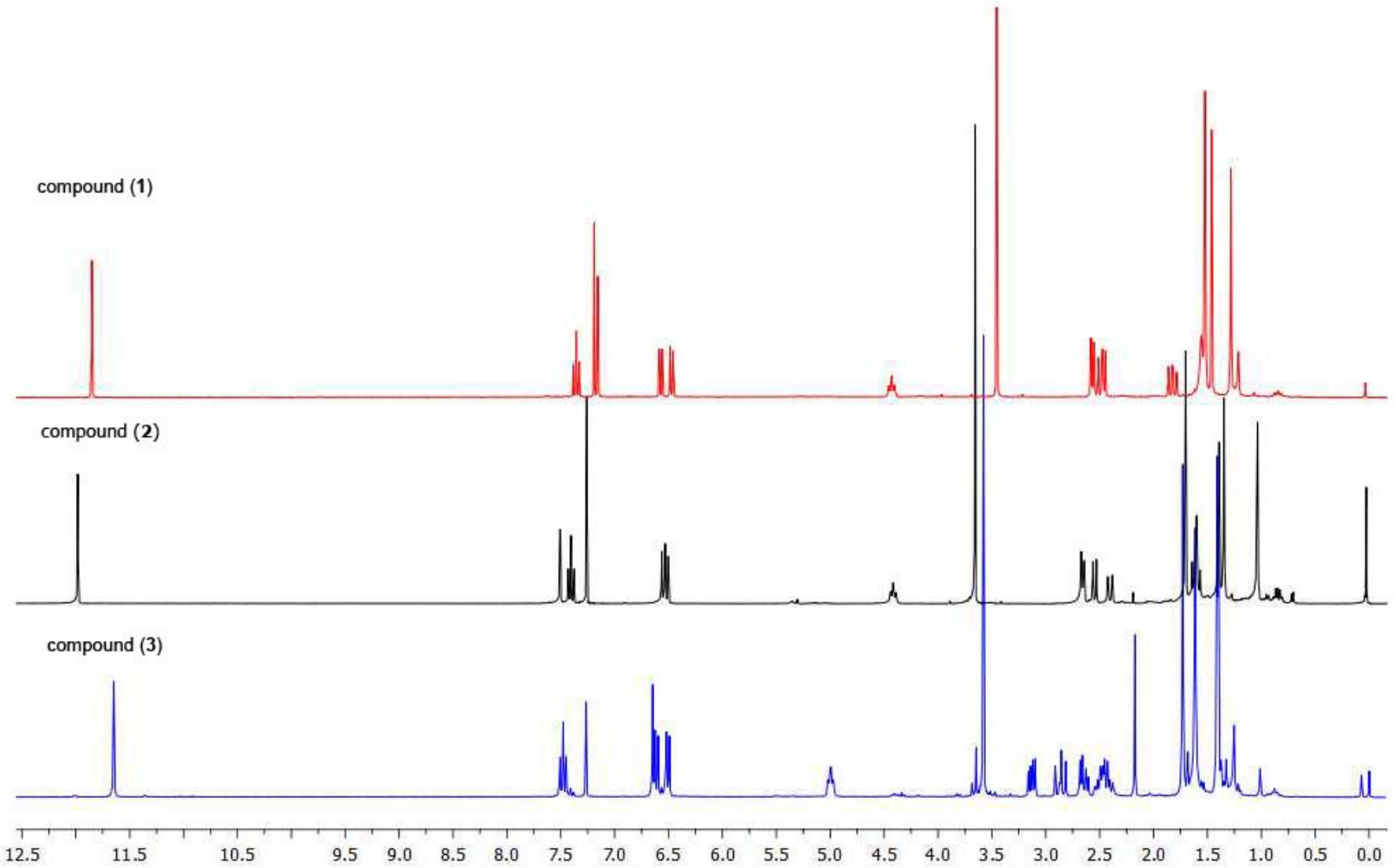

Figure A28. Overlay of ^{1}H NMR spectra of **1**-**3**

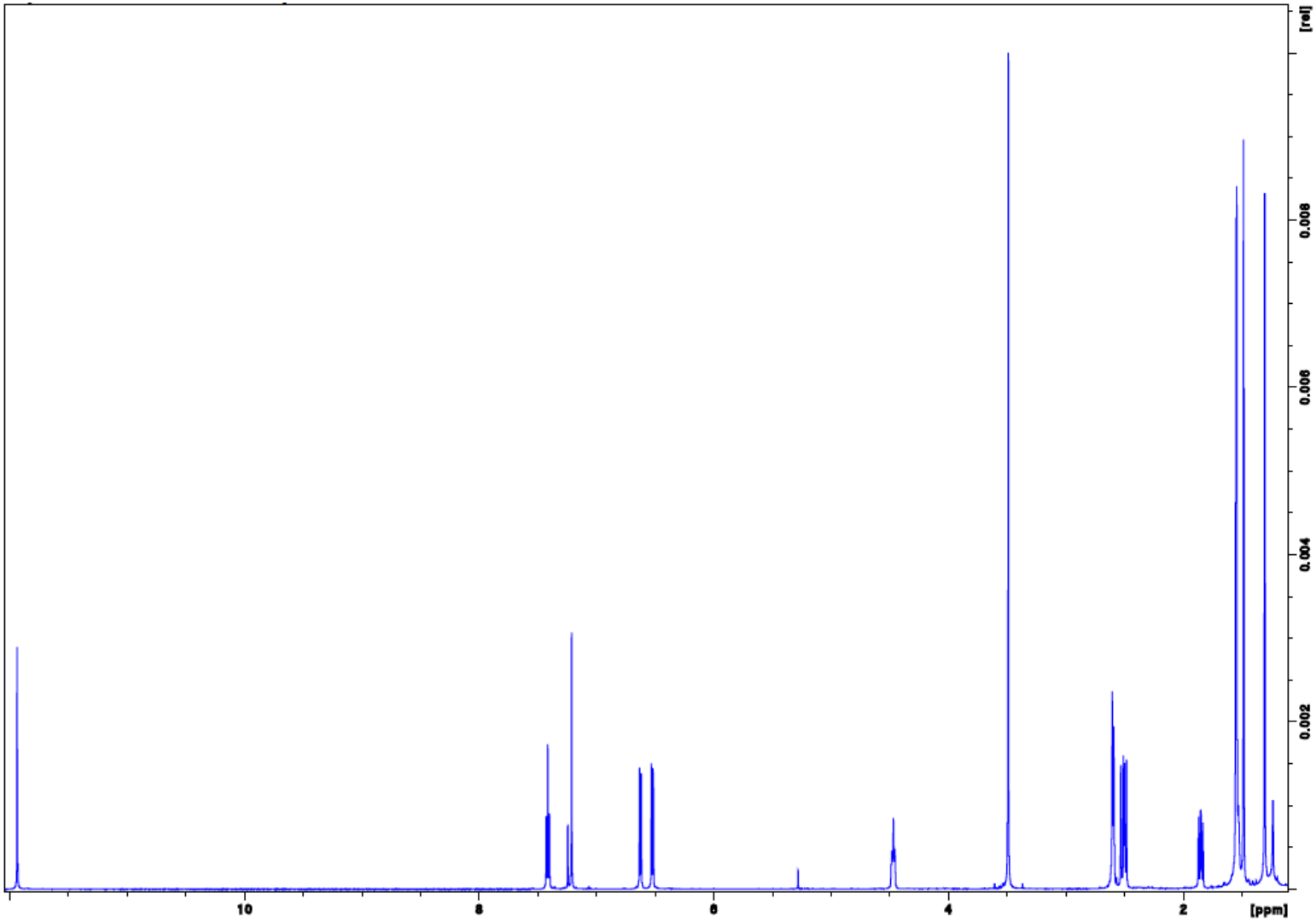

Figure A29. ^{1}H NMR (600 MHz, $CDCl_3$) spectrum of (+)-Neocaged-xanthone (**1**)

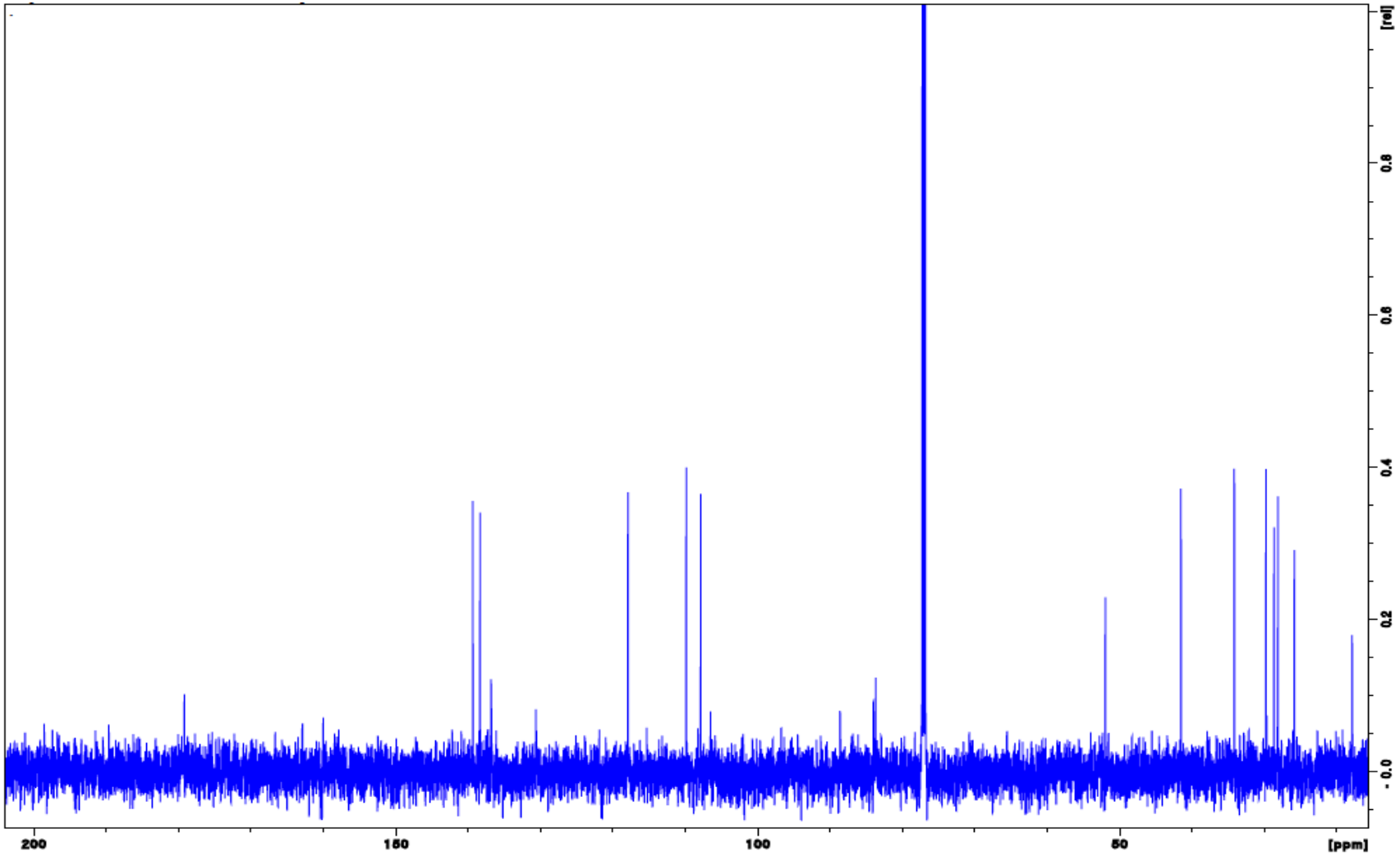

Figure A30. ^{13}C NMR (150 MHz, $CDCl_3$) spectrum of (+)-Neocaged-xanthone (**1**)

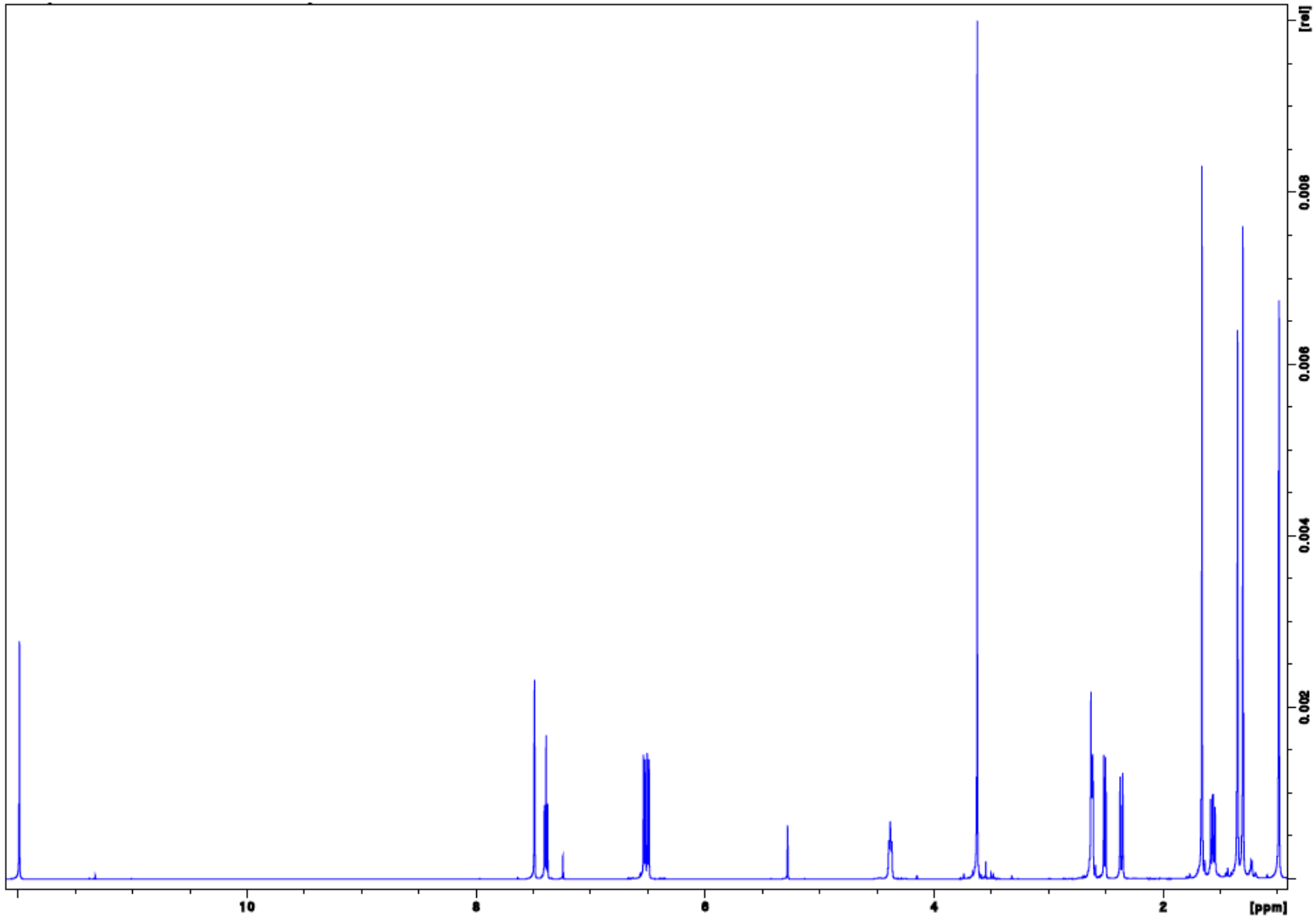

Figure A31. ^{1}H NMR (600 MHz, $CDCl_3$) spectrum of (+)-Caged-xanthone (**2**)

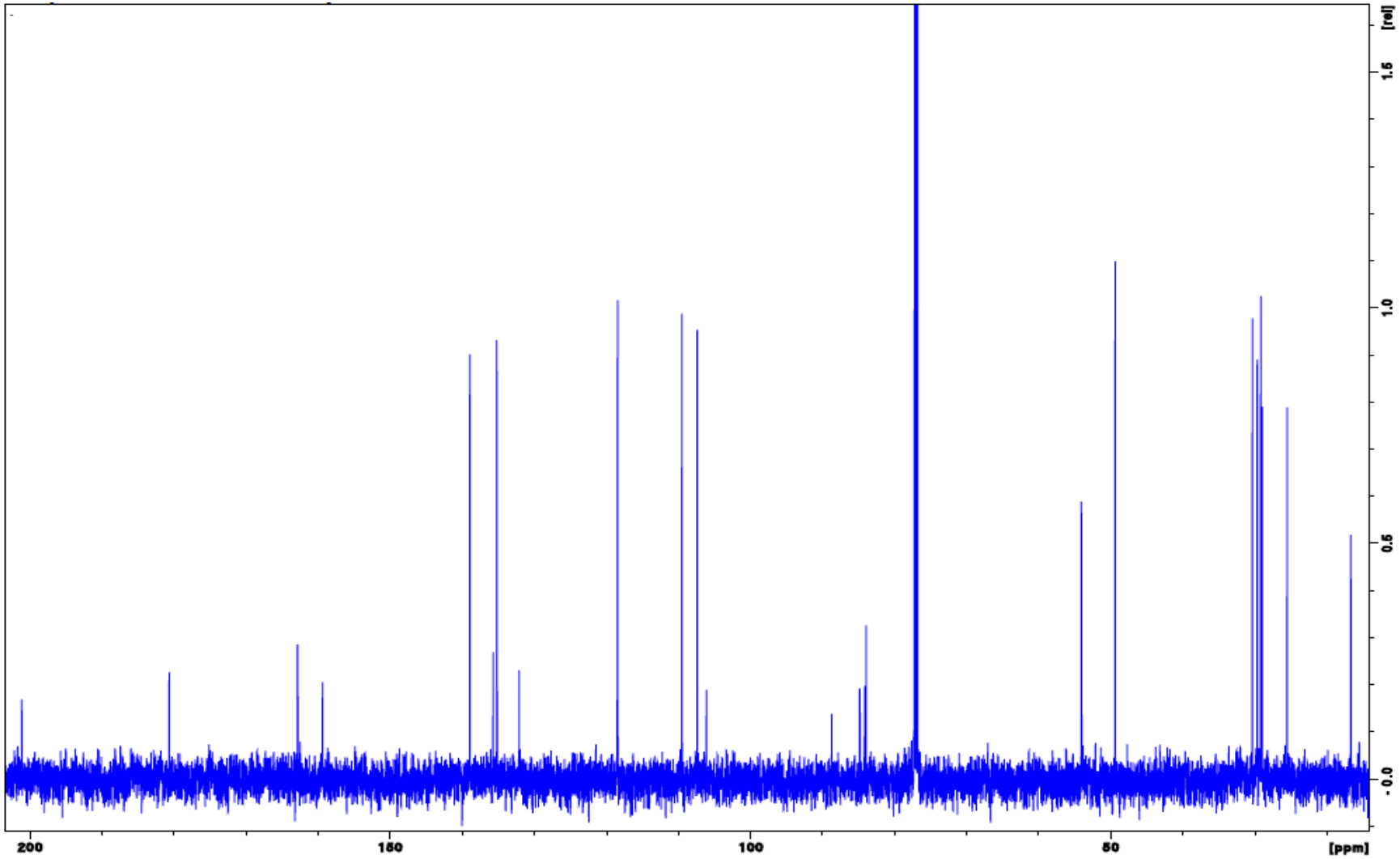

Figure A32. ^{13}C NMR (150 MHz, $CDCl_3$) spectrum of (+)-Caged-xanthone (**2**)

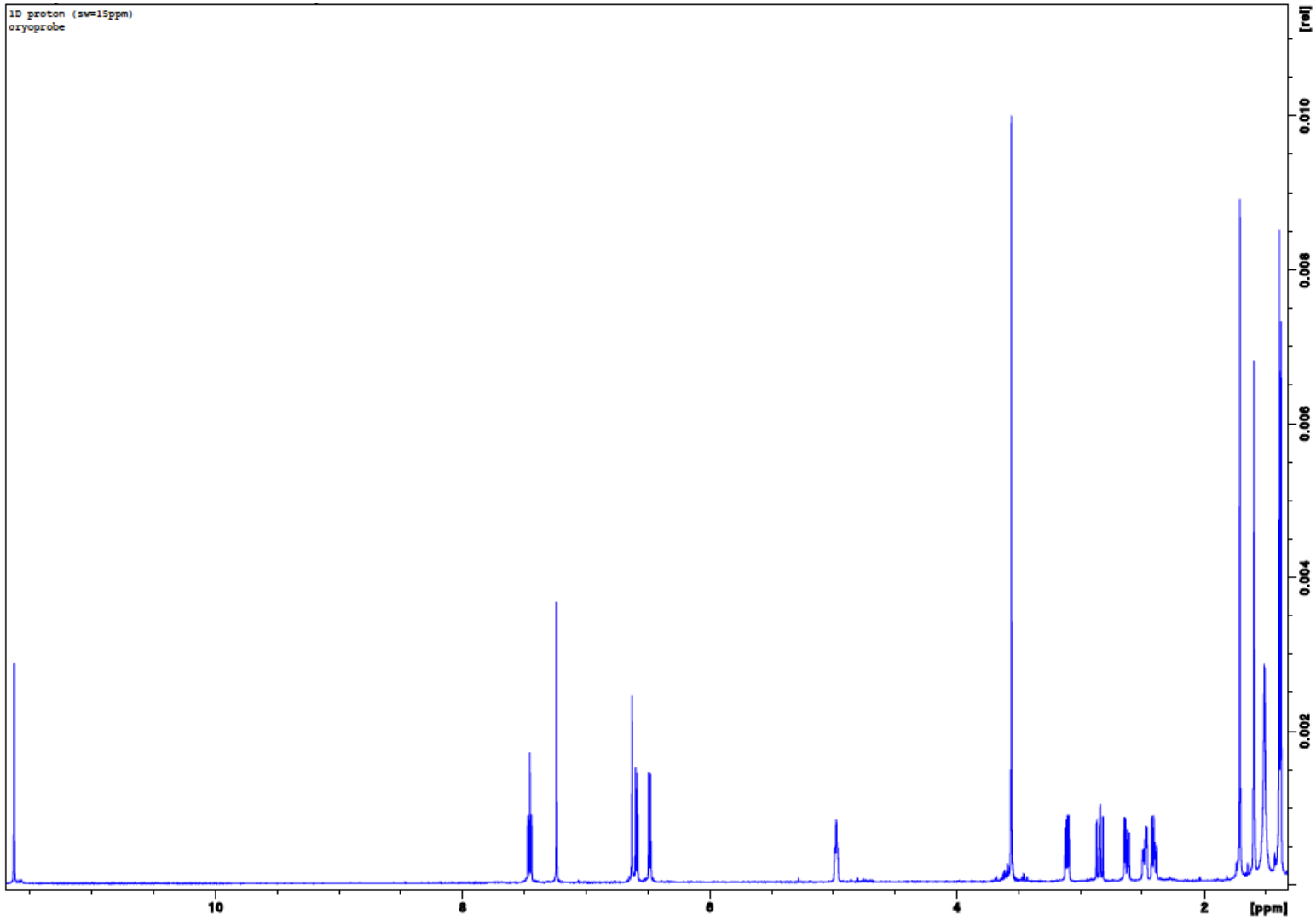

Figure A33. ^{1}H NMR (600 MHz, $CDCl_3$) spectrum of (+)-Rearranged caged-xanthone (**3**)

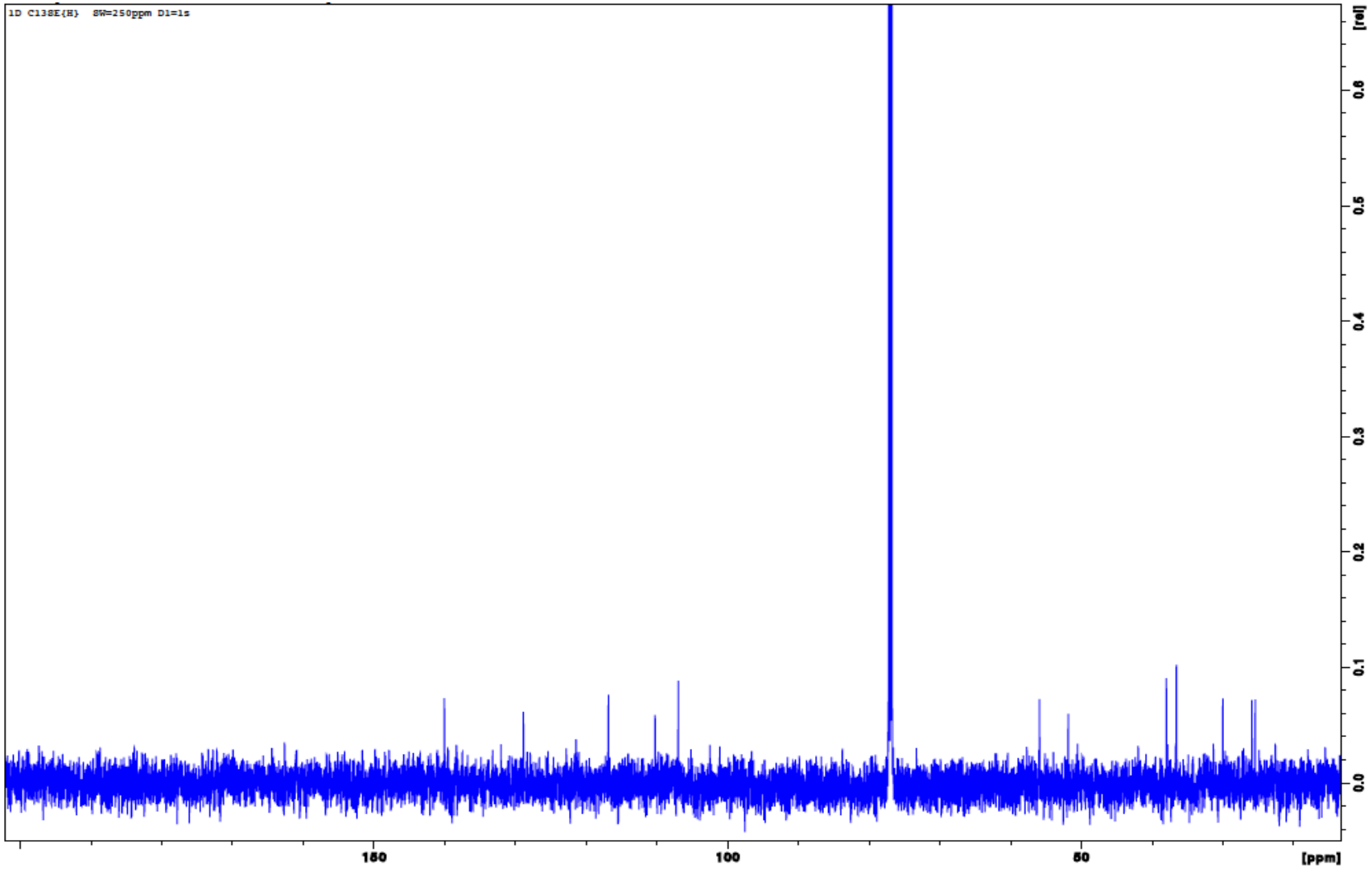

Figure A34. ^{13}C NMR (150 MHz, $CDCl_3$) spectrum of (+)-Rearranged caged-xanthone (**3**)

JOURNAL OF NATURAL PRODUCTS

Article

pubs.acs.org/jnp

Three Types of Cytotoxic Natural Caged-Scaffolds: Pure Enantiomers or Partial Racemates

Nawong Boonnak,*[,†] Suchada Chantrapromma,*[,‡] Hoong-Kun Fun,[§,¶] Supreeya Yuenyongsawad,[⊥] Brian O. Patrick,[∥] Wisanu Maneerat,[∥] David E. Williams,[∥] and Raymond J. Andersen[∥]

[†]Faculty of Traditional Thai Medicine, Prince of Songkla University, Hat-Yai, Songkhla 90112, Thailand

[‡]Department of Chemistry, Faculty of Science, Prince of Songkla University, Hat-Yai, Songkhla 90112, Thailand

[§]X-ray Crystallography Unit, School of Physics, Universiti Sains Malaysia, 11800 USM, Penang Malaysia

[⊥]Department of Pharmacognosy and Pharmaceutical Botany, Faculty of Pharmaceutical Sciences, Prince of Songkla University, Hat-Yai, Songkhla 90112, Thailand

[∥]Department of Chemistry and Earth, Ocean & Atmospheric Sciences, University of British Columbia, Vancouver, BC V6T 1Z1, Canada

[¶]Department of Pharmaceutical Chemistry, College of Pharmacy, King Saud University, Riyadh 11451, Saudi Arabia

Supporting Information

ABSTRACT: Two rare new natural products, the neocaged-xanthone pruniflorone T (**1**) and the rearranged caged-xanthone pruniflorone U (**3**), and the known caged-xanthone cochinchinone C (**2**) were isolated from the roots of *Cratoxylum formosum* ssp. *pruniflorum*. The unique structures of **1**−**3** were determined by analysis of NMR and X-ray diffraction data. The X-ray data of **1**−**3** revealed that they all exist with both enantiomers in their crystal packing. Separation of **1**−**3** by chiral HPLC led to the isolation of three pairs of enantiomers, (−)-**1**/(+)-**1**, (−)-**2**/(+)-**2**, and (−)-**3**/(+)-**3**, and their absolute configurations were determined by analysis of single-crystal X-ray diffraction and ECD spectroscopic data. A 1:1 mixture of **1** and **3** showed potent in vitro cytotoxicity against an MCF-7 human breast cancer cell line with an IC_{50} value of 0.11 μg/mL.

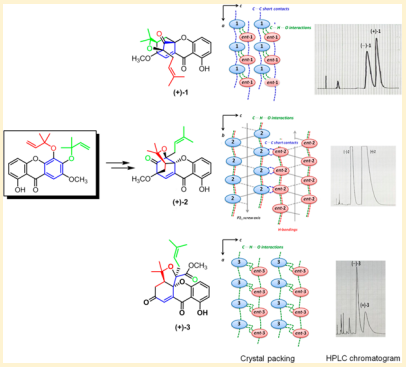

Natural caged-xanthones have been widely isolated from tropical plants in the genus *Garcinia*.[1−5] Many of the isolated caged-xanthones show interesting antibacterial,[6] anti-HIV-1,[4] and cytotoxic activities.[5,7−10] Gambogic acid, a well-known caged-xanthone, exhibited strong cytotoxicity against various human cancer cell lines including BCG-823 gastric carcinoma,[11] SMMC-7721 hepatoma,[12] and SPC-A1 lung cancer[9] cells. Moreover, gambogic acid has been used as an anticancer drug in the People's Republic of China for the treatment of patients with breast carcinoma by intravenous injection.[7,9] The previous results suggested that the unusual caged motif was important for the bioactivity.[13−16] Only a few neocaged-xanthones, structural isomers of caged-xanthones, and rearranged caged-xanthones, degraded products of caged-xanthones, have been identified. Herein, we report the isolation of three different types of caged-scaffolds represented by pruniflorone T (**1**), a new neocaged-xanthone, pruniflorone U (**3**), a rearranged caged-xanthone, and cochinchinone C (**2**), a known caged-xanthone,[17] from the roots of *Cratoxylum formosum* ssp. *pruniflorum*. The structures of **1**−**3** were elucidated by analysis of NMR spectroscopic and single-crystal X-ray diffraction data. Compounds **1**−**3** were evaluated for in vitro cytotoxicity against the MCF-7 human breast cancer cell line.

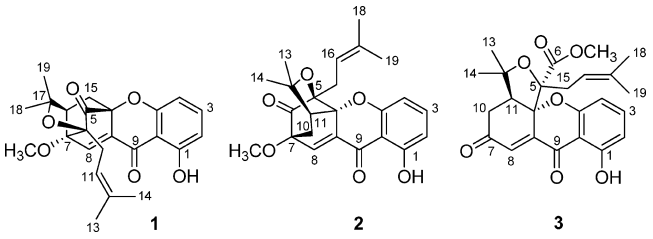

RESULTS AND DISCUSSION

Neocaged-xanthone pruniflorone T (**1**) was assigned a molecular formula of $C_{23}H_{26}O_5$ on the basis of ^{13}C NMR spectroscopic data and an HREIMS ion at m/z 382.1774 $[M - CO]^{+}$.[17] A single-crystal X-ray diffraction analysis of **1** (Figure 1) showed that the main skeleton of **1** was a neocaged-xanthone type. The UV spectrum of **1** showed absorption bands at 242, 293, 329, and 396 nm, which were similar to those of the known caged-xanthone cochinchinone C (**2**).[17] Its IR spectrum indicated the presence of a hydroxy (3445 cm^{-1})

Received: December 7, 2013
Published: June 18, 2014

dx.doi.org/10.1021/np400996k | *J. Nat. Prod.* 2014, 77, 1562−1571

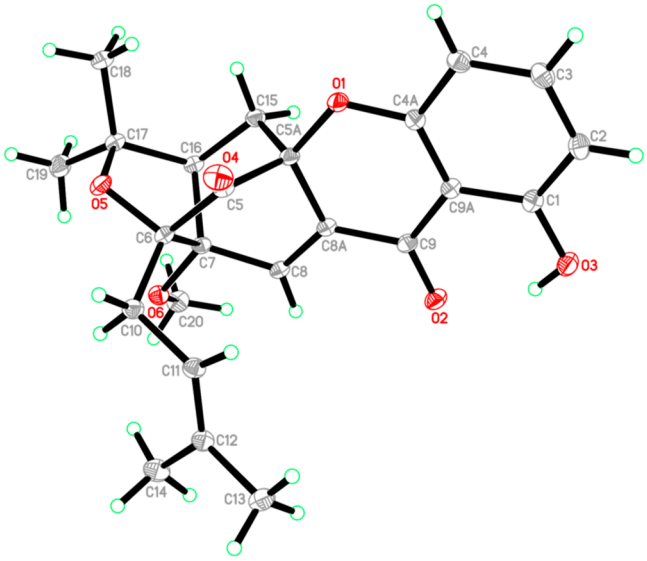

Figure 1. ORTEP diagram of neocaged-xanthone pruniflorone T (**1**).

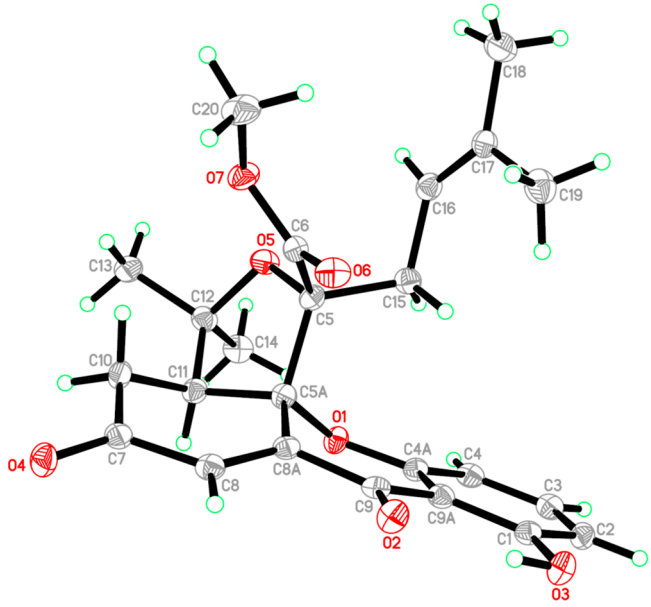

Figure 2. ORTEP diagram of rearranged caged-xanthone pruniflorone U (**3**).

functionality along with unconjugated (1747 cm^{-1}) and conjugated (1645 cm^{-1}) ketone carbonyls.

The ^1H and ^{13}C NMR spectroscopic data of **1** (Table 1) were similar to those of the known caged-xanthone **2**[17] (Table 1 and Figure S28) including the presence of ^{13}C NMR resonances typical of unconjugated and conjugated ketone carbonyls at δ_C 198.4 (C-5) and 179.2 (C-9). The ^1H NMR spectrum of **1** (Table 1) revealed the hydrogen-bonded phenolic proton at δ_H 11.88 (s, 1-OH) and an ABM spin system for three aromatic protons at δ_H 7.36 (t, J = 8.4 Hz, H-3), 6.57 (dd, J = 0.6, 8.4 Hz, H-4), and 6.47 (dd, J = 0.6, 8.4 Hz, H-2), respectively. Resonances assigned to an olefinic proton at

Table 1. ^1H and ^{13}C NMR Spectroscopic Data of 1−3 in $CDCl_3$

	neocaged-xanthone (**1**)		caged-xanthone (**2**)		rearranged caged-xanthone (**3**)	
position	δ_C,[a] type	δ_H[b] (J in Hz)	δ_C,[a] type	δ_H[b] (J in Hz)	δ_C,[a] type	δ_H[b] (J in Hz)
1-OH	162.9 C	11.88 s	162.9 C	12.10 s	162.6 C	11.65 s
2	109.8 CH	6.47 dd (0.6, 8.4)	109.5 CH	6.55 dd (0.9, 8.4)	110.2 CH	6.61 br d (8.4)
3	139.3 CH	7.36 t (8.4)	138.9 CH	7.41 t (8.4)	140.8 CH	7.48 t (8.4)
4	107.8 CH	6.57 dd (0.6, 8.4)	107.4 CH	6.52 dd (0.9, 8.4)	106.9 CH	6.51 br d (8.4)
4a	160.0 C		159.4 C		159.5 C	
5a	83.5 C		88.8 C		90.9 C	
5	198.4 C		84.1 C		95.1 C	
6	84.0 C		201.1 C		171.7 C	
7	88.6 C		84.8 C		197.0 C	
8	138.3 CH	7.16 s	135.3 CH	7.51 d (1.2)	128.9 CH	6.65 s
9	179.2 C		180.7 C		185.3 C	
8a	130.7 C		132.1 C		145.8 C	
9a	106.5 C		106.1 C		107.8 C	
10	28.1 CH_2	2.54 d (7.8)	29.7 CH_2	2.39 br d (13.2)	37.9 CH_2	2.86 dd (12.6, 16.5)
				1.58 dd (9.6, 13.2)		2.64 dd (6.6, 16.5)
11	117.9 CH	4.42 br t (7.8)	49.4 CH	2.53 d (9.6)	55.9 CH	3.13 dd (6.6, 12.6)
12	136.7 C		83.9 C		84.7 C	
13	25.8 CH_3	1.50 s	30.4 CH_3	1.68 s	30.0 CH_3	1.73 s
14	17.8 CH_3	1.50 s	29.0 CH_3	1.32 s	25.4 CH_3	1.41 s
15	34.2 CH_2	2.48 br d (12.9)	29.2 CH_2	2.64 d (7.8)	36.6 CH_2	2.46 m
		1.80 dd (9.6, 12.9)				
16	41.6 CH	2.44 d (9.6)	118.4 CH	4.41 br t (7.8)	116.9 CH	4.99 br t (6.9)
17	83.6 C		135.7 C		136.3 C	
18	29.8 CH_3	1.43 s	25.5 CH_3	1.37 s	17.9 CH_3	1.40 s
19	28.6 CH_3	1.25 s	16.7 CH_3	1.01 s	25.9 CH_3	1.62 s
6-OCH_3					51.8 CH_3	3.58 s
7-OCH_3	51.9 CH_3	3.44 s	54.1 CH_3	3.64 s		

[a]Measured at 75 MHz. [b]Measured at 300 MHz.

dx.doi.org/10.1021/np400996k | J. Nat. Prod. 2014, 77, 1562−1571

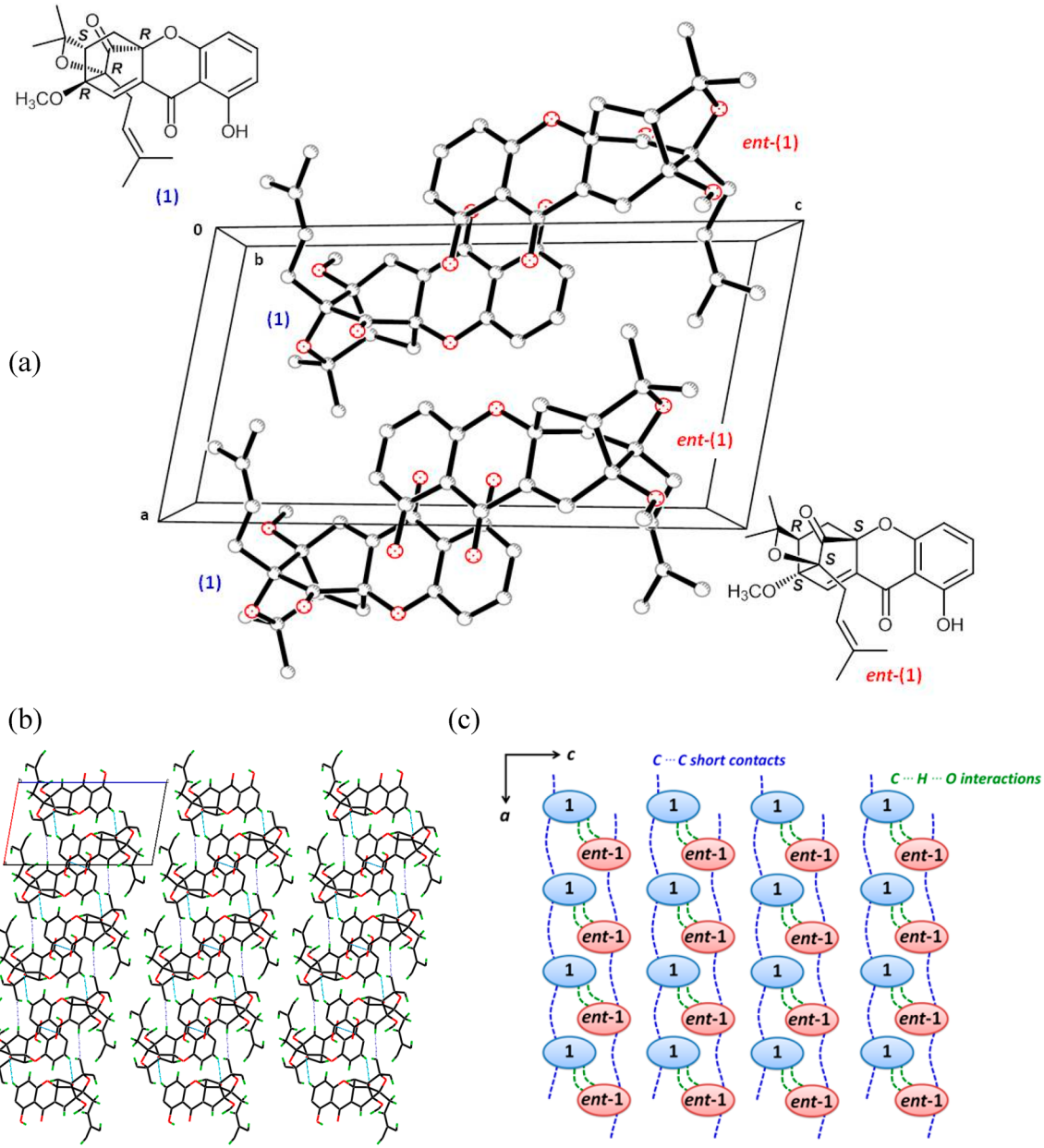

Figure 3. Crystal structure of neocaged-xanthone **1**. (a) Crystal packing of **1** showing the nonsuperimposition of molecule **1** ((5a*R*,6*R*,7*R*,16*S*)-**1**) and molecule *ent*-**1** ((5a*S*,6*S*,7*S*,16*R*)-**1**). (b) Intermolecular interactions and molecular arrangement of **1**. (c) Schematic representation of interactions between molecule **1** (blue oval) and molecule *ent*-**1** (red oval) in the crystal packing.

δ_H 7.16 (s, H-8), a methoxy group at δ_H 3.44 (s, 7-OCH_3), and an isoprenyl group at δ_H 4.42 (br t, J = 7.8 Hz, H-11), 2.54 (d, J = 7.8 Hz, H_2-10), and 1.50 (s, H_3-13/H_3-14) were also identified in the ^{1}H NMR spectrum. A methine proton resonance at δ_H 2.44 (H-16) showed vicinal coupling (J = 9.6 Hz) with the proton resonance at δ_H 1.80 (H-15), and the latter also showed geminal coupling (J = 12.9 Hz) with the proton resonance at δ_H 2.48 (H-15), indicating the presence of a $-CH_2-CH-$ subunit. In the HMBC spectrum of **1** (Figure S8), the diastereotopic methylene protons H_2-15 were correlated to C-5, C-9, C-5a, and C-8a, whereas the C-16 methine proton was correlated to C-6, C-7, and C-17, indicating that the $-CH_2$-15 and $-CH$-16 carbons were linked to C-5a and C-7, respectively. Furthermore, strong HMBC correlations from H-10 to C-5, C-6, and C-7 confirmed the attachment of an isoprenyl side chain to C-6. Therefore, the structure of compound **1** was assigned as a neocaged-xanthone, namely, pruniflorone T.

The rearranged caged-xanthone pruniflorone U (**3**) was assigned a molecular formula of $C_{24}H_{26}O_7$ on the basis of ^{13}C NMR spectroscopic data (Table 1) and an HREIMS ion at m/z 426.1684 $[M]^+$. The single-crystal X-ray diffraction analysis of **3** (Figure 2) showed that the main skeleton of **3** was a rearranged caged-xanthone. The UV spectrum of **3** showed absorption bands at 243, 252, 312, and 385 nm. IR absorptions at 3615, 1748, 1710, and 1633 cm^{-1} implied the existence of a hydroxy and three carbonyl groups. The presence of the carbonyl functionalities was confirmed by the observation of resonances at δ_C 197.0 (C-7), 185.3 (C-9), and 171.7 (C-6) in the ^{13}C NMR data (Table 1).

The ^{1}H NMR spectrum of **3** (Table 1) revealed resonances assigned to a hydrogen-bonded phenolic proton at δ_H 11.65 (s,

dx.doi.org/10.1021/np400996k | *J. Nat. Prod.* 2014, 77, 1562−1571

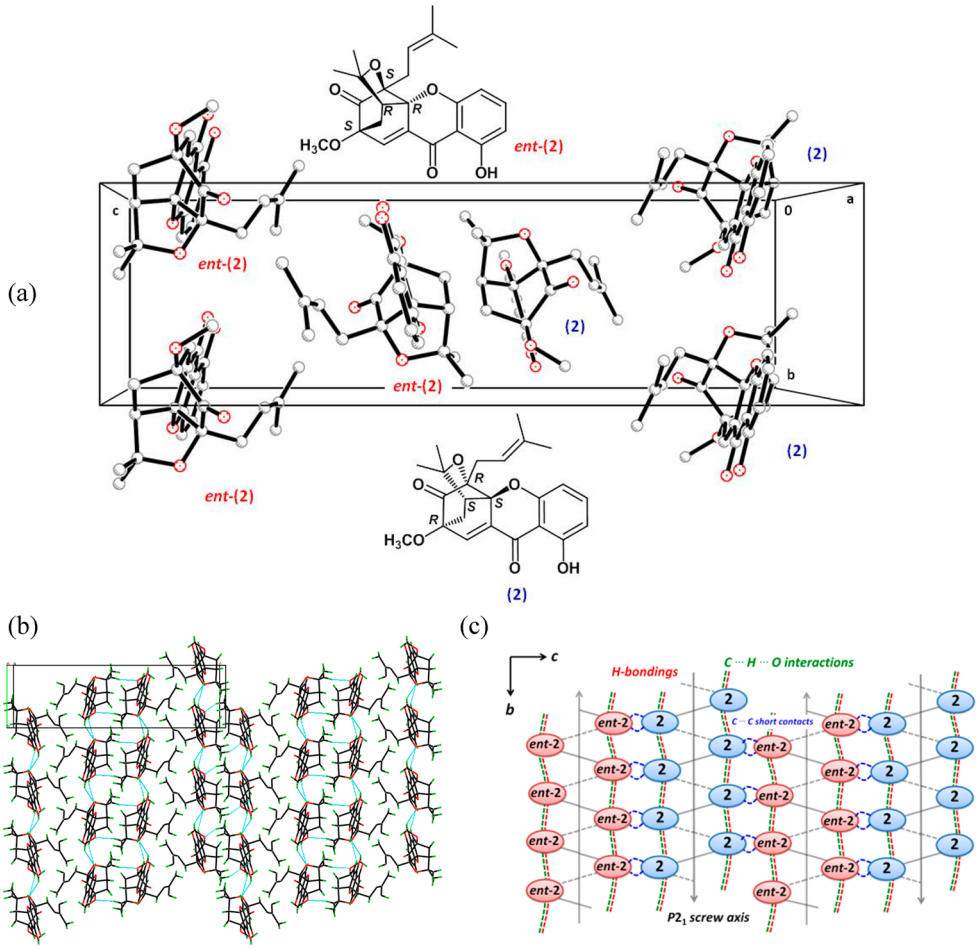

Figure 4. Crystal structure of caged-xanthone **2**.[18] (a) Crystal packing of **2** showing the nonsuperimposition of molecule **2** ((5*R*,5a*S*,7*R*,11*S*)-**2**) and molecule *ent*-**2** ((5*S*,5a*R*,7*S*,11*R*)-**2**). (b) Intermolecular interactions and molecular arrangement of **2**. (c) Schematic representation of interactions between molecule **2** (blue oval) and molecule *ent*-**2** (red oval) in the crystal packing.

1-OH) and three aromatic protons that coupled as an ABM system at δ_H 7.48 (t, J = 8.4 Hz, H-3), 6.61 (br d, J = 8.4 Hz, H-2), and 6.51 (br d, J = 8.4 Hz, H-4). A proton resonance at δ_H 6.65 (s) was assigned to the C-8 olefinic proton. The resonance at δ_H 3.13 (dd), assigned to the methine proton H-11, showed small (J = 6.6 Hz) and large (J = 12.6 Hz) coupling constants with the nonequivalent C-10 methylene proton resonances at δ_H 2.64 and 2.86, respectively. In the NOESY spectrum, a diastereotopic C-10 methylene proton at δ_H 2.64 showed a correlation with H-11 (δ_H 3.13), which indicated that the orientation of a diastereotopic C-10 methylene proton at δ_H 2.64 should be β-oriented. The attachment of an α,β-unsaturated cyclohexenone moiety at C-8a and C-5a was assigned by the HMBC correlations from the H-8 (δ_H 6.65) resonance to the C-9, C-5a, C-8a, and C-10 resonances and from H-10 (δ_H 2.86) to C-5a.

The ^{1}H NMR spectrum of **3** also showed resonances at δ_H 1.73 (s, H_3-13) and 1.41 (s, H_3-14) assigned to a 2,2-dimethyltetrahydrofuran ring. The attachment of the tetrahydrofuran ring at C-11 and C-5a was confirmed by the HMBC correlations between H-10 (δ_H 2.86) and C-7, C-11, C12, and C-5a. Resonances typical of an isoprenyl group were present at δ_H 4.99 (br t, J = 6.9 Hz, H-16), 2.46 (m, H_2-15), 1.62 (s, H_3-19), and 1.40 (s, H_3-18). The attachment of isoprenyl and methyl ester groups at C-5 was confirmed by the HMBC correlations between H_2-15 (δ_H 2.46) and C-5, C-5a, and C-6 and between 6-OCH_3 (δ_H 3.58) and C-6 shown in Figure S26. Therefore, the structure of compound **3** was assigned as a rearranged caged-xanthone, namely, pruniflorone U.

The X-ray analyses of **1**−**3** revealed that both **1** (CCDC 727003) and **3** (CCDC 774999) crystallized in a centrosymmetric triclinic $P\bar{1}$ space group (containing an inversion center), whereas **2**[18] crystallized in a centrosymmetric monoclinic $P2_1/c$ space group (containing a c-glide plane). Owing to the fact that crystals of an enantiomerically pure compound cannot crystallize in a space group that contains an inversion center, mirror plane, or glide plane,[19] and the crystals of **1**−**3** crystallalized in space groups containing an inversion center (for **1** and **3**) and a glide plane (for **2**), it was apparent that the crystals of **1**−**3** are racemates.

The crystal packings of **1**−**3** as shown in Figures 3−5 revealed that molecules **1**, **2**, and **3** cannot be superimposed on molecules *ent*-**1**, *ent*-**2**, and *ent*-**3**, respectively. In these diagrams, molecules **1** and **3** are related to molecules *ent*-**1** and *ent*-**3** by inversion,[19] whereas molecule **2** is related to molecule *ent*-**2** by a c-glide plane.[19] Therefore, the X-ray data obtained for **1**−**3** showed that single crystals of **1**−**3** exist as racemates. Moreover, the X-ray data in Figures 3b−5b and Figures 3c−5c showed that the crystals of **1**−**3** were stabilized by intermolecular interactions between two enantiomers (using blue and red ovals in Figures 3c−5c) in their crystal lattices.

dx.doi.org/10.1021/np400996k | J. Nat. Prod. 2014, 77, 1562−1571

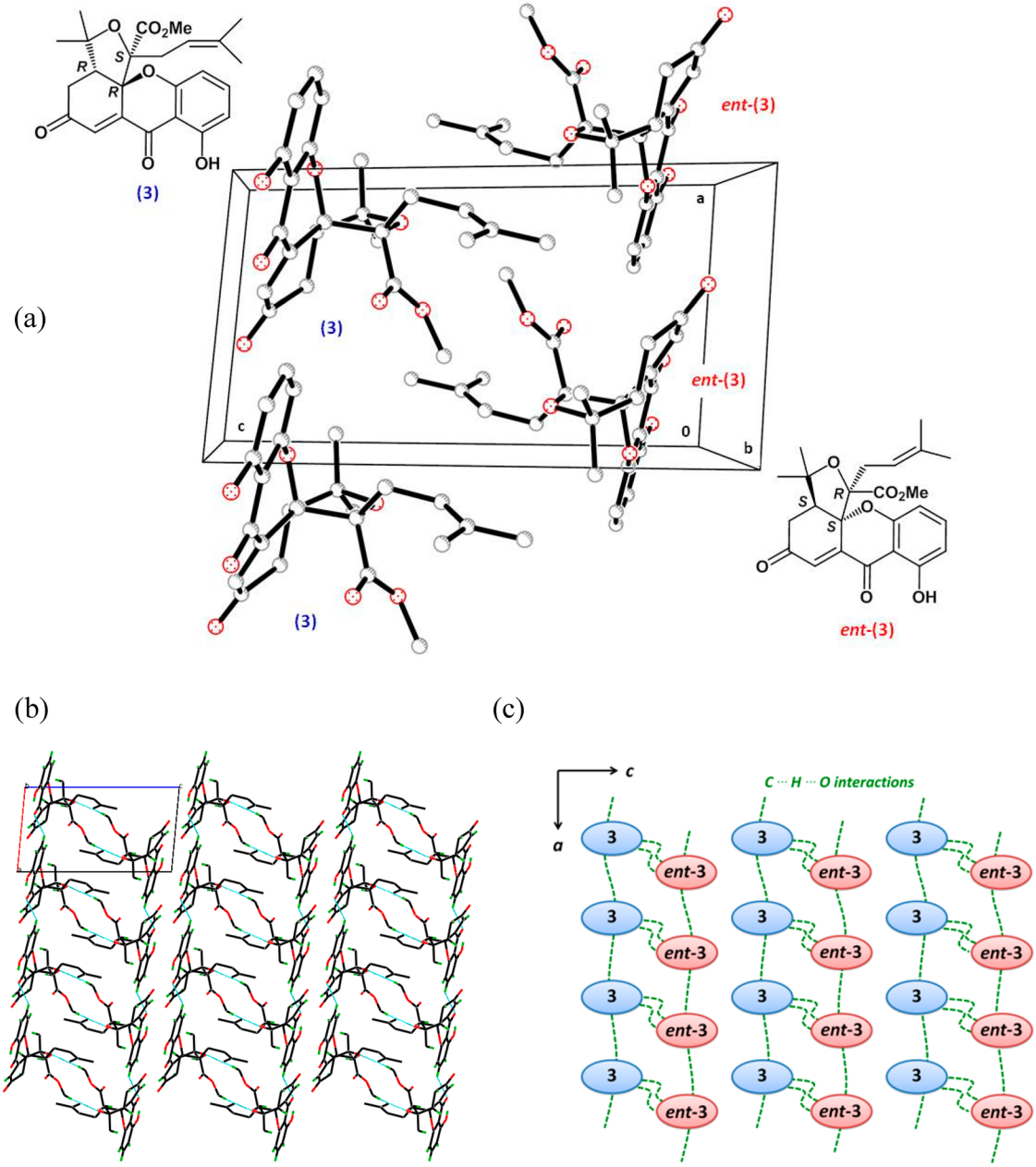

Figure 5. Crystal structure of rearranged caged-xanthone **3**. (a) Crystal packing of **3** showing the nonsuperimposition of molecule **3** ((5*S*,5a*R*,11*R*)-**3**) and molecule *ent*-**3** ((5*R*,5a*S*,11*S*)-**3**). (b) Intermolecular interactions and molecular arrangement of **3**. (c) Schematic representation of interactions between molecule **3** (blue oval) and molecule *ent*-**3** (red oval) in the crystal packing.

Surprisingly, the specific rotations of the isolated samples of **1**−**3** are +14 (*c* 0.1, $CHCl_3$), +125 (*c* 0.1, $CHCl_3$), and −24 (*c* 0.1, $CHCl_3$), respectively, demonstrating that the bulk samples of **1**−**3** are optically active, whereas the X-ray data of **1**−**3** showing that they contained both enantiomers in their crystal packing suggest that they are racemates. The combination of both observations suggests that the isolated samples of **1**−**3** are partial racemates. A previous report by Thoison and co-workers[2] showed that bractatin, a caged-xanthone isolated from *Garcinia bracteata* leaves, was a parital racemate that could be separated using a chiral column to give two peaks in an HPLC chromatogram. The partial racemization of **1** and **2** can be explained by the proposed biosynthesis shown in Scheme 1, in which the Claisen rearrangement step generates intermediates **1** and **2** as partial racemates.[20] This infers that Claisen rearrangement to give **1** and **2** might proceed via a mixture of nonenzymatic and enzymatic processes. Scheme 1 proposes that the caged motif construction occurs via a Diels−Alder reaction, affording the partial *rac*-**1** and partial *rac*-**2**, respectively, whereas partial *rac*-**3** would be formed via a ring expansion and degradation of partial *rac*-**2**.

The above results implied that compounds **1**−**3** were partial racemates. To clarify this assumption, we have further subjected all compounds to HPLC separation on a chiral column to determine the ratio of the two enantiomers in each mixture. The chiral HPLC analysis of each of the isolated samples **1**−**3** showed well-resolved peaks of two enantiomers in unequal ratios (Figure 6). The ratios of two enantiomers of compound **1**−**3** were as follows: 1.0:1.1 for the mixture of (−)-**1** [(1.1 mg), $[\alpha]^{25}_D$ = −61] and (+)-**1** [(1.2 mg), $[\alpha]^{25}_D$ = +79] in

dx.doi.org/10.1021/np400996k | *J. Nat. Prod.* 2014, 77, 1562−1571

Scheme 1. Plausible Biosynthesis of 1−3

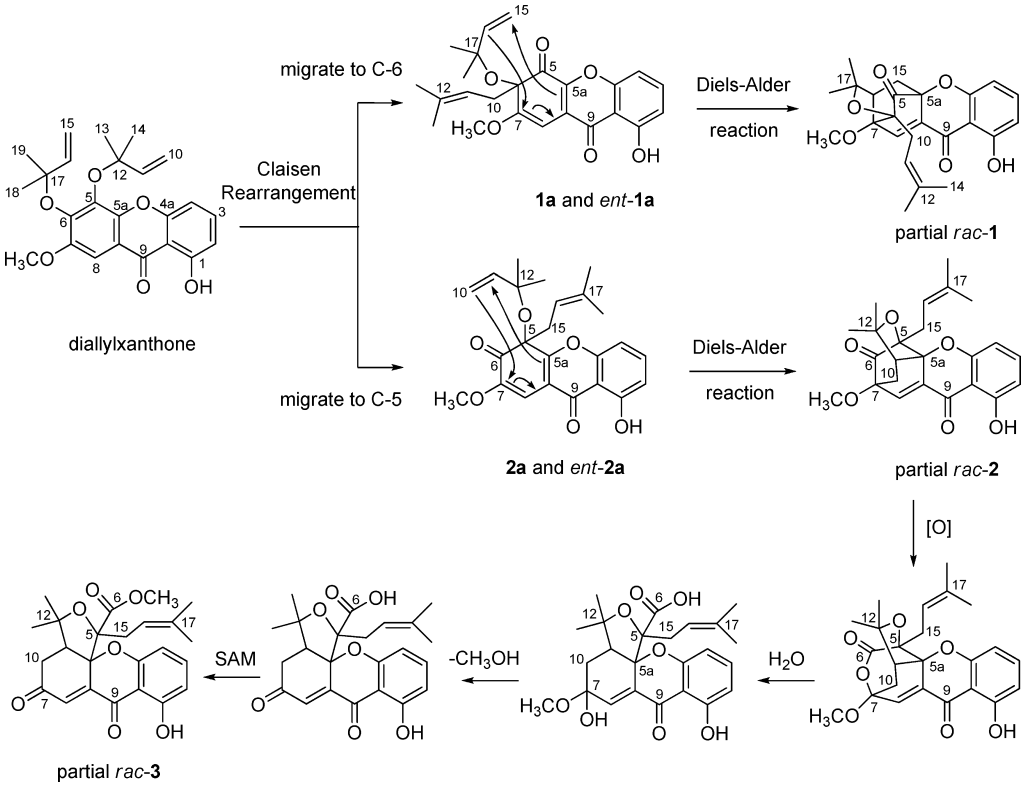

compound **1** (Figure 6a); 1.0:1.9 for the mixture of (−)-**2** [(1.8 mg), $[\alpha]^{25}_{D}$ = −459] and (+)-**2** [(3.4 mg), $[\alpha]^{25}_{D}$ = +509] in compound **2** (Figure 6b); and 1.1:1.0 for the mixture of (−)-**3** [(0.8 mg), $[\alpha]^{25}_{D}$ = −161] and (+)-**3** [(0.7 mg), $[\alpha]^{25}_{D}$ = +172] in compound **3** (Figure 6c), respectively. Comparison of the spectroscopic data of (−)-**1**/(+)-**1** with **1**, (−)-**2**/(+)-**2** with **2**, and (−)-**3**/(+)-**3** with **3** revealed that the ^{1}H and ^{13}C NMR spectra of each of the isolated enantiomers (Figures S29−S34) and their precursor mixtures in an achiral environmental were identical. These results confirmed our hypothesis that compounds **1**−**3** were partial racemates.

To establish the absolute configuration of the three different caged-scaffolds **1**−**3**, pure enantiomers of each scaffold [(−)-neocaged-xanthone pruniflorone T (**1**), (−)-caged-xanthone cochinchinone C (**2**), and (−)-rearranged caged-xanthone pruniflorone U (**3**)] were further recrystallized in CH_2Cl_2 to obtain single crystals for X-ray structure determination using Cu Kα radiation. Yellow plate-like single crystals of the (−)-neocaged-xanthone **1** were monoclinic, with a = 8.4151(3) Å, b = 8.0906(3) Å, c = 15.1668(5) Å and chiral space group $P2_1$. From the X-ray data analysis, the absolute configuration of (−)-neocaged-xanthone pruniflorone T (**1**) (Figures 7 and 9) was established as 5a*R*, 6*R*, 7*R*, and 16*S* through the refinement of Flack's parameter [x = 0.01(2)].

Moreover, (+)-neocaged-xanthone **1** showed the opposite sign in terms of the Cotton effects in the electronic circular dichroism (ECD) curve (Figure 8) and specific rotation as compared with the (−)-neocaged-xanthone **1**, but their NMR data were identical in an achiral environmental. Thus, the absolute configuration of (+)-neocaged-xanthone **1** (Figure 9) is (5a*S*, 6*S*, 7*S*, 16*R*).

The absolute configuration of (−)-caged-xanthone cochinchinone C (**2**) was confirmed to be the same as (−)-**1** based on single-crystal X-ray diffraction analysis. The yellow needle single crystals of the (−)-caged-xanthone **2** were orthorhombic, with a = 7.2698(8) Å, b = 11.4350(1) Å, c = 24.6320(3) Å and chiral space group $P2_12_12_1$. The X-ray diffraction analysis using anomalous scattering of Cu Kα radiation resulted in a Flack parameter of 0.02(3), which showed that the absolute configuration of (−)-caged-xanthone cochinchinone C (**2**) (Figures 10 and 12) was (5*R*, 5a*S*, 7*R*, 11*S*).

The signs of the ECD Cotton effects and specific rotations of (+)-cochinchinone C (**2**) and (−)-cochinchinone C (**2**) were opposite (Figure 11). Therefore, the absolute configuration of (+)-cochinchinone C (**2**) (Figure 12) was (5*S*, 5a*R*, 7*S*, 11*R*).

Finally, yellow needle single crystals of the (−)-rearranged caged-xanthone pruniflorone U (**3**) were monoclinic, with a = 13.4658(12) Å, b = 7.9997(7) Å, c = 20.8660(2) Å and with a chiral space group $P2_1$. The absolute configuration of (−)-rearranged caged-xanthone pruniflorone U (**3**) was assigned as (5*S*, 5a*R*, 11*R*) by the single-crystal X-ray diffraction analysis (Figures 13 and 15) with a Flack parameter of 0.02(3).

In a similar way, the absolute configuration of (+)-pruniflorone U (**3**) (Figure 15) was assigned as (5*R*, 5a*S*, 11*S*) by comparison of the ECD curve (Figure 14) and specific rotation with those of (−)-pruniflorone U (**3**) (see Experimental Section).

Only stable compounds of sufficient quantity were evaluated for in vitro cytotoxicity against the MCF-7 human breast cancer cell line (Table 2). Cochinchinone C (**2**) exhibited better activity than pruniflorone T (**1**) and pruniflorone U (**3**), with an IC_{50} value of 0.36 μg/mL. Interestingly, a 1:1 mixture of **1** and **3** significantly increased the cytotoxicity against MCF-7 compared with the pure forms (**1** and **3**), with an IC_{50} value of 0.11 μg/mL.

dx.doi.org/10.1021/np400996k | *J. Nat. Prod.* 2014, 77, 1562−1571

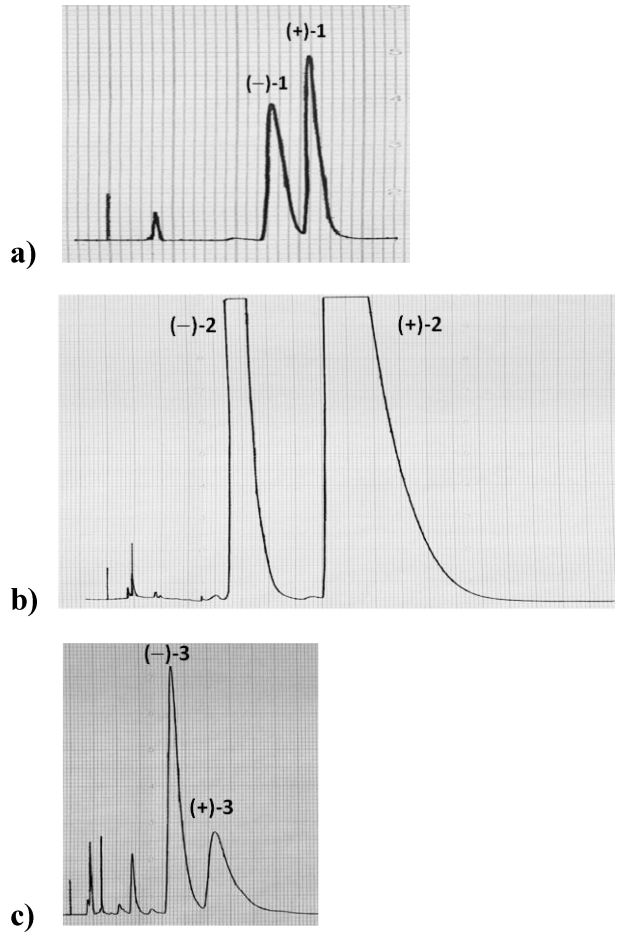

Figure 6. Chiral HPLC using a Chiral Pack AD-H, 5 μm, 4.6 × 250 mm column, with detection at 225 nm and a flow rate of 1 mL/min. (a) Chiral HPLC chromatogram of (−)-neocaged-xanthone **1** and (+)-neocaged-xanthone **1** by using 1:99 *i*PrOH−*n*-hexane as eluent. (b) Chiral HPLC chromatogram of (−)-caged-xanthone **2** and (+)-caged-xanthone **2** by using 0.5:99.5 *i*PrOH−*n*-hexane as eluent. (c) Chiral HPLC chromatogram of (−)-rearranged caged-xanthone **3** and (+)-rearranged caged-xanthone **3** by using 1:99 *i*PrOH−*n*-hexane as eluent.

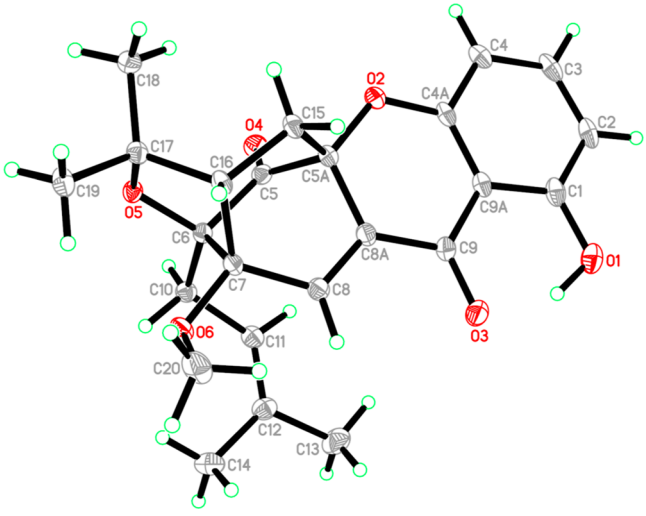

Figure 7. ORTEP diagram of (−)-neocaged-xanthone pruniflorone T (**1**).

EXPERIMENTAL SECTION

General Experimental Procedures. Optical rotations were measured on a JASCO P-1020 polarimeter. Ultraviolet (UV) absorption spectra were measured on a SPECORD S 100 (Analytikjena) spectrophotometer. Infrared spectra (IR) were recorded on a PerkinElmer 783 FTS FT-IR spectrometer. The ^{1}H and ^{13}C NMR spectra were recorded on 300 MHz Bruker FTNMR Ultra Shield and 600 MHz Bruker AV-600 spectrometers in $CDCl_3$ with TMS as the internal standard. Chemical shifts are reported in δ (ppm), and coupling constants (J) are expressed in hertz. Electronic circular dichroism spectra were recorded on a JASCO J-810 CD spectropolarimeter. Mass spectra were measured on a MAT 95 XL mass spectrometer (Thermo Finnigan). Chiral HPLC was performed on a Chiralpak AD-H column of 4.6 × 250 nm and attached to the photodiode array detector. Quick column chromatography (QCC) and column chromatography (CC) were carried out on silica gel (Merck) type 100 (0.063−0.20 mm) and silica gel 60 F_{254} (Merck) with a gradient system of acetone−*n*-hexane or as otherwise stated, or silica gel 60 RP-18 (40−63 μm) (Merck) with pure MeOH.

Plant Material. Roots of *C. formosum* ssp. *pruniflorum* were collected in May 2004 from Nong Khai Province, in the northeastern part of Thailand. Identification was made by Prof. Puangpen Sirirugsa, Department of Biology, Faculty of Science, Prince of Songkla University, and a specimen (No. 0012677) was deposited at the Prince of Songkla University Herbarium.

Extraction and Isolation. Air-dried roots of *C. formosum* ssp. *pruniflorum* (5.30 kg) were extracted with CH_2Cl_2 (2 × 20 L, for 5 days) at room temperature. The crude CH_2Cl_2 extract was evaporated under reduced pressure to afford a brownish crude (60.0 g) extract, which was subjected to QCC on silica gel using *n*-hexane as the first eluent and then increasing polarity with acetone to give six fractions (F1−F6). Fraction F2 was separated by QCC eluting with a gradient of CH_2Cl_2−*n*-hexane (0−70% over 120 min) to afford 11 subfractions (F2A−F2K). Subfraction F2B was further purified by QCC with a gradient of EtOAc−*n*-hexane (0−40% over 90 min) to give six subfractions (F2B1−F2B6). Subfraction F2B4 was further purified by CC eluting with 30% acetone−*n*-hexane to give nine subfractions (F2B4A−F2B4I). Subfraction F2B4F was further purified by CC eluting with 30% CH_2Cl_2−*n*-hexane to give **1** (4.3 mg), **2** (80.3 mg), and mixture of β-sitosterol and stigmasterol (7.5 mg). Compound **1** was recrystallized in $CHCl_3$−MeOH (9:1, v/v) to yield yellow needle single crystals. Subfraction F2B4E was further separated by CC on reversed-phase silica gel C_{18} eluting with MeOH to give **2** (15.5 mg) and **3** (3.5 mg). Compound **3** was recrystallized in $CHCl_3$−MeOH (9:1, v/v) to yield yellow needle single crystals.

*Pruniflorone T (**1**):* yellow powder, mp 167−169 °C; $[\alpha]^{25}_{D}$ +14 (*c* 0.1, $CHCl_3$); UV ($CHCl_3$) λ_{max} (log ε) 242 (3.36), 293 (3.34), 329 (3.54), 396 (2.78) nm; IR (neat) ν_{max} 3445, 1747, 1645 cm^{-1}; HREIMS $[M - CO]^+$ *m*/*z* 382.1774 for $C_{23}H_{26}O_5$ $[M - CO]^+$ (calcd 382.1780); EIMS *m*/*z* (rel int) (a parent ion at *m*/*z* 410 was not observed), 382 (3) $[M - CO]^+$, 313 (10), 279 (20), 256 (23), 178 (18), 167 (33), 149 (75), 127 (28), 113 (40), 111 (26), 99 (40), 97 (34), 85 (77), 83 (84), 71 (100), 69 (57).

*Chiral HPLC Separation and ECD Spectroscopic Data of (−)-**1** and (+)-**1**.* Separation of the two enantiomers of partial *rac*-**1** (2.3 mg) was performed by semipreparative HPLC on an enantioselective column (Chiral Pack AD-H 5 μm, 4.6 mm × 25 mm, eluent *n*-hexane−*i*PrOH, 99:1 v/v, 1 mL/min). Compound (−)-**1** (first eluted) {(1.1 mg), $[\alpha]^{25}_{D}$ −61 (*c* 0.4, CH_2Cl_2), mp 215−217 °C} and (+)-**1** (second eluted) {(1.2 mg), $[\alpha]^{25}_{D}$ +79 (*c* 0.8, CH_2Cl_2), mp 212−214 °C} were obtained. ECD spectra of compounds (−)-**1** (0.02 mg/mL) and (+)-**1** (0.12 mg/mL) were recorded at 25 °C in CH_2Cl_2, with a path length of 0.2 cm, bandwidth 2 nm, data pitch 0.5 nm, scan rate 200 nm/min, and response 4 s. UV absorption spectra were recorded at 25 °C in CH_2Cl_2 in the 200−500 nm region.

*Cochinchinone C (**2**):* yellow powder, mp 158−159 °C; $[\alpha]^{25}_{D}$ +125 (*c* 0.1, $CHCl_3$); UV ($CHCl_3$) λ_{max} (log ε) 262 (3.28), 310 (4.06), 350 (3.82), 400 (3.35) nm; IR (neat) ν_{max} 3428, 1746, 1644, 1604 cm^{-1}; HREIMS $[M - CO]^+$ *m*/*z* 382.1785 for $C_{23}H_{26}O_5$ [M −

dx.doi.org/10.1021/np400996k | *J. Nat. Prod.* 2014, 77, 1562−1571

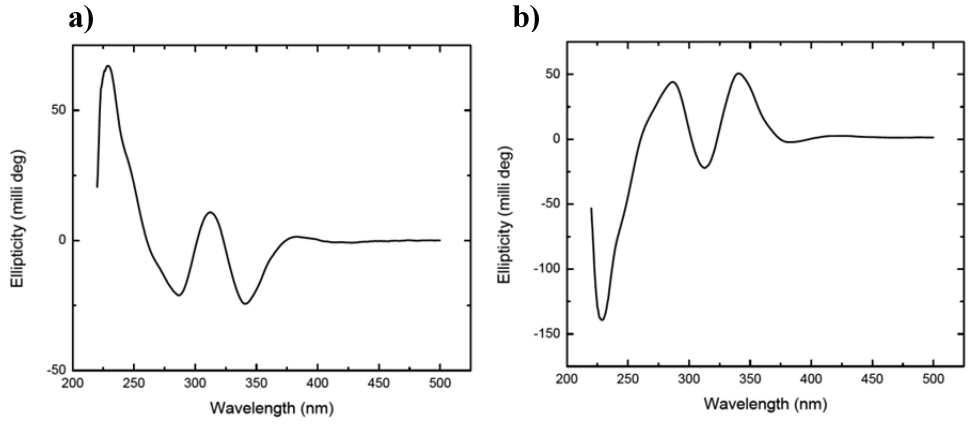

Figure 8. ECD spectra recorded in CH_2Cl_2. (a) (−)-Neocaged-xanthone pruniflorone T (**1**) (0.02 mg/mL). (b) (+)-Neocaged-xanthone pruniflorone T (**1**) (0.12 mg/mL) (path length of 0.2 cm, bandwidth 2 nm, data pitch 0.5 nm, scan rate 200 nm/min, and response 4 s).

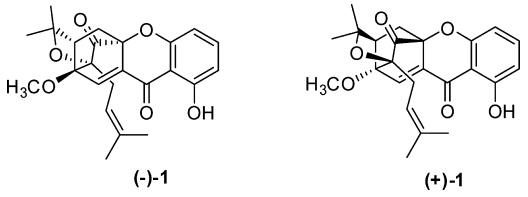

Figure 9. Absolute configurations of (−)-(5a*R*,6*R*,7*R*,16*S*)-**1** and (+)-(5a*S*,6*S*,7*S*,16*R*)-**1**.

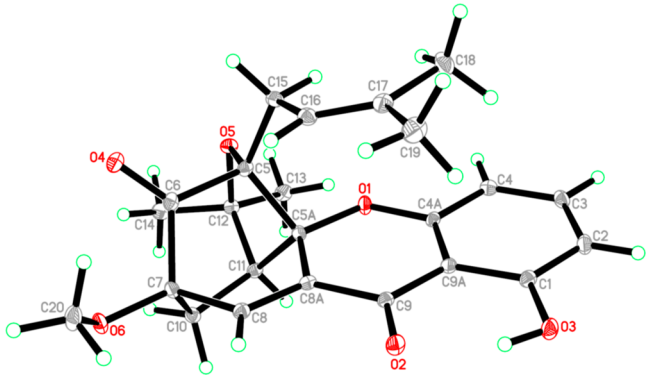

Figure 10. ORTEP diagram of (−)-caged-xanthone cochinchinone C (**2**).

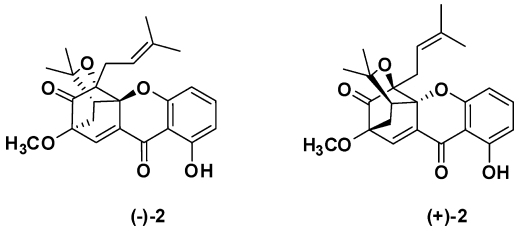

Figure 12. Absolute configurations of (−)-(5*R*,5a*S*,7*R*,11*S*)-**2** and (+)-(5*S*,5a*R*,7*S*,11*R*)-**2**.

CO]$^+$ (calcd 382.1780); EIMS *m*/*z* (rel int) (a parent ion at *m*/*z* 410 was not observed), 382 [M − CO]$^+$ (48), 313 (100), 285 (32), 271 (9), 243 (16), 227 (5), 203 (5), 137 (8), 69 (7).

Chiral HPLC Separation and ECD Spectroscopic Data of (−)-2 and (+)-2. Separation of the two enantiomers of partial *rac*-**2** (5.2 mg) was performed by semipreparative HPLC on an enantioselective column (Chiral Pack AD-H 5 μm, 4.6 mm × 25 mm, eluent *n*-hexane−*i*PrOH, 99.5:0.5 v/v, 1 mL/min). Compound (−)-**2** (first eluted) {(1.8 mg), $[\alpha]^{25}_D$ −459 (*c* 0.7, CH_2Cl_2), mp 163−164 °C} and (+)-**2** (second eluted) {(3.4 mg), $[\alpha]^{25}_D$ +509 (*c* 0.7, CH_2Cl_2), mp 166−167 °C} were obtained. ECD spectra of compounds (−)-**2** (0.02 mg/mL) and (+)-**2** (0.13 mg/mL) were recorded at 25 °C in CH_2Cl_2, with a path length of 0.2 cm, bandwidth 2 nm, data pitch 0.5 nm, scan rate 200 nm/min, and response 4 s. UV absorption spectra were recorded at 25 °C in CH_2Cl_2 in the 200−500 nm region.

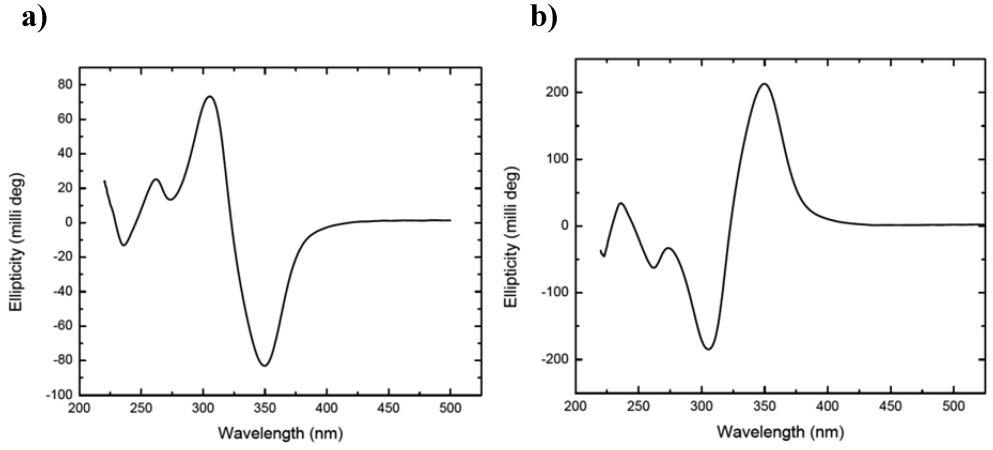

Figure 11. ECD spectra recorded in CH_2Cl_2. (a) (−)-Caged-xanthone **2** (0.02 mg/mL). (b) (+)-Caged-xanthone **2** (0.13 mg/mL) (path length of 0.2 cm, bandwidth 2 nm, data pitch 0.5 nm, scan rate 200 nm/min, and response 4 s).

dx.doi.org/10.1021/np400996k | *J. Nat. Prod.* 2014, 77, 1562−1571

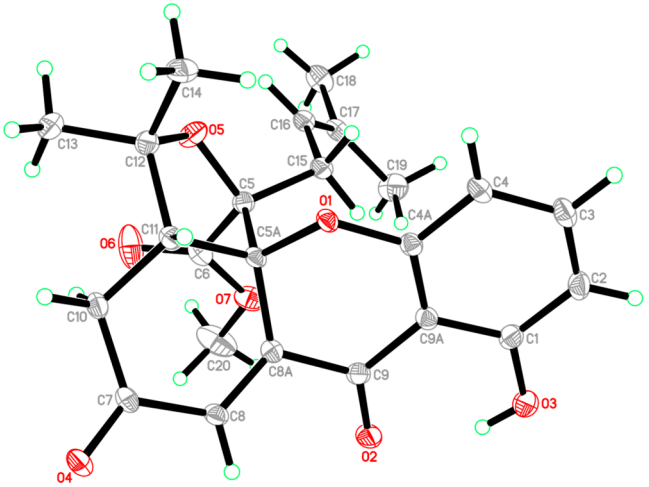

Figure 13. ORTEP diagram of (−)-rearranged caged-xanthone pruniflorone U (**3**).

*Pruniflorone U (**3**):* yellow powder, mp 97−99 °C; $[\alpha]^{25}_{D}$ −24 (*c* 0.1, $CHCl_3$); UV ($CHCl_3$) λ_{max} (log ε) 243 (3.93), 252 (3.91), 312 (4.01), 385 (3.37) nm; IR (neat) ν_{max} 3615, 1748, 1710, 1633 cm^{-1}; HREIMS *m*/*z* 426.1684 for $C_{24}H_{26}O_7$ (calcd 426.1679); EIMS *m*/*z* (rel int) 426 $[M]^+$ (2), 382 (7), 313 (13), 270 (100), 242 (19), 227 (42), 213 (9), 200 (8), 137 (8), 69 (7).

*Chiral HPLC Separation and ECD Spectroscopic Data of (−)-**3** and (+)-**3**.* Separation of the two enantiomers of partial *rac*-**3** (1.5 mg) was performed by semipreparative HPLC on an enantioselective column (Chiral Pack AD-H 5 μm, 4.6 mm × 25 mm, eluent *n*-hexane−*i*PrOH, 99:1 v/v, 1 mL/min). Compound (−)-**3** (first eluted) {(0.8 mg), $[\alpha]^{25}_{D}$ −161 (*c* 0.2, CH_2Cl_2), mp 150−152 °C} and (+)-**3** (second eluted) {(0.7 mg), $[\alpha]^{25}_{D}$ +172 (*c* 0.5, CH_2Cl_2), mp 147−148 °C} were obtained. ECD spectra of compounds (−)-**3** (0.02 mg/mL) and (+)-**3** (0.14 mg/mL) were recorded at 25 °C in CH_2Cl_2, with a path length of 0.2 cm, bandwidth 2 nm, data pitch 0.5 nm, scan rate 200 nm/min, and response 4 s. UV absorption spectra were recorded at 25 °C in CH_2Cl_2 in the 200−500 nm region.

Cytotoxicity Assay. The cancer cell line MCF-7 (human breast adenocarcinoma) was grown in Dulbecco's modified Eagle medium−nutrient mixture F12 (D-MEM/F12) supplemented with 10% fetal bovine serum. Cells were seeded in 96 wells (3000 cell/well) and allowed to adhere for 24 h at 37 °C with 5% CO_2 in a fully humidified incubator. Then 100 μL of 25 μg/mL crude extract or 5-fold-diluted pure compound in medium (final concentration 0.008, 0.04, 0.2, 1, and 5 μg/mL) was dispensed into wells of the cell plates and incubated further for 72 h. After removal of the sample medium, the cells were topped up with 200 μL of D-MEM/F12 medium and incubated. After 72 h, cells were fixed with cold 40% trichloroacetic acid, kept at 4 °C for 1 h, and washed with tap water. The viable cells were assayed by using sulforhodamine B following the method of Skehan and co-workers.[21] The absorbance was measured at 492 nm using a microplate reader. The results were based on the ability of the extracts to inhibit cell growth compared to control (cells in media without extract) and calculated for IC_{50} using probit analysis. Camptothecin, which was used as a standard, showed cytotoxic activity at <0.024 μg/mL.[22]

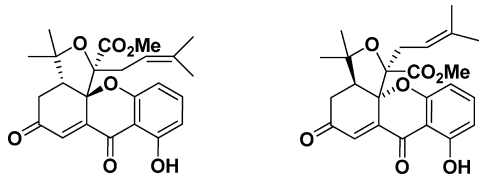

Figure 15. Absolute configurations of (−)-(5*S*,5a*R*,11*R*)-**3** and (+)-(5*R*,5a*S*,11*S*)-**3**.

Table 2. Cytotoxicity of 1−3 against the MCF-7 Human Breast Cancer Cell Line

	1	2	3	1 + 3[a]	camptothecin
IC_{50} (μg/mL)	>5	0.36	>5	0.11	<0.024

[a]A 1:1 mixture of **1** and **3**.

■ ASSOCIATED CONTENT

Ⓢ Supporting Information

NMR spectra of compounds **1**, (+)-**1**, **2**, (+)-**2**, **3**, and (+)-**3**. X-ray crystallographic data of **1**, **3**, (−)-**1**, (−)-**2**, and (−)-**3**. This material is available free of charge via the Internet at http://pubs.acs.org.

■ AUTHOR INFORMATION

Corresponding Authors

*E-mail: nawong.b@psu.ac.th. Tel: +66-7428-2704. Fax: +66-7428-2709.
*E-mail: suchada.c@psu.ac.th.

Notes

The authors declare no competing financial interest.

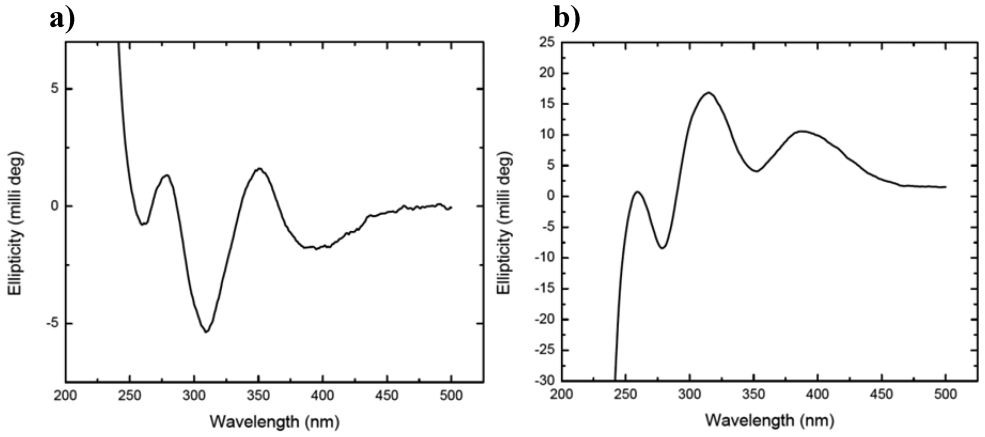

Figure 14. ECD spectra recorded in CH_2Cl_2. (a) (−)-Rearranged caged-xanthone pruniflorone U (**3**) (0.02 mg/mL). (b) (+)-Rearranged caged-xanthone pruniflorone U (**3**) (0.14 mg/mL) (path length of 0.2 cm, bandwidth 2 nm, data pitch 0.5 nm, scan rate 200 nm/min, and response 4 s).

dx.doi.org/10.1021/np400996k | *J. Nat. Prod.* 2014, 77, 1562−1571

■ ACKNOWLEDGMENTS

The research was supported by a grant from the Prince of Songkla University, contract no. TTM560546S. N.B. thanks the Department of Chemistry, Faculty of Science, Prince of Songkla University, for the research facilities. S.C. and H.K.F. also thank the Universiti Sains Malaysia for APEX DE2012 grant no. 1002/PFIZIK/910323. N.B. thanks Assoc. Prof. Dr. Chatchanok Karalai for his useful suggestions.

■ REFERENCES

(1) Asano, J.; Chiba, K.; Tada, M.; Yoshii, T. *Phytochemistry* **1996**, *41*, 815−820.
(2) Thoison, O.; Fahy, J.; Dumontet, V.; Chironi, A.; Riche, C.; Tri, M. V.; Sevenet, T. *J. Nat. Prod.* **2000**, *63*, 441−446.
(3) Rukachaisirikul, V.; Painuphong, P.; Sukpondma, Y.; Koysomboon, S.; Sawangchote, P.; Taylor, W. C. *J. Nat. Prod.* **2003**, *66*, 933−938.
(4) Reutrakul, V.; Anantachoke, N.; Pohmakotr, M.; Jaipetch, T.; Sophasan, S.; Yoosook, C.; Kasisit, J.; Napaswat, C.; Santisuk, T.; Tuchinda, P. *Planta Med.* **2007**, *73*, 33−40.
(5) Shadid, K. A.; Shaari, K.; Abas, K. F.; Israf, D. A.; Hamzah, A. S.; Syakroni, N.; Saha, K.; Lajis, N. H. *Phytochemistry* **2007**, *68*, 2537−2544.
(6) Sukpondma, Y.; Rukachaisirikul, V.; Phongpaichit, S. *Chem. Pharm. Bull.* **2005**, *53*, 850−852.
(7) Han, Q.-B.; Wang, Y.-L.; Yang, L.; Tso, T.-F.; Qiao, C.-F.; Song, J.-Z.; Xu, L.-J.; Chen, S.-L.; Yang, D.-J.; Xu, H.-X. *Chem. Pharm. Bull.* **2006**, *54*, 265−267.
(8) Cao, S.-G.; Sng, V. H. L.; Wu, X.-H.; Sim, K.-Y.; Tan, B. H. K.; Pereira, J. T.; Goh, S. H. *Tetrahedron* **1998**, *54*, 10915−10924.
(9) Wu, Z.-Q.; Guo, Q.-L.; You, Q.-D.; Zhao, L.; Gu, H.-Y. *Biol. Pharm. Bull.* **2004**, *27*, 1769−1764.
(10) Yu, J.; Guo, Q.-L.; You, Q.-D.; Lin, S.-S.; Li, S.; Gu, H.-Y.; Zhang, H.-W.; Tan, Z.; Wang, X. *Cancer Chemother. Pharmacol.* **2006**, *58*, 434−443.
(11) Liu, W.; Guo, Q.-L.; You, Q.-D.; Zhao, L.; Gu, H.-Y.; Yuan, S.-T. *World J. Gastroenterol.* **2005**, *11*, 3655−3659.
(12) Yang, Y.; Yang, L.; You, Q.-D.; Nie, F.-F.; Gu, H.-Y.; Zhao, L.; Wang, X.-T.; Guo, Q.-L. *Cancer Lett.* **2007**, *256*, 259−266.
(13) Zhang, H.-Z.; Kasibhatla, S.; Wang, Y.; Herich, J.; Guastella, J.; Tseng, B.; Drewe, J.; Cai, S.-X. *Bioorg. Med. Chem.* **2004**, *12*, 309−317.
(14) Kuemmerle, J.; Jiang, S.; Tseng, B.; Kasibhatla, S.; Drewe, J.; Cai, S.-X. *Bioorg. Med. Chem.* **2008**, *16*, 4233−4241.
(15) Li, N. G.; You, Q. D.; Huang, X. F.; Wang, J. X.; Guo, Q. L.; Chen, X. G.; Li, Y.; Li, H. Y. *Chin. Chem. Lett.* **2007**, *18*, 659−662.
(16) Wang, J.; Zhao, L.; Hu, Y.; Guo, Q.; Zhang, L.; Wang, X.; Li, N.; You, Q. *Eur. J. Med. Chem.* **2009**, *44*, 2611−2620.
(17) Mahabusarakam, W.; Nuangnaowarat, W.; Taylor, W. C. *Phytochemistry* **2006**, *67*, 470−474.
(18) Chantrapromma, S.; Boonnak, N.; Fun, H.-K. *Acta Crystallogr.* **2005**, *E61*, o3505−o3507.
(19) Glusker, J. P.; Lewis, M.; Rossi, M. *Crystal Structure Analysis for Chemistry and Biologists*; John Wiley & Sons: NJ, 1994.
(20) Hayden, A. E.; Xu, H.; Nicolaou, K. C.; Houk, K. N. *Org. Lett.* **2006**, *8*, 2989−2992.
(21) Skehan, P.; Storeng, R.; Scudiero, D.; Monks, A.; McMahon, J.; Vistica, D.; Warren, J. T.; Bokesch, H.; Kenney, S.; Boyd, M. R. *J. Natl. Cancer Inst.* **1990**, *82*, 1107−1112.
(22) Salae, A. W.; Karalai, C.; Ponglimanont, C.; Kanjana-Opas, A.; Yuenyongsawad, S. *Can. J. Chem.* **2010**, *88*, 922−927.

■ NOTE ADDED AFTER ASAP PUBLICATION

This paper published to the Web on June 18, 2014, with an added affiliation to Hoong-Kun Fun, and updated values in Table 2. The corrected version reposted on June 20, 2014.